



Title : **Investigation of the Use of Biogas in a Gas Hob and the Feasibility of Upgrading it on a Household Scale**

Author : **Trautmann, Christina (TRTCHR002)**

Course : **MEC 5061Z - Dissertation presented towards the partial fulfilment of a Master of Science in Sustainable Energy Engineering**

Date : **January 2012**

University of Cape Town
Department of Mechanical Engineering
Energy Research Centre

Title : **Investigation of the Use of Biogas in a Gas Hob and the Feasibility of Upgrading it on a Household Scale**

Author : **Trautmann, Christina (TRTCHR002)**

Course : **MEC 5061Z – Dissertation presented towards the partial fulfilment of a Master of Science in Sustainable Energy Engineering degree**

Supervisor : **A-Prof. Harro von Blottnitz**

Co-Supervisor : **Dr. Brett Cohen**

Date : **January 2012**

University of Cape Town
Department of Mechanical Engineering
Energy Research Centre

Plagiarism Declaration

I know that plagiarism is wrong. Plagiarism is using another's work and to pretend that it is one's own.

I have used the American Psychological Association (APA) as the convention for citation and referencing. Each significant contribution to, and quotation in, this dissertation from the work, or works of other people has been attributed and has cited and referenced.

This dissertation is my own work.

I have not allowed, and will not allow, anyone to copy my work with the intention of passing it off as his or her own work.

I acknowledge that copying someone else's assignment or essay, or part of it, is wrong, and declare that this is my own work.

Name: Christina Trautmann

Date: 2012

Abstract

The production and use of biogas on a household scale is becoming more common. The biogas is mainly used for lighting and cooking. Since some households may already be using sophisticated gas appliances prior to investing in an anaerobic digester and might not wish to downgrade to relatively simple and robust biogas appliances, a need to investigate the compatibility of biogas with a standard household appliance was identified. A gas hob was chosen. Special biogas appliances are typically required because biogas has a low methane content compared to natural gas; a possible need to upgrade the biogas was thus also identified. Biogas upgrading is regularly performed on a larger scale, but is a fairly expensive and complex process.

Two hypotheses were formulated: the first stated that, unless modified, a standard gas hob could not operate on a gas that had the same composition as biogas; while the second stated that it was expected that the costs of a simple and robust household scale absorber for the upgrading of biogas would be significant compared to the possible economic advantages of using this device.

In order to test the first hypothesis, a standard gas hob was tested with a range of synthesized gas mixtures that represented biogas as well as various levels of upgraded biogas. The gas mixtures were composed of 60 to 100 % methane, with the balance being carbon dioxide. The aim of this experimental work was to determine if biogas upgrading was required and, if it was, to what methane concentration it needed to be upgraded. In addition to testing different gas mixtures, the design of hobs was analysed in order to determine the ease with which they may be modified to become compatible with biogas.

The experimental work produced two main findings. The first was that increasing the injector size increased the water heating rate and efficiency, and allowed for the ignition of a lower quality gas. Thus a standard gas hob could be modified in order to run on biogas, i.e. the injector size would need to be changed and the air-intake would need to be adjusted. Secondly, it was shown that upgraded biogas also improved the water heating rate and efficiency, and that a methane content of 80% was considered a sufficient level of biogas upgrading in order to be compatible with a standard hob.

An absorber was determined to be the most appropriate upgrading technology. The second hypothesis was thus tested through the theoretical design of a household scale absorber. The absorber was designed to upgrade the biogas while in use. The flow rate of the upgraded biogas was specified by the flow rate required to produce a 3 kW flame in a hob, while the required composition was specified by the experimental findings (80% methane). A stripper was not included in the design and the column was restricted to operating at ambient conditions.

An aqueous K_2CO_3 solution was determined to be a suitable solvent. A packed column type absorber was chosen due its suitability to the small scale. The column diameter and a height were calculated to be 3 to 4 cm and 5 to 15 cm respectively. The cost to operate the absorber was determined to be more than the value of LPG gas replaced by the biogas and thus prohibitive unless the produced potassium bicarbonate solution had fertilizer value.

The experimental work found that the hob could either be modified to run on a gas with a low methane content, or that the unmodified hob would be compatible with a gas containing 80% methane. The high cost of upgrading the biogas resulted in the latter option being unfeasible. It was thus concluded that the modification of a standard gas hob was preferable over upgrading of the biogas in an absorber without solvent regeneration. It is recommended that raw biogas be tested in a modified gas hob, but also that future work consider an absorber-stripper combination, informed by experimental data for an absorber operating at such a small scale.

Acknowledgements

Firstly, I would like to thank Harro for being an all-round great supervisor. His guidance and valuable feedback was greatly appreciated.

I would also like to thank the following people:

Waldo Kurtz, who went out of his way to help me build the rig and much more, even on the weekend

Ilhaam Dalwai, who sat with me for many hours at the GC testing gas samples

Eghsaan Matthews and Joachim Macke for providing invaluable assistance

Greg Austin for providing feedback and taking this research to the next level

Brett Cohen for co-supervising this dissertation

Mark Williamson, Shireen Govender, Ann Steiner, Frances Pocock, Mymoena van der Fort, Gideon Kaufman for general assistance

I would like to give a special thanks to Nicholas Schiller for all the advice and never-ending support.

Lastly I would like to thank the Centre for Renewable and Sustainable Energy Studies at Stellenbosch University, the Department of Science and Technology and the South African National Research Institute (SANERI) for funding my master's degree.

Table of Contents

1. Introduction	1
1.1. Background	1
1.2. Objectives	3
1.3. Strategy to Achieve Objectives	4
1.4. Dissertation Overview	5
2. Literature Review.....	6
2.1. Biogas Technology	6
2.1.1. <i>Biogas Digesters</i>	6
2.1.2. <i>Biogas Production</i>	8
2.2. Gas Hobs	10
2.3. Biogas Upgrading.....	13
2.3.1. <i>Introduction</i>	13
2.3.2. <i>Physical Absorption</i>	15
2.3.3. <i>Chemical Absorption</i>	16
2.3.4. <i>Adsorption</i>	17
2.3.5. <i>Membrane Separation</i>	17
2.3.6. <i>Cryogenic Separation</i>	18
2.4. Concluding Notes on the Literature Review	19
3. Approach and Methods.....	20
3.1. Hypotheses	20
3.2. Experimental Work	21
3.2.1. <i>Equipment</i>	21
3.2.2. <i>Method of Analysis</i>	25
3.2.3. <i>Experimental Approach</i>	27
3.2.4. <i>Experimental Procedure</i>	29
3.2.5. <i>Experimental Error</i>	30
3.3. Absorber Design	32
3.3.1. <i>Comparison and Feasibility</i>	32
3.3.2. <i>Design Basis</i>	33
3.3.3. <i>Design Approach</i>	34
4. Experimental Results and Discussion	36
4.1. Variation of Water Heating Power with Gas Composition	36
4.2. Variation of Flame Power with Gas Composition	41
4.3. Hob Efficiency	44
4.4. Cut-Off Compositions	51
4.5. Error Analysis.....	53
4.6. Conclusions and Recommendations from the Experiments.....	55
4.6.1. <i>Summary</i>	55
4.6.2. <i>Conclusions</i>	56
4.6.3. <i>Recommendations</i>	57
5. Absorber Design	59

5.1.	Mass Balance	59
5.2.	Selection of Solvent	61
5.3.	Equilibrium Solubility Data	63
5.4.	Calculation of the Liquid-to-Gas Ratio.....	64
5.5.	Choice of Equipment	68
5.6.	Column Diameter	70
5.7.	Packed Tower Height.....	72
5.7.1.	<i>Mass Transfer Theory</i>	72
5.7.2.	<i>Height Calculation</i>	75
5.8.	Results	80
5.9.	System Configuration and Integration	82
5.10.	Financial Viability.....	84
5.11.	Conclusions and Recommendations from the Absorber Design	86
5.11.1.	<i>Conclusions</i>	86
5.11.2.	<i>Recommendations</i>	86
6.	Conclusions and Recommendations.....	88
6.1.	Purpose and Motivation	88
6.2.	Hypotheses	88
6.3.	Experimental Work.....	89
6.3.1.	<i>Approach</i>	89
6.3.2.	<i>Summary of Findings</i>	89
6.4.	Absorber Design	91
6.4.1.	<i>Approach</i>	91
6.4.2.	<i>Summary of Findings</i>	92
6.5.	Conclusions.....	92
6.6.	Recommendations.....	94
	References	95
	Appendix A	98
	<i>Methane Material Safety Data Sheet</i>	98
	<i>Photographs of the Experimental Apparatus</i>	100
	<i>Gas Chromatograph Details</i>	103
	Appendix B	104
	<i>Raw Data</i>	104
	Appendix C.....	108
	<i>Gas Composition</i>	108
	<i>Flow Rate</i>	108
	<i>Energy Transferred to the Water</i>	110
	<i>Flame Power</i>	111
	<i>Efficiency</i>	111
	<i>Error Analysis</i>	112
	Appendix D	113
	<i>Raw Biogas Flow Rate</i>	113
	<i>Equilibrium Solubility Data</i>	113

<i>Correlations and Correction Factors</i>	114
<i>Absorber Design: Sample Calculations</i>	117

List of Tables

Table 1 Composition of biogas and natural gas (Deublein & Steinhauser, 2008)	9
Table 2 Comparison of various upgrading technologies (de Hullu et al., 2008).....	15
Table 3 Composition of biogas immediately after the treatment with different solvents (Tippayawong & Thanompongchart, 2010)	17
Table 4 Equipment Specification	22
Table 5 Whirlpool gas hob injector table (Whirlpool Corporation, n.d.).....	24
Table 6 Measured variables	25
Table 7 Overview of experiments	30
Table 8 Key for the graph legends	36
Table 9 Pooled standard deviation	54
Table 10 Calculation of gas flow rate (¹ Sandler, 1999).....	60
Table 11 Comparison between physical and chemical solvents (Green & Perry, 2008)	61
Table 12 Calculated solvent flow rate at 1.2 and 1.5 times the minimum rate	66
Table 13 Characteristics of Random Packings used in Calculations	69
Table 14 Column dimensions.....	80
Table 15 Price comparison.....	84
Table 16 Hob Efficiency Summary	90
Table 17 Gas Chromatograph details (SGE Analytical Science, 2011)	103
Table 18 Raw data.....	104
Table 19 Cut-off compositions: Raw data.....	107
Table 20 Data used to calculate the pooled standard deviation.....	112
Table 21 Equilibrium solubility data (Park, Shim, Lee, & Lee, 1997)	113

List of Figures

Figure 1 Flow diagram of the strategy to achieve objectives.....	4
Figure 2 Floating drum biogas digester (Fraenkel, 1986)	7
Figure 3 Fixed dome biogas digester (Fraenkel, 1986)	7
Figure 4 Diagram of the BiogasPro-6 (left) and BiogasPro-6D (right) (Agama Energy (a), 2011)	8
Figure 5 Burner diagram (adapted from Zanussi, n.d.).....	10
Figure 6 Biogas burner diagram (Khandelwal & Gupta, 2009)	11
Figure 7 Total number of biogas upgrading plants from 1987 to 2009 (Petersson & Wellinger, 2009)	13
Figure 8 Costs to upgrade biogas (Persson, 2003).....	14
Figure 9 Experimental setup	23
Figure 10 Whirlpool gas hob (AKT 30I IX) (Whirlpool Corporation, n.d.)	24
Figure 11 Water heating power versus gas composition (constant supply and operating pressure, high range)	37
Figure 12 Water heating power versus gas composition (constant supply and operating pressure, medium range).....	38
Figure 13 Water heating power versus gas composition (constant supply and operating pressure, low range)	39
Figure 14 Water heating power versus gas composition (constant methane flow rate).....	40
Figure 15 Flame power versus gas composition (constant supply and operating pressure, high range)	41
Figure 16 Flame power versus gas composition (constant supply and operating pressure, medium range).....	42
Figure 17 Flame power versus gas composition (constant supply and operating pressure, low range)	43
Figure 18 Supply pressure versus hob efficiency (constant gas composition of 99.95% methane and operating pressure of 2 kPa)	44
Figure 19 Operating pressure versus hob efficiency (constant gas composition of 99.95% methane and supply pressure)	45
Figure 20 Operating pressure versus hob efficiency (constant methane flow rate of 1.25 kW and supply pressure).....	46

Figure 21 Flow rate versus hob efficiency (constant gas composition of 99.95% methane and supply pressure).....	47
Figure 22 Flow rate versus hob efficiency (constant gas composition of 99.95% methane and operating pressure of 2 kPa).....	47
Figure 23 Gas composition versus hob efficiency (constant methane flow rate of 1.25 kW and supply pressure).....	48
Figure 24 Gas composition versus hob efficiency (constant operating and supply pressure, high range)	49
Figure 25 Gas composition versus hob efficiency (constant operating and supply pressure, mid range).....	49
Figure 26 Gas composition versus hob efficiency (constant operating and supply pressure, low range)	50
Figure 27 Cut-off compositions below which ignition was not possible	51
Figure 28 Mass balance diagram	60
Figure 29 Design diagram, showing the gas absorption concentration relationships (Sinnott, 2005)	64
Figure 30 Design diagram for CO ₂ dissolved water (Henry's constant from Green & Perry (2008)).....	65
Figure 31 Design diagram for CO ₂ dissolved in a 5 mass % K ₂ CO ₃ solution (equilibrium data from Park et al. (1997)).....	66
Figure 32 Design diagram for CO ₂ dissolved in a 10 mass % K ₂ CO ₃ solution (equilibrium data from Park et al. (1997)).....	67
Figure 33 Concentration profile for absorption with chemical reaction (Richardson, Harker, & Backhurst, 2002).....	73
Figure 34 Nomenclature for material balances in a counter-current packed-tower absorber (Richardson et al., 2002)	74
Figure 35 System Integration.....	82
Figure 36 Experimental apparatus.....	100
Figure 37 Whirlpool gas hob	101
Figure 38 Gas hob, showing burner heads and caps	101
Figure 39 Burner head, with injection candle and injector nozzle	102
Figure 40 Small burner in operation with a weak flame that was not well-dispersed by the burner crown	102
Figure 41 Small burner in operation with large, strong flames.....	103

Figure 42 Air calibration chart for metric series rotameter tube size 7 with float type A, showing $\pm 3.5\%$ error bars	108
Figure 43 Sample chart, showing graphs plotted for flow rates at different pressures	109
Figure 44 Generalised pressure drop correlation (Sinnott, 2005).....	114
Figure 45 Percentage flooding correction factor (Sinnott, 2005).....	115
Figure 46 Factor for H_G for Berl saddles (Sinnott, 2005)	115
Figure 47 Factor for H_L for Berl saddles (Sinnott, 2005)	116

Nomenclature

Roman letters:

A	- Cross-sectional area
a	- Effective interfacial area of packing
a_w	- Effective wetted area of the packing
b	- Big
Ca(OH)_2	- Calcium hydroxide
CH_4	- Methane
CO_2	- Carbon dioxide
C_t	- Concentration ($C_t = \frac{\rho_L}{M_s}$)
D	- Diffusivity
d	- Dry
D_c	- Column diameter
DEA	- Diethanolamine
d_p	- Packing size
$f_1, f_2,$ and f_3	- Viscosity, density and surface tension correction factors relative to water
F_p	- Packing factor
g	- Gravitational constant
GC	- Gas chromatograph
G_M and L_M	- Inert gas and liquid phase molar velocities per cross-sectional area respectively
H	- Henry's Law constant
H_2	- Hydrogen
H_G and H_L	- Heights of the individual gas and liquid phase transfer units
H_2O	- Water
H_{OG} and H_{OL}	- Heights of the overall transfer units based on the gas and liquid phase respectively
H_2S	- Hydrogen sulphide
K_3	- Correction factors
K_2CO_3	- Potassium carbonate
KHCO_3	- Potassium bicarbonate
k_G	- Gas film mass transfer coefficient
K_G	- Overall mass transfer coefficient based on the gas film
k_L	- Liquid film mass transfer coefficient
L	- Liquid molar flow rate
LPG	- Liquefied petroleum gas
L_w	- Liquid mass flow rate per cross sectional area
N_2	- Nitrogen

N_A	- Mass transfer flux
NaOH	- Sodium hydroxide
N_{OG} and N_{OL}	- Number of transfer units based on the gas and liquid phase respectively
MEA	- Monoethanolamine
m_{eL}	- Slope of the equilibrium line
m_{OL}	- Slope of the operating line
M_s	- Molecular mass of the solvent
MSDS	- Material Safety Data Sheet
P	- Operating pressure
p_A	- Partial pressure of substance A in the gas
R	- Ideal gas constant
s	- Small
SABS	- South African Bureau of Standards
Sc_V and Sc_L	- Schmidt numbers based on the gas and liquid phase respectively
V	- Volume
V_w	- Gas mass flow rate per cross sectional area
w	- Wet
X	- Mole ratio in the liquid phase
x_A	- Mole fraction of A in the liquid
Y	- Mole ratio in the gas phase
y_A	- Mole fraction of A in the gas phase
Z	- Height [m]
ZAR	- South African Rand

Greek letters:

ρ_V and ρ_L	- Gas and liquid densities
μ_L	- Liquid viscosity
Ψ_h	- Correction factors
ϕ_h	- Correction factors
σ_c	- Critical surface tension of the packing material
σ_L	- Liquid surface tension

Subscripts:

A	- Substance A
B	- Bulk
e	- Equilibrium
G	- Gas
i	- Interface
L	- Liquid
p	- Packing

- 1 - Bottom of absorber
- 2 - Top of absorber

1. Introduction

1.1. Background

Biogas is produced when organic material is anaerobically decomposed by bacteria. It is a methane-rich gas, which can be used as an energy source. It may be produced on a large scale and used in combined heat and power plants, as a vehicle fuel, or as a replacement for natural gas (Petersson & Wellinger, 2009). Biogas may also be produced on a household scale in micro-biogas digesters, and used as a household energy source. Household scale biogas production and usage forms the focus of this dissertation.

The use of biogas, produced in household-scale biogas digesters, is becoming more common in domestic settings, with over 44 million households globally already benefiting from this technology (REN21, 2011). Government programs have promoted the use of biogas systems, with the addition of approximately 22 million biogas systems from 2006 to 2010 in China alone (REN21, 2011). The main domestic biogas uses are cooking, heating and lighting.

Raw biogas is of a lower quality compared to typical household gases, including natural gas and liquefied petroleum gas (LPG), for which typical household appliances are designed. It is, however, similar to natural gas, as it is mainly composed of methane (CH_4). It differs in that natural gas is 83 to 98% methane, while biogas contains far more inert gases and only 55 to 70% methane (Deublein & Steinhauser, 2008). It thus has a relatively lower calorific value and a greater volume of biogas is required for the same energy provision as natural gas. Standard gas appliances may thus either not work at all or not perform optimally when run on biogas.

In order to utilize the biogas, it is thus necessary to either modify standard appliances or purchase appliances that have been specially designed to run on biogas. Another option, which appears not to have been seriously explored on a household scale, is to upgrade the biogas.

To obtain a better understanding of the options of using biogas on a household scale, it is instructive to consider a specific appliance more closely. The focus of this dissertation is primarily on more affluent households and on home-industry scale restaurants and conference centres, which constitute a thus far under-explored sector for the use of biogas. These establishments typically have access to electric lighting, and choose to use gas cooking appliances as gas may possibly be cheaper than using electricity, or may offer greater flexibility or speed in the kitchen compared to their electric equivalents. A gas hob was thus chosen for closer consideration.

Biogas produced on an industrial scale often needs to be upgraded before it may be used; the main step is the removal of carbon dioxide (CO₂) (Petersson & Wellinger, 2009). Upgrading biogas on a household scale may be seen as an unnecessary expense and complication.

A need to test a standard gas hob in order to establish whether it could work with raw biogas was thus identified. Failing this, it would need to be tested with upgraded biogas to determine at what minimum methane content the appliances would work. In this way it may be determined if the biogas would need to be upgraded, and to what extent it should be upgraded, in order to be used in standard gas appliances.

1.2. Objectives

This dissertation focuses on both the performance of biogas in a standard household gas hob and the design of an absorber, which may be used to upgrade biogas on a household scale. The benefits and disadvantages of each option are also compared.

The two main objectives of this dissertation are:

1. To investigate the performance of a standard gas hob run on synthesized biogas, with varying methane content.
2. To design a CO₂ absorber that may be used in a household biogas digester system.

The investigation into the performance of a standard home appliance through experimental work includes the following sub-objectives:

- Determine the minimum methane composition of biogas required to be used in a standard gas hob, which will provide the design basis of the absorber;
- Identify hob components that must be modified in order for the hob to run on biogas and how they could be changed; and
- Determine the possible benefits and disadvantages of using upgraded biogas, rather than raw biogas, in a gas hob.

The viability of the absorber will depend on the following criteria:

- It will need to be financially viable, in that it should not cost more to operate than the value of the gas produced.
- It should require little or no maintenance. As the digester units are privately-owned, small-scale installations, the absorber should be as self-sufficient as possible.
- The absorber should not produce waste streams that require additional treatment or special handling and disposal.
- In relation to the financial restriction, the absorber should not be disproportionately large, as this will increase the cost excessively as well as be impractical.
- The upgraded gas should be of a quality which is suitable to be used in readily available, standard gas equipment.

1.3. Strategy to Achieve Objectives

This section outlines the approach taken in order to achieve the stated objectives.

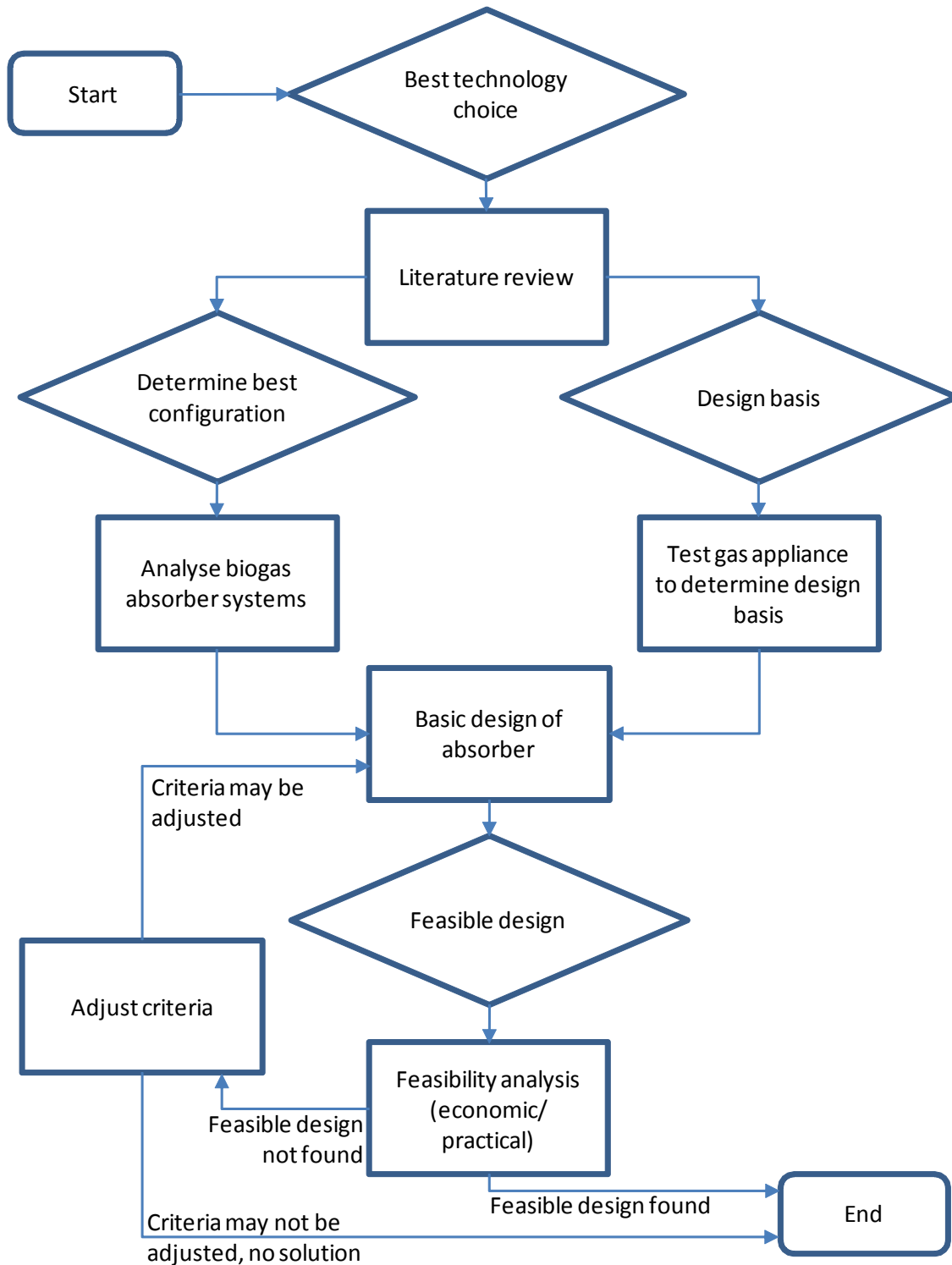


Figure 1 Flow diagram of the strategy to achieve objectives

Figure 1 illustrates the approach followed in order to achieve the objectives. Firstly, upgrading technology to be investigated will be informed by the literature review. From there the best configuration and the design basis will be determined concurrently. The best configuration of how the absorber will be integrated into the biogas digester system will be decided based on a mass and energy analysis, taking into account the typical usage of the biogas in a household. The design basis will be determined through the experimentation with a household appliance for operation on raw and improved biogas. The experimental work will be replicable, and designed to identify the effects of key identified parameters.

Once the system configuration and design basis have been determined, the absorber can be designed. The design will need to be tested for economic and practical feasibility. If a feasible design is not found, the design criteria may be reconsidered and possibly adjusted. Once it has been determined if a feasible design has been found or not, the dissertation can be concluded and recommendations can be made.

1.4. Dissertation Overview

The development of the dissertation follows the strategy outlined above. This introduction is followed by a literature review, which discusses biogas digester technology, gas appliances, and biogas upgrading technology. The approach and methodology that was followed are then discussed. The two results chapters form the central part of the dissertation. Chapter 4 presents the experimental work which was carried out on the household gas appliance; and Chapter 5 discusses the design of the absorber. The final chapter concludes the dissertation and presents recommendations.

2. Literature Review

This chapter provides a detailed review of household biogas production and usage, appropriate theory and related prior research that is used in Chapter 3 to justify the approach and methods employed in this dissertation. Firstly, the main types of household biogas digesters are discussed, including their basic operating principles and biogas production. This is followed with information on the design of a standard gas hob and how it compares to a biogas hob. Lastly, a review of biogas upgrading technologies is provided, with a focus on use on a small scale. The theory on the design of the chosen upgrading technology is not included in the literature review, but rather integrated into the actual design in Chapter 5.

2.1. Biogas Technology

2.1.1. Biogas Digesters

The two main types of small-scale biogas digesters are fixed dome and floating drum. These are presented in Figure 2 and Figure 3. Figure 2 illustrates the design of a floating drum digester, which was developed in India. It has a rigid digester chamber, which is divided into two parts. There is a separate, steel drum, which floats on top of the digester. As the floating drum collects the biogas, which is produced in the digester chamber, it rises. Thus the height of the drum provides an indication of the volume of gas that has been produced. The pressure in the system is constant for this digester type and is essentially dictated by the weight of the drum relative to its cross-sectional area. (Fraenkel, 1986)

The fixed dome digester (Figure 3) was developed in China. It has a rigid, fixed volume structure, which is typically buried underground. The pressure increase caused by the biogas production forces the level of the slurry to decrease by displacing the slurry into a separate tank. The difference between the levels of the slurry in the digester and the displacement tank provide an indication of the available pressure in the system. The available pressure is the driving force which allows the biogas to flow through a pipeline to be used in an appliance. The greater the amount of biogas produced, the greater the available pressure. This is thus a fixed volume system, with varying pressure. A pressure gauge may be used to estimate the amount of biogas produced. (Fraenkel, 1986)

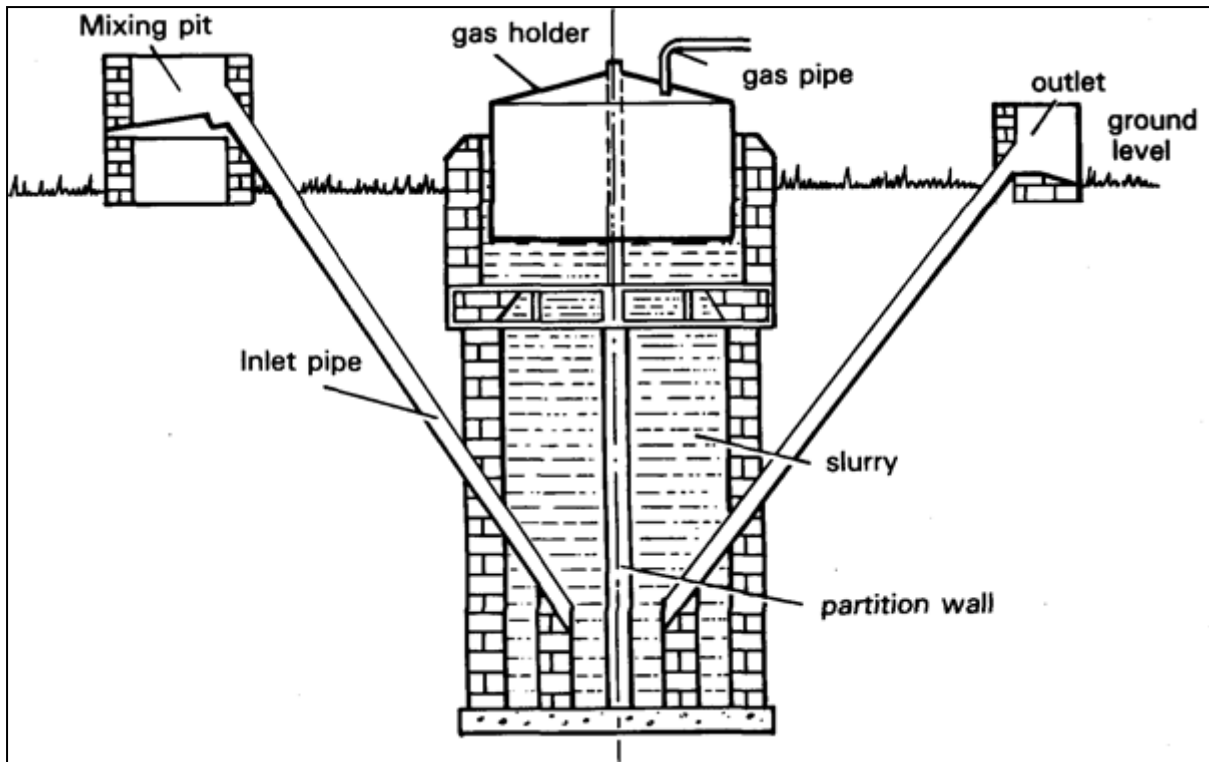


Figure 2 Floating drum biogas digester (Fraenkel, 1986)

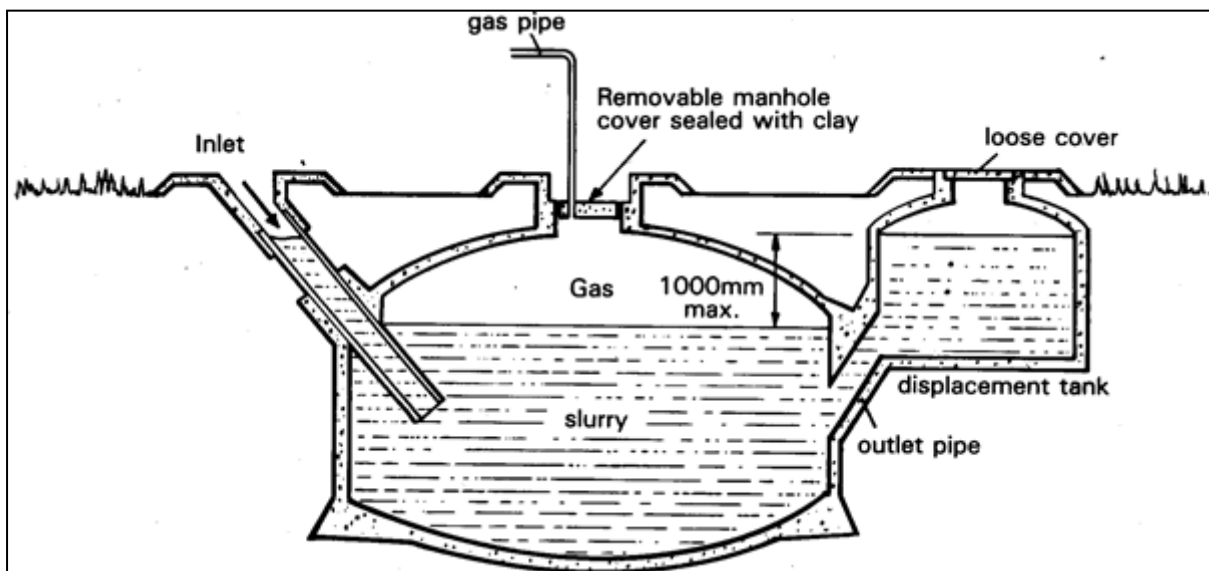


Figure 3 Fixed dome biogas digester (Fraenkel, 1986)

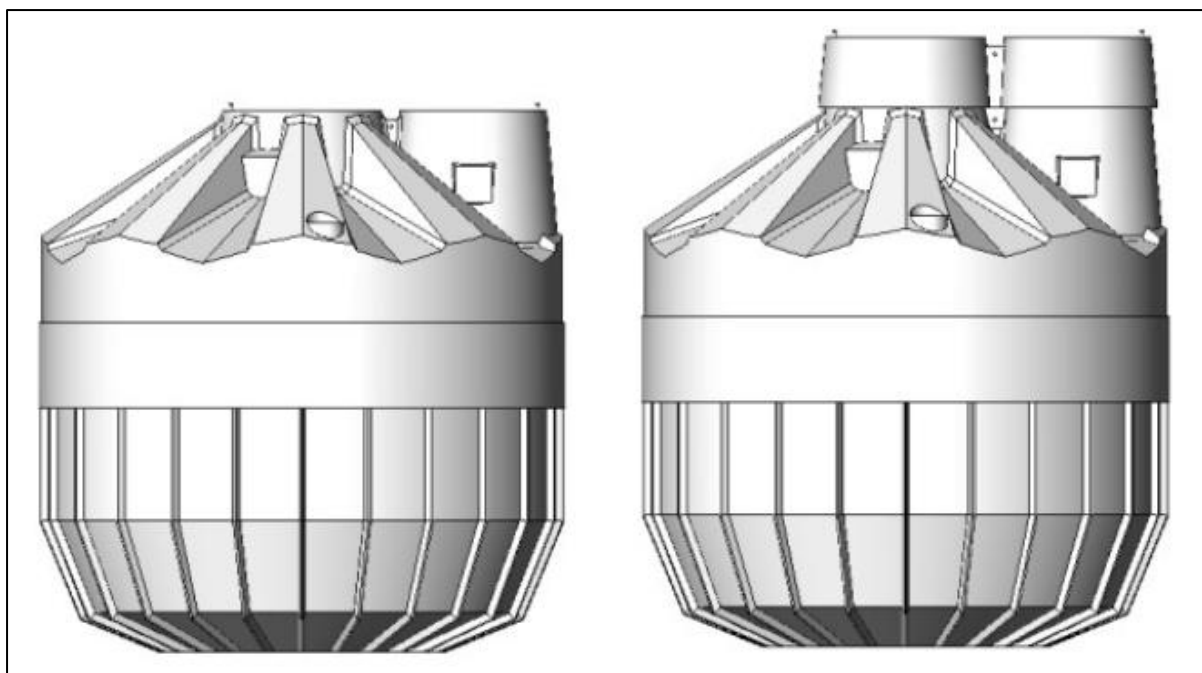


Figure 4 Diagram of the BiogasPro-6 (left) and BiogasPro-6D (right) (Agama Energy (a), 2011)

The fixed dome digester type is the most common type (Austin, 2011) and is the type on which the experimental work is based. Many variations on the fixed dome design exist; one of particular interest to this dissertation is Agama's pre-fabricated BiogasPro, shown in Figure 4. It has a capacity of 6 m³ and the ability to produce up to 1.9 m³ of biogas daily (Agama Energy (b), 2011).

2.1.2. Biogas Production

The composition and production rate of biogas depends on many factors, including: the amount and type of feed stock fed into the digester; the ambient temperature; and the current state of the digester, for example, the pH. Table 1 provides a comparison of various types of biogases and natural gases. Biogas is typically composed of 55-70% methane (CH₄) and 30-45% carbon dioxide (CO₂), as well as small amounts of water vapour, nitrogen and sulphur compounds (mainly hydrogen sulphide (H₂S)) (Deublein & Steinhauser, 2008). It has a lower methane content than natural gas, which sometimes also contains other hydrocarbons, and thus the calorific value is not as high as that of natural gas.

The pressure with which the biogas is supplied to the appliance depends on the amount of biogas which has been produced; the more biogas that has been produced, the greater the pressure. A minimum supply pressure is required to overcome the pressure drop in the pipeline connecting the digester to an appliance, including all additional fittings. If the biogas is used for an extended period, the supply pressure will decrease significantly since

the rate of biogas production is relatively slow compared to its consumption in an appliance. Based on the experience of the biogas research group within the Chemical Engineering Department at the University of Cape Town, a 6 m³ Agama BiogasPro biogas digester will typically provide a supply pressure of 2 to 7 kPa. Classic fixed dome digesters, such as those being installed under the auspices of the African Biogas Partnership in Ethiopia, have been observed to run supply pressures of up to 10 kPa (Melamu, 2011).

Table 1 Composition of biogas and natural gas (Deublein & Steinhauser, 2008)

Gas composites/ features	Natural gases			Biogases		
	Group H (GUS)	Group H (North Sea)	Group L (Holland)	Sewage gas	Agricultural gas	Landfill gas
Methane vol-%	98	86.5	83	65 - 75	45 - 75	45 - 55
Other hydro carbons vol-%	<1	<11	<5	-	-	-
Carbon dioxide vol-%	0.08	1.5	1.3	20 - 35	25 - 55	25 - 30
Nitrogen vol-%	0.8	1.1	10.6	3.4	0.01 - 5	10 - 25
Oxygen vol-%	0.05	0.05	0.05	0.5	0.01 - 2	1 - 5
Hydrogen sulphide mg/Nm ³	5	5	5	<8000	10 - 30 000	<8000
Mercaptan sulphur mg/Nm ³	6	6	6	-	<0.1 - 30	n.a.
Total sulphur mg/Nm ³	30	30	30	n.a.	n.a.	n.a.
Gross calorific value kWh/Nm ³	11.7	11.99	10.26	6.6 - 8.2	5.5 - 8.2	5.0 - 6.1
Net calorific value kWh/Nm ³	9.98	10.85	9.27	6.0 - 7.5	5.0 - 7.5	4.5 - 5.5
Relative humidity %	60	60	60	100	100	<100

2.2. Gas Hobs

The options for utilizing a standard hob with biogas include: upgrading the biogas to achieve a higher quality gas which will work with standard equipment; modifying the equipment so it may be used with raw biogas; or a combination of both. This section will deal with the basics of how standard hobs, as well as biogas hobs, work; while the next section will focus on options for upgrading the biogas.

A hob is made up of one or more burners, on each of which a pot may be placed. Burners are classified according to their size; a rapid burner is large and will take a large pot, while a semi-rapid burner is smaller and accommodates a smaller pot. A rapid burner consumes more gas than a semi-rapid burner, as it needs to heat a larger area. A biogas hob will usually only have one or two burners, depending on the rate of biogas production; while a standard hob usually has two or four burners.

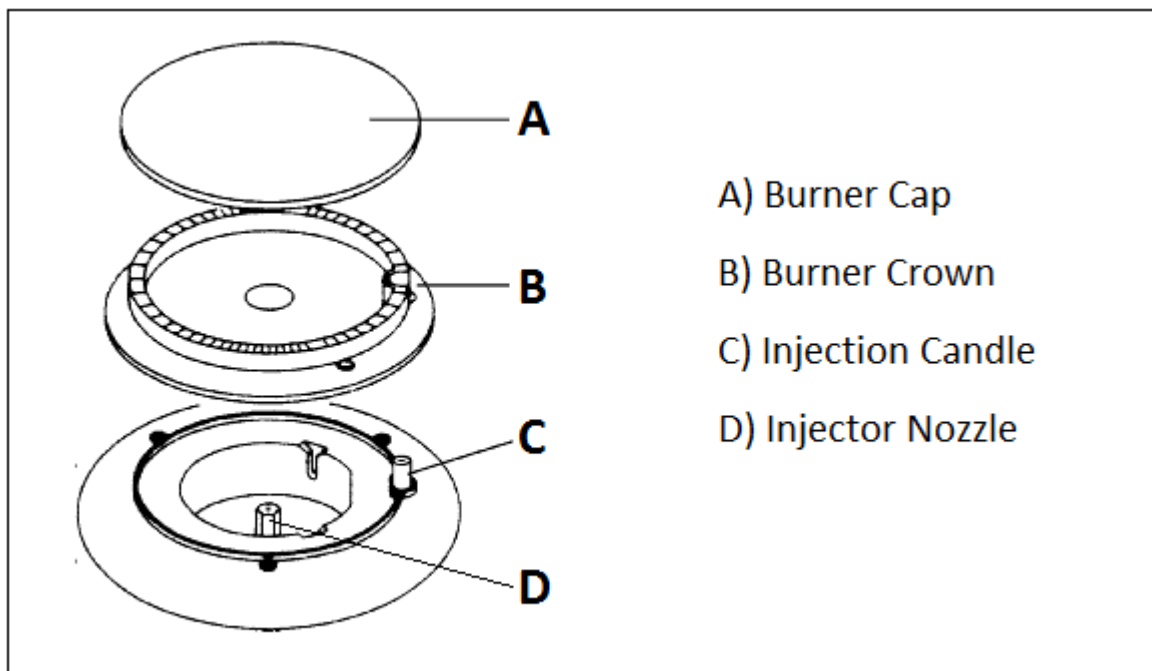


Figure 5 Burner diagram (adapted from Zanussi, n.d.)

A diagram of a burner typically found on a standard hob is shown in Figure 5. The gas flows through D, the injector nozzle, where it is lit by C, the injection candle. The burner crown and cap disperse the flame in order to provide even heating of the pot. The pot sits on a frame above the flames.

Biogas hobs are slightly different, more robust, and perhaps a bit more crude compared to standard hobs. A diagram of a typical biogas burner is shown in Figure 6. A gas tap allows the biogas to flow through the injector nozzle, into the mixing tube where air is mixed with the biogas. Air enters through the primary air openings. This feature is only present in some biogas hobs, but is present in all standard gas hobs. The air/biogas mixture exits through the burner ports where it is burnt at the burner head. The hob also includes pot supports and frame. (Khandelwal & Gupta, 2009)

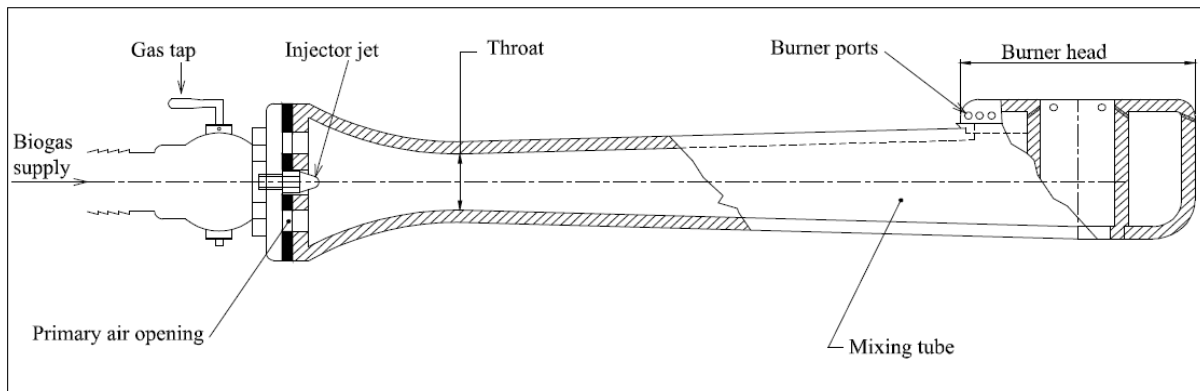


Figure 6 Biogas burner diagram (Khandelwal & Gupta, 2009)

A biogas hob typically needs to be corrosion resistant due to the H_2S content of the biogas, where that is not an important feature of a standard hob. Biogas hobs are thus constructed of corrosion-resistant materials, such as cast iron (Khandelwal & Gupta, 2009). This is important since the H_2S will need to be removed from the biogas if it is to be burnt in a standard gas hob.

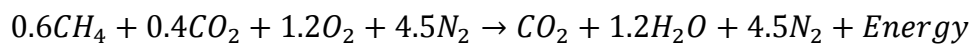
An injector nozzle, labelled as D in Figure 5, is a brass nozzle through which the gas flows. The injector diameter refers to the small opening in the centre of the injector. The size of the diameter is the key feature of the hob which is chosen according to the type of gas used and the size of the burner. The size of the diameter determines the flow rate of the gas. The flow rate and the calorific value of the gas directly affect the power rating of the burner. The flow rate of a gas with a low calorific value would need to be higher than that of a gas with a high calorific value; thus requiring an injector with a larger diameter. Also, since a greater flow rate is required for a rapid burner compared to a semi-rapid burner, a larger injector nozzle is required for a rapid burner.

Liquefied petroleum gas (LPG) is used in South Africa and natural gas is more widely used throughout the world, thus hobs that are imported into South Africa typically arrive ready to be used with natural gas (Whirlpool, 2011). The injectors with smaller diameters, which are needed for use with LPG, are supplied additionally. The natural gas injectors are then

replaced with LPG injectors during the installation of the hob. The injector is a small part, which is easy to change with a socket spanner. Injectors, to be used with biogas, will need to be bigger than natural gas injectors.

In addition to the injector size, another important design feature is the allowance for pre-combustion air-intake and mixing. Air intake ports may not be present, be a fixed size, or be adjustable (Khandelwal & Gupta, 2009). According to Perry et al. (1997), burners that are designed for partial premixing with air, make use of an inspirator system. The biogas flows through an orifice, which creates a pressure difference and draws in air through the air-intake ports. These gases are mixed in the mixing tube, resulting in a fuel-rich mixture. The gas to air mixture ratio is determined by the ratio of the diameter of the orifice and the mixing tube. Secondary combustion air is supplied at the flame.

Oxygen is required for methane to burn; the stoichiometry of the reaction dictates the ratio of air to biogas necessary for combustion. The following is a balanced reaction for the complete combustion of biogas and air, with the biogas containing 60% methane and 40% CO₂, and the air containing 79% nitrogen and 21% oxygen (Khandelwal & Gupta, 2009).



Thus the requirement for complete combustion is a ratio of one volume of biogas to 5.7 volumes of air, or 15% biogas in air (Khandelwal & Gupta, 2009). If the same exercise is carried out for natural gas (assuming 85% methane and no other hydrocarbons), the ratio is about one volume of natural gas to 8 volumes of air, or 11% natural gas in air.

It is good practise to ensure a small excess of air is present for complete combustion, and to prevent the flame from becoming too rich. This may be accomplished by pre-mixing the biogas with some of the required air before it is burnt. If no air-intake is included in the hob design, the biogas will still burn due to the oxygen present in the surrounding air, but the flame will be yellow, less compact; will not burn as hot; and carbon monoxide and soot will be formed. On the other hand, if too much air is present, the flame will be cooler and the cooking time will be extended. The air intake thus needs to be adjusted on the hob in order to find the optimal air to biogas ratio, and to produce a blue flame. Biogas will only burn in the range of 9 to 17% in air when the biogas composition is 60% CH₄ 40% CO₂. (Khandelwal & Gupta, 2009)

There are a number of other factors which need to be taken into consideration when designing a hob, such as the volume of the burner manifold to permit adequate mixing of the air and biogas; size, shape and number of burner holes which stabilize the flame; and the size and shape of the burner (Khandelwal & Gupta, 2009). These are all aspects of the design which cannot be altered, and will not be discussed further. The most important aspects of hob which can be altered fairly easily to possibly accommodate the use of biogas in a standard hob are the injector size and, only for some designs, the air intake.

2.3. Biogas Upgrading

2.3.1. Introduction

As the price of oil and natural gas increases and renewable energy targets are set, the production of biogas, and thus also the number of upgrading plants, is increasing. For certain applications, such as vehicle fuel and for injection into the gas grid, biogas needs to be upgraded. Biogas upgrading is being carried out on a fairly large scale, with almost 100 upgrading plants reported to be in operation in 2009 in Europe, Japan, Canada and the USA (Pettersson & Wellinger, 2009). There has been a great increase in the number of plants over the last 20 years, as illustrated in Figure 7.

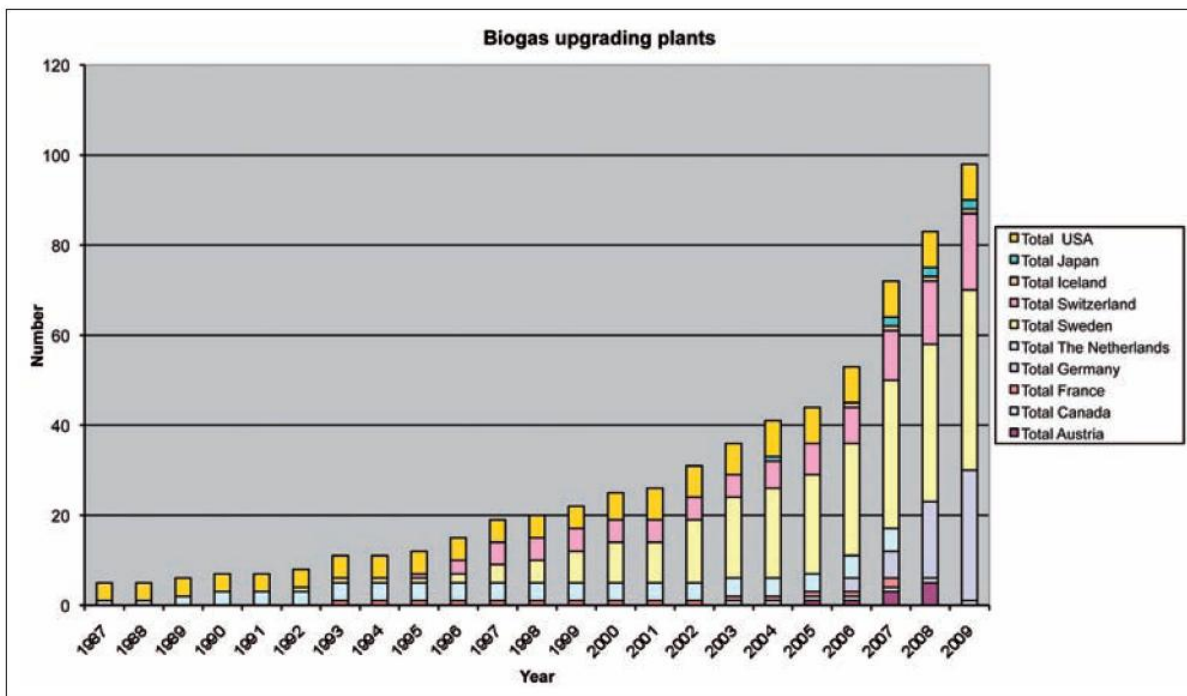


Figure 7 Total number of biogas upgrading plants from 1987 to 2009 (Pettersson & Wellinger, 2009)

Biogas upgrading consists of removing corrosive H_2S , which will damage equipment, as well as carbon dioxide, which dilutes the methane, lowering the calorific value of biogas. Since upgrading increases the cost of biogas significantly, much research has been carried out to optimize the various upgrading processes. It is important for the process to be energy efficient as well as minimising the emission of methane, as its greenhouse gas effect is 25 times that of carbon dioxide (IPCC, 2007). The requirements for upgraded biogas vary for

different countries and for various applications. The focus of this dissertation is on CO₂ removal, since the calorific value is the primary concern.

Figure 8 illustrates the impact of the plant scale on the total costs to upgrade biogas. Persson (2003) reports that this information was taken from various sources, including plants, suppliers, and literature. The currency, SEK, is the Swedish krona. Costs are 2003 values, and value added tax (VAT) is not included. The total costs include capital, operating, repair and maintenance costs. They are significantly higher for smaller plants, which is not favourable for household scale biogas upgrading.

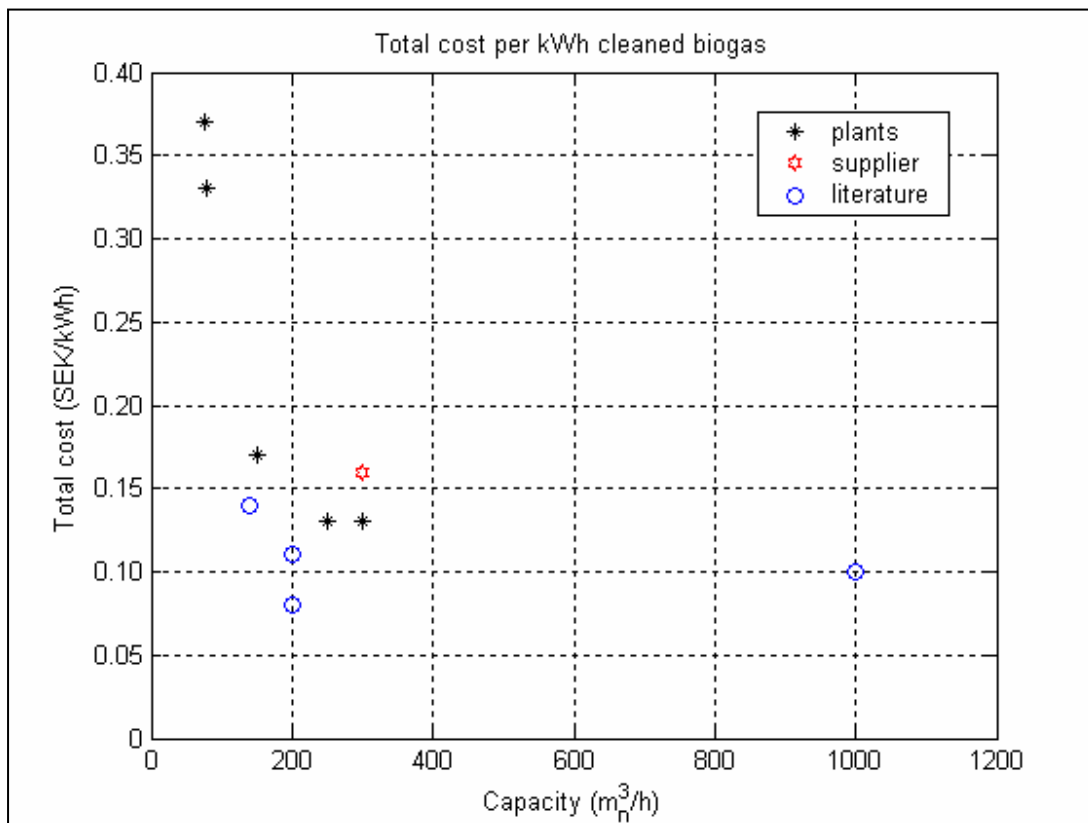


Figure 8 Costs to upgrade biogas (Persson, 2003)

There are a number of techniques that can be used to upgrade biogas, each with their own advantages and disadvantages, and level of maturity. Table 2 provides a list of the five main upgrading technologies, as well as the cost, yield and purity achievable for each on an industrial scale. In general the required purity may be different to what is presented in Table 2, which will influence the price. The price will also depend on the plant scale and local costs, including the cost of equipment, labour, and consumables (such as solvents and energy). The table should thus be used for comparative purposes only.

Table 2 Comparison of various upgrading technologies (de Hullu et al., 2008)

Technique	Cost of CO ₂ removal*	Total cost for CO ₂ and H ₂ S removal	Overall yield	Overall purity
	€/Nm ³ biogas	€/Nm ³ biogas	%	%
High pressure water scrubbing		0.15	94	98
Chemical absorption†	0.17	0.28	90	98
Pressure swing adsorption		0.26	91	98
Membrane separation	0.12	0.22	78	89
Cryogenic separation		0.40	98	91

* For processes where the cost for the removal of CO₂ and H₂S has been calculated separately

† Based on an amine solvent

2.3.2. Physical Absorption

Absorption involves contacting two immiscible phases, gas and liquid, in order to achieve the transfer of one or multiple substances from one phase to the other; in this case the substance is CO₂. The mass transfer between the phases is due to diffusion, which occurs across the gas-liquid interface. The process typically takes place in a counter-current absorption column, packed with a special material to create a high surface area for better gas-liquid contacting. There are two types, physical and chemical absorption, which are both favourable for biogas upgrading since they can handle low biogas flow rates, are cost effective, and are the least complicated (Kapdi et al., 2004).

High pressure water scrubbing is an example of physical absorption. It is the most common commercially available upgrading technique (Pettersson & Wellinger, 2009), and is also the cheapest and provides a high purity and yield (de Hullu et al., 2008). The removal of both CO₂ and H₂S are possible. Carbon dioxide is not very soluble in water at atmospheric pressure, but since solubility increases with pressure, the absorption is carried out at an elevated pressure where the solubility is higher. The biogas and water thus requires compressing prior to absorption. Once the water has passed through the absorption column, it can be regenerated in a packed desorption column, where it counter-currently contacted with air and then cooled (Pettersson & Wellinger, 2009). The recirculation of water containing dissolved H₂S is, however, not recommended as it is not removed during the regeneration stage (Wheeler et al., 2000).

Kapdi et al. (2006) designed a high pressure water scrubber to reduce CO₂ in biogas from 40 to 5 %. Pressurised water and biogas (1 MPa) were contacted counter-currently in a scrubber that was 150 mm in diameter, 4.5 m high, and packed to a height of 3.5 m. The scrubber was designed to process 120 m³ of raw biogas per day, operating for 8 hours per day. The water usage was not specified. The study investigated the financial feasibility of

this process, including the compression and bottling of the scrubbed biogas. It was found to be profitable if the gas was sold for use as a vehicle fuel in India.

An organic solvent, such as polyethylene glycol, is another physical solvent which may be used for the absorption of carbon dioxide. Polyethylene glycol is a better solvent than water for the absorption of carbon dioxide, thus requiring a smaller plant and less solvent for the same separation. The saturated solvent can be regenerated with air or by heating and/or depressurizing; although if dissolved H₂S is present, the solvent should be stripped with steam or an inert gas. Various organic solvents are available commercially, including Selexol® and Genosorb® (Petersson & Wellinger, 2009; Wheeler et al., 2000).

2.3.3. Chemical Absorption

Chemical absorption is different to physical absorption as the solute reacts chemically with the solvent and can thus be carried out at atmospheric pressure. There are many types of chemical solvents available that are suitable for the removal of CO₂. The most common are: aqueous solutions of amines, including monoethanolamine (MEA) and diethanolamine (DEA); and aqueous alkaline salt solutions, including potassium carbonate (K₂CO₃) (Green & Perry, 2008). The spent solvent can be regenerated by heating, but since chemical bonds need to be broken, more energy is typically required compared to a physical solvent (Kapdi et al., 2004). Chemical absorption can also produce a high purity product, with a high yield of methane (de Hullu et al., 2008). The cost of this technology will vary according to the type of solvent used.

Tippayawong and Thanompongchart (2010) investigated the absorption of CO₂ and H₂S from biogas in a packed column using three different solvents, including aqueous solutions of sodium hydroxide (NaOH), calcium hydroxide (Ca(OH)₂) and MEA. The column was 70 mm in diameter, 1 m high, and packed to a height of 700 mm with 42 mm plastic bioballs. The system pressure was slightly higher than atmospheric pressure. The composition of the gas immediately after the start up is presented in Table 3; a high purity product was initially produced. Since the solvent was recycled without regeneration, the efficiency decreased until the solvents were saturated. The gas and solvent flow rates were not provided in this paper; these are important variables without which, comparisons with other systems are impossible. The regeneration of the solvents and the costs of such systems were not investigated.

Table 3 Composition of biogas immediately after the treatment with different solvents (Tippayawong & Thanompongchart, 2010)

Component	Unit	Inlet	NaOH	Ca(OH) ₂	MEA
CH ₄	%	53.1	95.5	95	98
CO ₂	%	46.8	3.2	4	1.3
H ₂ S	ppm	2150	0	0	0

2.3.4. Adsorption

Adsorption involves the contacting of a gas and a solid, enabling the transfer of a component in the gas to the solid. The component is either attracted by weak van der Waals forces and moves into the cavities of molecular sieves, such as zeolites and activated carbon (Kapdi et al., 2004; Wheeler et al., 2000); or it reacts chemically with an adsorptive material, such as sodium hydroxide (Eze, 2010).

Pressure swing adsorption is the term for an industrial process, which makes use of adsorption and pressure for the purification of gases. According to Table 2, pressure swing adsorption is relatively expensive, but can produce a high purity gas with low methane losses. Carbon dioxide is removed by its adsorption onto a solid molecular sieve under pressure in a column. The adsorptive material is regenerated when the column is depressurized; this is carried out in stages. The adsorption of H₂S is irreversible, and moisture can destroy the adsorptive material, both should thus be removed before entering the adsorption column. (Petersson & Wellinger, 2009)

Eze (2010) carried out a study that demonstrated the upgrading of biogas on a household scale. H₂S was removed through adsorption with iron filings, and CO₂ was removed through adsorption with solid sodium hydroxide. The flow rate of biogas, quantities of iron filings and sodium hydroxide, and the time taken for the adsorptive material to reach saturation was not provided. The adsorptive material would need to be replaced periodically as it became saturated. The experiment was shown to reduce the H₂S in the biogas from 1.2 to 0.4 %, and the CO₂ from 26 to 12 %, although decrease in adsorption due to saturation over time was not investigated. The methane composition increased from 62 to 74 %. The time taken to boil 500 ml of water was improved from 6.44 (raw biogas) to 5.13 (upgraded biogas) minutes. The cost of this process was not investigated.

2.3.5. Membrane Separation

Membrane separation is essentially the filtration of gas through a membrane which is permeable to certain compounds, such as carbon dioxide, while it retains other compounds,

such as methane, under high pressures. Different membranes offer different efficiencies, for example an acetate-cellulose polymer offers a 20 and 60 times higher permeability to CO₂ and H₂S, respectively, compared to CH₄, under pressures of 25 to 40 bar (Kapdi et al., 2004). The required pressure depends on the type of membrane. Referring to Table 2, the process is relatively inexpensive, even when the necessary, additional H₂S removal is considered; however, this technology produces the lowest yield and purity. It is mainly used for the upgrading of landfill gas (Petersson & Wellinger, 2009).

2.3.6. Cryogenic Separation

Cryogenic separation is based on the liquefaction of CO₂ by the staged cooling and compressing the biogas. Various end conditions have been reported: -90°C and 40 bar was reported by de Hullu et al. (2008), while -45°C and 80 bar was reported by Kapdi et al. (2004). This technology has the advantage of producing a high purity product in the liquid state, which is compact and easy to transport. It is, however, the most expensive of all the technologies that have been discussed, as well as being least mature (Petersson & Wellinger, 2009).

2.4. Concluding Notes on the Literature Review

The purpose of the literature review was to provide information on biogas and biogas digesters, and compare biogas and standard gas hobs. Amongst the various design features of a hob, two features that can be altered fairly easily in order for a standard hob to run on biogas were found to be the injector size and the air intake.

In addition, a review of various upgrading techniques was carried out. High pressure water scrubbing was found to be the least expensive technology, although the final costs depend on the system size and configuration. The scale of the upgrading system has a significant effect on the costs, with small scale systems corresponding to the highest costs. The various technologies will be compared and assessed in terms of suitability for use on a household scale in chapter 3.

3. Approach and Methods

This chapter presents the hypotheses of this dissertation, as well as the approach and methods used in order to test the hypotheses, including the experimental work and the absorber design.

3.1. Hypotheses

In relation to the objectives of this dissertation, stated in Chapter 1, and informed by the literature review in Chapter 2, the following two hypotheses are proposed for testing:

- 1 *Unless the size of its inlet nozzle can be enlarged and its ratio of air intake to fuel gas flow suitably adjusted, it will not be possible to operate a standard gas hob on a gas that has the same composition as biogas.*

- 2 *The desire for a simple and robust device to upgrade biogas on a household scale will be matched with significantly higher costs compared to equivalent devices on an industrial scale.*

These hypotheses are the basis for the experimental work and the absorber design, respectively.

3.2. Experimental Work

The purpose of the experimental work was to investigate the performance of a standard gas hob with varying operating conditions and thus to generate data to support the first hypothesis. The operating conditions that were chosen aimed to represent the range of conditions that could be expected if the hob was operated on biogas, or varying levels of upgraded biogas.

3.2.1. Equipment

Figure 9 provides a diagram of the experimental setup, with Table 4 providing the description of each item in the diagram. Photographs of the experimental apparatus may be found in Appendix A.

The gas cylinders and regulators, indicated as section A in Figure 9, were located in an area allocated for gas cylinders, approximately 4 metres from sections B and C. Sections B and C were located in a fume hood with gas extraction. A fume hood was required since methane is a flammable gas; the methane Material Safety Data Sheet (MSDS) is provided in Appendix A. Section B was fixed to a wooden stand, with section C located next to it. Section C consisted of the gas hob and a line, which connected the hob to section B. The line was approximately 1 metre long.

Both the methane and CO₂ cylinders were at high pressures; for example, the full methane cylinder was initially at 200 bar. Since the pressure required for the experiments was only slightly higher than atmospheric, two-stage pressure regulation was required to lower the pressure sufficiently.

Ball valves 1 and 2 provided means to allow or stop the flow of each gas from the cylinders to the rest of the rig; while needle valves 1 and 2 could be used to control the flow rate of each gas. The non-return valves were installed in order to try to prevent the flow of one of the gases back along the line of the other gas, thus inhibiting the flow of the other gas. This would happen if the supply pressures of each gas were not exactly equal.

Since biogas contains water vapour, some of the experiments were carried out with 'wet' gas. Water vapour was added to the gas mixture by bubbling the gas through water. The wetting apparatus consisted of a cylinder filled with water approximately half way, at a temperature of 20°C. The gas line was extended into the cylinder, below the water level. The gas would then bubble through the water and exit through the gas line at the top of the cylinder. Although the water absorbs some methane and carbon dioxide, the volume of water was small and the solubilities were fairly low under the experimental conditions (the mole fractions for carbon dioxide and methane dissolved in water, at 20°C and with a solute

partial pressure of 1 atm, are approximately 7.06×10^{-4} and 2.81×10^{-5} respectively (Poling et al., 2008)). It was thus assumed that the water was saturated with carbon dioxide and methane during the runs.

The final pressure gauge before the hob was used to measure the operating pressure of the stove. This pressure was lower than the closed system pressure, and thus required a pressure gauge which indicated a low pressure range (0 – 16 kPa). It was necessary to install a valve, which could isolate the gauge, so that the gauge was not over-pressurized.

Table 4 Equipment Specification

Label	Name	Description
C-1	Methane cylinder	50 litre cylinder
C-2	CO ₂ cylinder	50 litre cylinder
C-3	Wetter	150 ml cylinder for gas-water contacting
R-1,3	Pressure regulators	First-stage pressure regulation, 700 kPa max outlet
R-2,4	Pressure regulators	Second-stage pressure regulation, 200 kPa max outlet
PG-1,4	Pressure gauges	Indicate pressure in the range of 0 - 25 MPa
PG-2,5	Pressure gauges	Indicate pressure in the range of 0 - 1 600 kPa
PG-3,6	Pressure gauges	Indicate pressure in the range of 0 - 100 kPa
PG-7	Pressure gauge	Indicates pressure in the range of 0 - 16 kPa
BV-1,2,3	Ball valves	Open or close to allow or stop flow
BV-4	3-way plug valve	Allows flow in one of two directions
NV-1,2	Needle valves	Control of flow rate
FM-1	Rotameter	Indicates methane flow rate (7 ml diameter, 0 - 30 cm)
FM-2	Rotameter	Indicates CO ₂ flow rate (0 - 5 litres/min air)
NRV-1,2	Non-return valves	Prevents flow back along the line
S-1	Gas hob	Gas burner
P-1	Inlet point	Inlet for injecting water into C-3
P-2	Sample point	Gas sampling point

A Whirlpool, two-plate gas hob was used; Table 5 provides the details supplied with the hob and a diagram of the gas hob is given in Figure 10. The hob had both a rapid and semi-rapid burner, which will also be referred to as a big and small burner respectively, in this dissertation. The type of burner refers to the burner size, which in turn indicates the pot size which should be used on the burner. The Whirlpool hob manual specifies that a 16 to 22 cm diameter pot should be used on the semi-rapid burner, while a 24 to 26 cm diameter pot should be used on the rapid burner (Whirlpool Corporation, n.d.). A 16 cm diameter pot was used in the experiments.

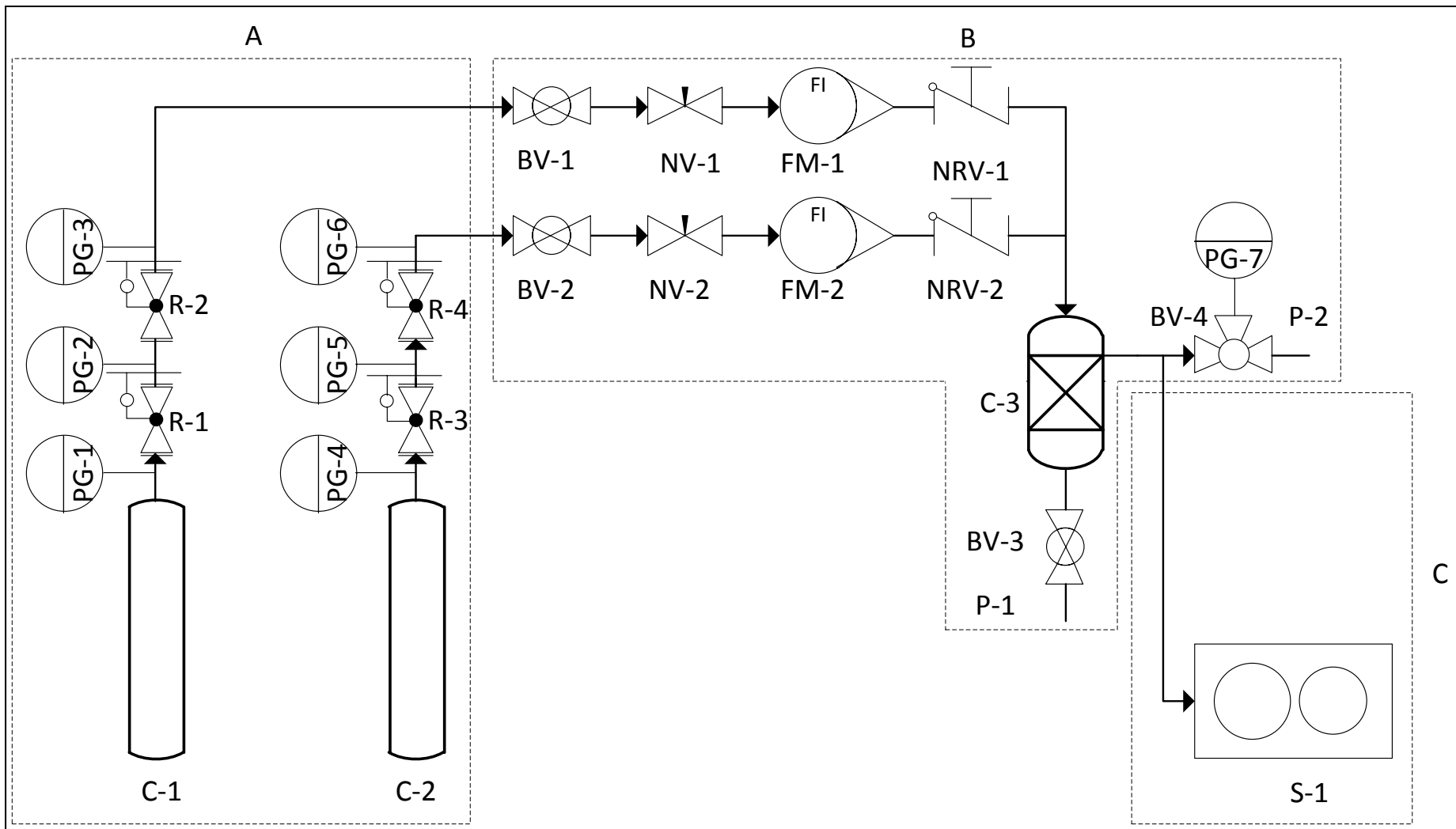


Figure 9 Experimental setup

Table 5 Whirlpool gas hob injector table (Whirlpool Corporation, n.d.)

Gas	Type of burner	Injector diameter (mm)	Rated thermal flow rate [kW]	Rated consumption		Reduced heat capacity [kW]	Gas pressure [mbar]		
							min.	rat.	max.
Natural Gas	rapid	1.28	3	286	l/h	0.6	17	20	25
	semi-rapid	0.95	1.65	157	l/h	0.35			
LPG	rapid	0.87	3	218	g/h	0.6	25	30	35
	semi-rapid	0.67	1.65	120	g/h	0.35			

With reference to Table 5: a range of injectors were supplied with the hob, with each size indicated for a specific type of gas and burner size. The natural gas injectors are larger than the LPG injectors. The rated thermal flow rate refers to the potential power of the gas stream, while the reduced heat capacity refers to the energy that is transferred to the pot. This indicates that the expected efficiency of the hob is 20%. The gas pressure is the recommended operating pressure range of the hob.

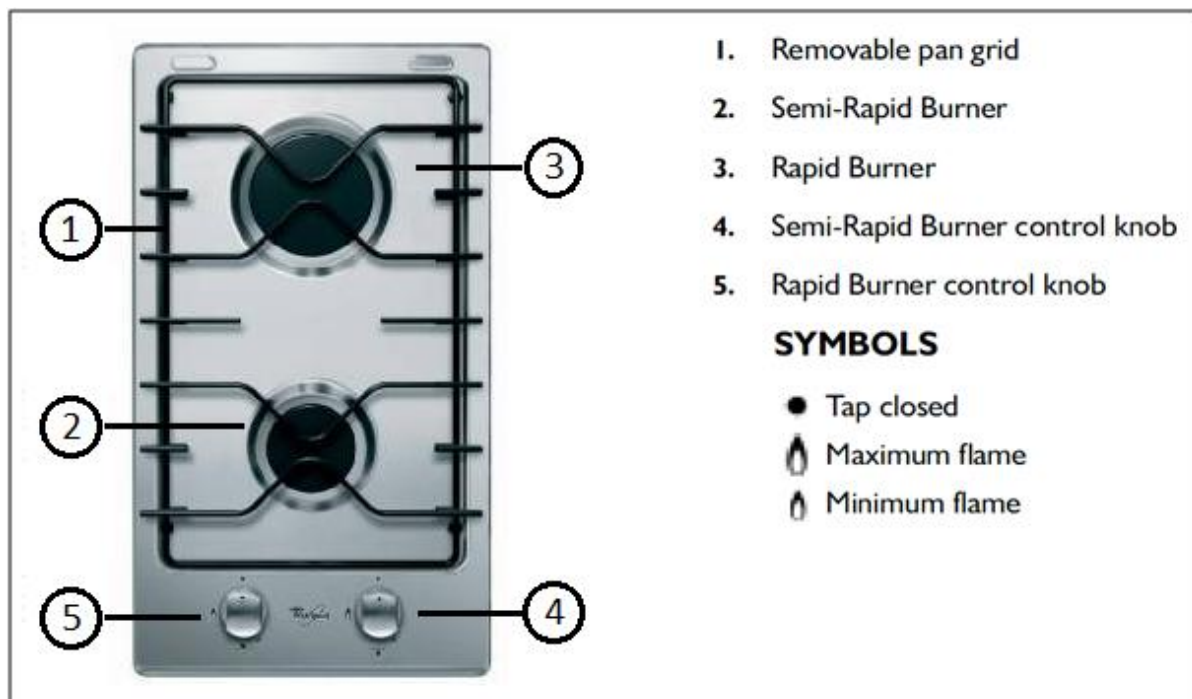


Figure 10 Whirlpool gas hob (AKT 30I IX) (Whirlpool Corporation, n.d.)

3.2.2. Method of Analysis

The details of how each variable was measured and processed are listed in this section, with sample calculations provided in Appendix C.

Measured Variables

The variables that were recorded during each run, as well as the measuring devices, are listed in Table 6. The burner and injector size were also noted. For the cut-off composition tests, only supply pressure, flow rates and burner size were recorded. The set of raw data may be found Appendix B.

Table 6 Measured variables

Variable	Unit	Measuring device
Water to be heated	1 litre	Large beaker
Start and end temperatures	°C	Standard glass/ethanol thermometer
Time taken to heat the water	s	Stop watch
Methane flow rate	cm	Rotameter
CO ₂ flow rate	L/min	Rotameter
Supply and operating pressure	kPa	Pressure gauge

Gas Composition

A gas sample was taken for each test at the gas sampling point shown in Figure 9. Since there was pressure in the line, a complicated sampling method, such as the Ampule Method, was not necessary. Inflatable containers made of different materials were tested overnight to see how well they held pressure. Blue latex laboratory gloves held pressure the best, and were thus used for the gas sampling. In order to avoid the composition of the gas samples changing due to the permeation of different gases into and out of the glove, the gas analyses were all performed on the day that the samples were collected. Additionally, each glove was filled with the sample gas and emptied before the final sample was taken so that there was no sample contamination. A syringe was used to transfer the gas sample from the glove to an SGE Gas Chromatograph (GC), the details of which may be found in Table 17 in Appendix A. Each sample was analysed in duplicate.

The gas compositions needed to be calculated from the GC results, which are provided in the form of an area under a chromatograph. The ratio of the composition of a reference gas and its area was then be used to calculate the methane content of the gas sample. Since

two analyses were made for each sample, these were averaged and the standard deviation could be calculated.

Flow Rate

The rotameter measurements, which were taken for methane, needed to be processed further, as the rotameter was calibrated for air at standard temperature and pressure. The rotameter was marked in centimetres. A calibration chart (Figure 42, found in Appendix C) was provided with the rotameter, which could be used to read-off the flow rate, corresponding to the reading in centimetres, in litres per minute air. A correction factor was then used to account for the gas being methane instead of air. A further correction for pressure was also required. Since the pressure range was close to atmospheric, it was assumed that the ideal gas law applied.

In order to make the calculations easier the information from the calibration chart was transferred to an Excel spreadsheet. Based on this data, a table of methane flow rates was then calculated for a range of operating pressures. A chart was then created for each operating pressure, with the rotameter reading on the x-axis and the methane flow rate (in L/min) on the y-axis. A trend line was fitted to each set of data, and the resulting polynomial equation recorded. This equation could then be used to calculate the methane flow rate for each test.

The rotameter used to measure the flow rate of carbon dioxide was the smallest size available, but was slightly too big for the flow rates that were required for the experiments. Thus the carbon dioxide flow rate was calculated based on the methane flow rate and the composition of the gas. This value, however, was not very important.

The Water Heating Rate

The water heating power is essentially a measure of how long it took to heat water. The thermal energy transferred to the water in the pot was calculated by integrating the specific heat capacity of water (in the form of a fourth degree polynomial, dependent on temperature), and solving the resulting equation using the starting and final temperatures. The specific heat capacity data was sourced from Perry et al. (1997). The following equation was used in the calculations:

$$H = \int_{T_1}^{T_2} 2.7637 \times 10^5 - 2.0901 \times 10^3 T + 8.1250 T^2 - 1.4116 \times 10^{-2} T^3 + 9.3701 \times 10^{-6} T^4$$

Where: H is the heat that was transferred to the water
 T is the temperature [K]

The power relating to rate at which the heat was added to the water was then calculated by dividing the energy by the time taken to heat the water.

Flame Power

The flame power refers to the potential heat that could be released upon the combustion of a certain amount of methane. It was calculated by multiplying the methane flow rate with the calorific value of methane, and does not account for incomplete combustion or other inefficiencies.

Efficiency

The hob efficiency refers to the ratio of the water heating power and flame power, and represents the difference between the heat power which is potentially available and the actual heat which is transferred to the water. Factors which decrease the efficiency of a hob include: convective heat losses; conductive heat losses; incomplete combustion of methane; heating of inert gases; the use of a pot which is too small for the burner; not using a pot lid; and using a pot with an uneven bottom. Convective heat losses were fairly large during these experiments, as the hob was located in the fume hood, which caused a draught.

3.2.3. Experimental Approach

With all the parameters of the system considered, the experimental approach could be established. In order to try to reproduce conditions that would be expected in a real situation reflective of the first hypothesis, where biogas is produced near the home and used for cooking, the whole system had to be considered. The different components of the system will be discussed here, followed by the experimental procedure that was used.

Biogas

Firstly, biogas is typically composed of about 55-70% methane, with the balance being mainly CO₂ (Deublein & Steinhauser, 2008). Thus these two gases were combined in various compositions, with 55% methane being the lowest limit which was considered. Since a range of compositions needed to be tested, the gas mixtures were synthesised in a laboratory, rather than using real biogas. A limitation was that the effect of other components typically present in biogas, such as H₂S, were not considered in this work. The

effect of water vapour present in the biogas was included to a certain extent with the wetter, as described in section 3.2.1.

Supply Pressure

The second important variable in the system was the supply pressure. As was explained in section 2.1.1, the available supply pressure in the fixed dome biogas digester depends on the amount of biogas produced. The supply pressure is important for three reasons. Firstly, it is required to overcome the pressure drop along the line due to the line itself, as well as all the fittings in the line including the injector nozzle in the hob. There is thus a minimum required pressure, which is unique in each system. Secondly, the supply pressure affects the flow rate of the biogas; a higher flow rate can be achieved with a higher pressure. Lastly, the available supply pressure will decrease significantly with the use of the biogas for an extended period, as biogas production takes place at a much slower rate than burning gas in a hob. It was thus important to investigate the effect of supply pressure on the operation of the hob.

A range of supply pressures was required in order to account for the pressure variations in a real system, thus a supply pressure range needed to be determined. The supply pressure needed to be high enough to overcome the pressure drop across the system, which was relatively high due to all the fittings. The pressure drop for the dry runs, where no water was present in the wetting appliance, was lower than the wet runs. The range was thus determined by adjusting the supply pressure and checking firstly if the hob would light, and then checking and adjusting the operating pressure of the hob. The supply pressure range was chosen as 20 – 28 kPa for the dry runs and 22 – 32 kPa for the wet runs. Only some pressures in these ranges were chosen for closer assessment.

Operating Pressure

The recommended operating conditions of the gas hob also needed to be considered. Table 5 provides the various parameters for operating the hob with natural gas or LPG. The operating pressure at the stove was indicated to be 20 mbar (or 2 kPa) for natural gas. Since a gas of lower methane content compared to natural gas was used in the tests, the flow rate would need to be higher to achieve the same heating rate. It was thus expected that the operating pressure of the hob would be higher than that specified for natural gas for the same injector size. There was no indication of what the maximum possible operating pressure of the hob was.

The operating pressure of the hob could be controlled at the hob to a certain extent by adjusting the flame height knob. A range of operating pressures of 1 to 10 kPa was investigated, although the range of 1 to 3 kPa was looked at most closely.

Hob Modification

In addition to testing different gas mixtures, there was also the possibility of modifying the hob to be more suitable for a lower quality gas than for what it was designed. This was carried out in a limited way, by comparing the effect of the different injectors, which were provided with the hob. The two largest injector sizes were provided for natural gas: 0.95 and 1.28 mm.

The big burner was only tested with the larger size injector, while the small burner was tested with both. If the methane content of natural gas and biogas are considered to be 85% and 60% respectively, using ratios, the required injector size for the small burner to run on biogas could be predicted to be 1.34 mm. Although slightly smaller, it was anticipated that an injector size of 1.28 mm would be adequate for use in the smaller burner with a gas of lower quality than natural gas.

Additionally, the air-intake of the hob was set for natural gas. Although it is noted that the air-intake is an important design feature, it was decided that this feature would remain constant throughout the experiments and not explored further. It is recommended that the significance of this should be explored in future experiments.

3.2.4. Experimental Procedure

Table 7 provides an overview of the various sets of experiments that were carried out. The experiments consisted of timing how long a 16 cm diameter pot, containing one litre of water, would take to reach 50°C. All experiments were carried out for both size burners, under wet and dry conditions, with the small burner being tested with the two different size injectors.

Each set of experiments involved varying a system parameter in order to establish its effect on a calculated variable. Due to the nature of the system, when one parameter was varied, a second one also varied in order to keep the other parameters constant. For example, to determine the effect of a varying gas composition on the water heating rate, both the CH₄ and CO₂ flow rate were varied, while the operating and supply pressures remained constant.

Additionally, a set of tests were performed in order to establish cut-off compositions for a range of supply pressures. These tests essentially consisted of setting a supply pressure and varying the gas composition until the gas would no longer ignite. This information was important, as it provided a starting point from where a biogas absorber could be designed.

Table 7 Overview of experiments

Independent variable	Dependent (calculated) variable	Parameter 1	Parameter 2	Constant 1	Constant 2
Gas composition	Water heating rate	CH ₄ flow rate	CO ₂ flow rate	Supply pressure	Operating pressure
Gas composition	Water heating rate	CO ₂ flow rate	Operating pressure	CH ₄ flow rate	Supply pressure
Gas composition	Flame power	CH ₄ flow rate	CO ₂ flow rate	Supply pressure	Operating pressure
Supply pressure	Hob efficiency	Supply pressure	Total flow rate	Gas composition	Operating pressure
Operating pressure	Hob efficiency	Operating pressure	Total flow rate	Gas composition	Supply pressure
Operating pressure	Hob efficiency	Operating pressure	CO ₂ flow rate	CH ₄ flow rate	Supply pressure
Total flow rate	Hob efficiency	Operating pressure	Total flow rate	Gas composition	Supply pressure
Total flow rate	Hob efficiency	Supply pressure	Total flow rate	Gas composition	Operating pressure
Gas composition	Hob efficiency	Operating pressure	CO ₂ flow rate	CH ₄ flow rate	Supply pressure
Gas composition	Hob efficiency	CH ₄ flow rate	CO ₂ flow rate	Supply pressure	Operating pressure

3.2.5. Experimental Error

A number of steps were taken in order to account for error in the experiments. The sources of error included: the pressure gauges; rotameters; thermometer; stop watch; beaker used to measure the water; and the gas analysis. The error due to the pressure gauges, thermometer, beaker and stop watch was systematic and assumed to be minimal.

The accuracy of the methane rotameter due to the manufacturing process was given as $\pm 3.5\%$. A bias error in the rotameter reading was suspected, since at low flow rates, the float was below the zero line; although this was not corrected for, since the relative results were more important than the absolute results. All the gas samples were analysed in duplicate in the GC, thus allowing for the calculation of the standard deviation for every run.

Additionally, it was noted that the draught caused by the fume hood significantly reduced the efficiency of the hob. This was minimized by placing a shield in front of the hob.

3.3. Absorber Design

Based on the literature, it was hypothesised that the costs of a household scale biogas upgrading system would be significant compared to the possible economic advantages of using this system. In order to test this hypothesis, a household scale biogas upgrading device was designed, based on the composition of upgraded biogas that is acceptable for use in a standard gas hob, which was determined through experimental work and presented in chapter 4. The first step was to decide which technology would be the most appropriate for use on a small scale.

3.3.1. Comparison and Feasibility

For the purposes of upgrading biogas on a household scale, the feasibility of the various technologies need to be assessed in a different way compared to industrial scale upgrading. The criteria for assessment will be based on: financial feasibility, safety, environmental impact, ease of operation, and technology maturity.

Based on the costs given in Table 2, high pressure water scrubbing appears to be the least expensive option, followed by membrane separation and pressure swing adsorption. The cost of chemical and physical absorption will depend on the solvent choice. If the solvent is not regenerated, H₂S does not need to be removed beforehand and a stripper will not be required, which will be less expensive, but the cost of the solvent will be higher. Cryogenic separation is by far the most expensive, the least mature, least appropriate for use on a household scale, and can be ruled out as an option.

Since the absorber will be located in a residential setting, it was not desirable to choose a technology which required a high operating pressure and/or extreme operating temperatures. Thus high pressure water scrubbing, pressure swing absorption and membrane separation are not attractive.

The technology with the most potential for a high environmental impact is absorption, both chemical and physical. This will depend purely on the choice of solvent; if a solvent with a low environmental impact is chosen, the environmental impact will not be high. The other technologies will produce mainly water and gas-based waste streams, containing various levels of H₂S and methane. The environmental impacts of methane release are considered to be related to its global warming potential, and as such the recovery of methane in the upgraded biogas is a direct indicator of environmental impact.

By industrial standards, membrane separation, high pressure water scrubbing, and chemical absorption are the simplest to operate. Pressure swing adsorption is fairly difficult to operate as the adsorptive material needs to be regenerated in stages and it requires that

H₂S and water are removed before CO₂ removal. On a household level, it is the opinion of the author that low pressure absorption is the easiest to operate and maintain, since it is the only technology which does not require extreme and risky operating conditions.

Additionally, the low methane yield of membrane separation is not desirable considering the low amounts of methane produced in a household scale digester. The gas waste stream will also contain significantly more methane than the other technologies, which is not desirable in terms of the potent greenhouse gas effect of methane.

It may be concluded that absorption is the most promising technology for a household scale biogas upgrading system. Additionally, since a low pressure system is preferable, high pressure water scrubbing will not be considered. The choice of solvent and design of the absorber will be discussed further in section 5.

3.3.2. Design Basis

Before the absorber could be designed, the best system configuration needed to be determined. Since biogas is used for household applications such as cooking or lighting, the gas is usually only used for a few hours per day and not continuously. There are a number of possible system configurations that may be employed to upgrade the biogas. Different system configurations will influence the size of the scrubber, and thus the cost; three configurations were possible:

1. An inline absorber, which could upgrade the biogas as it is being used.
2. The other two options involved upgrading the gas continuously and either compressing it and storing it in an external gas canister, or
3. storing without compressing it.

The first option was considered to be the most practical and was thus used for the design of the absorber. If the absorber was found to be too large, the other options could have been reconsidered.

Since the appliance chosen for the experimental work was a gas hob, it seemed appropriate to use the required gas flow rate of the hob as the outlet flow rate of the absorber. Additionally, the required composition of the upgraded biogas that was determined from the experimental work was used to specify the composition of the absorber outlet.

3.3.3. Design Approach

The building of a prototype and its testing was out of the scope of this dissertation, thus the absorber design and financial feasibility evaluation was carried out based on theory alone.

The design of an absorber typically follows the following steps: (Green & Perry, 2008)

1. Choose a suitable solvent
2. Collect equilibrium solubility data: absorbers are designed based on mass-transfer principles. Gas absorption is limited by the equilibrium solubility of the system; equilibrium determines the maximum achievable separation. This data is used to determine the required solvent flow rate for a desired separation. It is considered the most time consuming, but also the most important step.
3. Calculation of the gas-to-liquid ratio, utilising the equilibrium solubility data and a design diagram
4. Choose absorber type, such as a tray or packed column
5. Liquid- and gas-handling capacity of the chosen contacting device: the column diameter is designed based on the pressure drop, gas and liquid flow rates, and absorber characteristics.
6. Determine the height of the contacting zone for the required separation: the height depends on the fluid properties and the efficiency of the column.
7. Internals specifications, such as liquid re-distribution and internal support in a packed column
8. Optimum solvent circulation rate determination for the best operation of the absorber and stripper
9. Specification of the operating temperatures, including the specification of heat to be added or removed if necessary
10. Specification of the operating pressures of the absorber and stripper
11. The mechanical design of each vessel

These steps apply to the design of an industrial scale absorber, and thus might not all apply to the design of a household scale absorber. The applicability of each step to a small scale absorber will thus be discussed.

Steps 1 to 6 are all definitely applicable to the design of any absorber and are covered in the detailed design along with the appropriate theory in chapter 5. Since the absorber was

anticipated to be small, no internal supports or liquid re-distribution were expected to be necessary.

The use of a stripper could be considered, although this would add significant complexities to the system as well as increasing the costs. The use of a stripper would result in the need for a taller absorber since the concentration of CH₄ in the recycled solvent would not be zero. Additionally, H₂S removal would be required prior to the absorber since it is typically more difficult to strip from the solvent compared to CH₄ (Pettersson & Wellinger, 2009). A stripper would increase the energy requirements of the system, since the solvent is stripped through heating. A stripper would thus increase the capital cost (due to the increased cost of the absorber; the cost of the H₂S removal; and the cost of the stripper) and the running cost (due to the increased energy requirements and the consumables required for the H₂S removal). It would also complicate the operation of the system. The benefit of a stripper would be the decreased cost of the solvent, as less would be required. It was decided that a stripper should not be included in the design.

To limit the capital cost, the absorber would need as few controls as possible. The operating temperature was thus restricted to ambient conditions, with no heat removal or addition stages in the absorber; and the operating pressure was restricted to the pressure of the digester, with an important restriction that the pressure drop should be minimal.

The financial viability of the absorber is an important aspect of the design. Since the use of a stripper was excluded, the cost of the solvent might be significant. It was thus decided that the feasibility would be determined by a comparison of the operating costs (i.e. the solvent costs) to upgrade a certain amount of biogas and the cost of LPG that would be needed to produce an equivalent amount of energy.

4. Experimental Results and Discussion

As discussed in chapter 3, a number of experiments were carried out to test the operation of a standard domestic gas hob with synthesised biogas of varying methane content. This chapter presents the most important results in processed form, as discussed in section 3.2.2, and discusses the key findings. Table 8 provides a key which explains the legend used in all of the graphs.

Table 8 Key for the graph legends

Position	Variable	Unit
First	Supply pressure	kPa
Second	Burner size	s (small) / b (big)
Third	Run type	d (dry) / w (wet)
Fourth	Injector size (not shown for the big burner)	1/100 mm
Fifth	Operating pressure	kPa

4.1. Variation of Water Heating Power with Gas Composition

Figures 11 to 13 provide plots of water heating rate versus gas composition for a set of runs where the supply and operating pressure were kept constant. The results are grouped on the three different graphs according to the magnitude of water heating power; from a high to low range. Figure 14 provides the results for runs where the supply pressure and the methane flow rate were constant. An intuitive result, which can be seen in all of these figures, is that the water heating rate increases with an increase in the methane composition of the gas. The important results to be noted are how the different runs compare to each other; each graph will thus be discussed in more detail.

It must be noted that when the supply and operating pressures were kept constant and the gas composition changed, the methane flow rate also varied. Conversely, when the supply pressure and methane flow rate were kept constant, the operating pressure varied.

Figure 11 provides the results for the runs which produced the highest water heating rate. These results were generally produced from runs with a mid to high supply pressure. The highest power was produced from runs with the small burner, while only one run with the

big burner was included in the high range. The big burner provided the lowest heating rate in the high category. The heating rates for the small burner were similar for runs where the supply pressure was different and the operating pressure constant; and for runs with a constant supply pressure and different operating pressures.

Figure 12 provides the results for runs which produced medium range heating rates. This range generally included runs with mid to low supply pressures. One cannot directly compare wet and dry runs with the same supply pressure, as the addition of water into the system created a slightly larger pressure drop. The wet runs, nevertheless, show similar results compared to their dry counterparts. With a supply and operating pressure of 22 kPa and 2 kPa respectively, the highest heating rates were observed for the dry run with the 0.95 mm injector, and the wet run with the 1.28 mm injector. For the same conditions, a lower heating rate was observed for the dry run with the 1.28 mm injector, while the lowest heating rate was produced on a wet run with the 0.95 mm injector (shown in Figure 13).

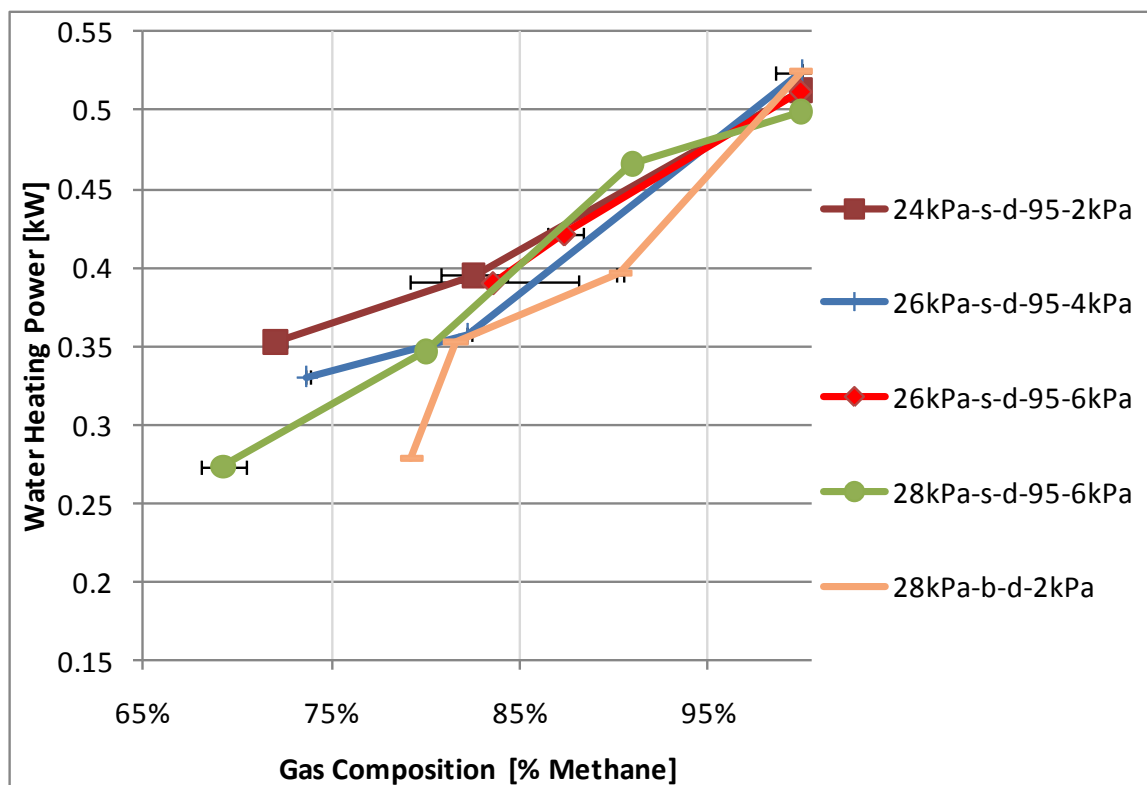


Figure 11 Water heating power versus gas composition (constant supply and operating pressure, high range)

Figure 13 provides the results for runs which produced low range heating rates. This range generally included runs with low supply pressures combined with the big burner. With a supply pressure of 22 kPa, the big burner produced the highest heating rate for the dry and

wet runs with operating pressures of 2 and 1 kPa respectively. The dry runs with operating pressures of 1 kPa and 3 kPa produced the lowest heating rates of all the runs.

On comparing all three graphs, a number of interesting trends may also be observed. With a supply pressure of 24 kPa, the small burner produced a better heating rate at an operating pressure of 2 kPa, compared to 3 kPa. This trend was not as pronounced for the big burner at 22 kPa (Figure 13) or for the small burner at 26 kPa (Figure 11). The operating pressure was controlled by adjusting the flame height at the hob. An increase in the operating pressure, along with a lower methane flow rate, resulted in a smaller flame. It would thus be intuitive that the heating rate would decrease with an increase in the operating pressure. This was not clear for all cases, suggesting a more complex explanation. Thus a definite conclusion cannot be made regarding the effect of different operating pressures on the water heating rate.

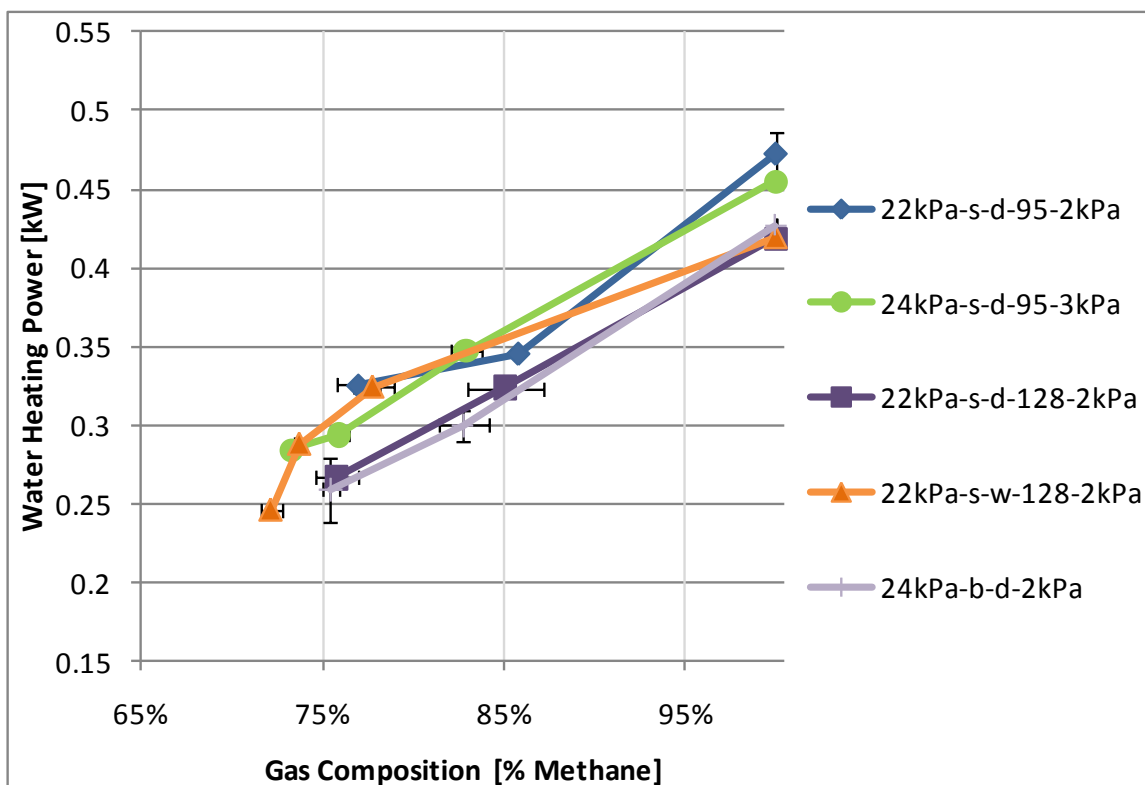


Figure 12 Water heating power versus gas composition (constant supply and operating pressure, medium range)

The small burner produced a higher heating rate at a supply pressure of 24 kPa, compared to 22 kPa, with the same operating pressure and injector size. Similarly, the big burner produced a heating rate in descending order from 28 to 22 kPa, at a constant operating pressure. In this case a clear conclusion may be made: for a constant operating pressure, the

water heating rate increased with an increase in the supply pressure. This conclusion may be directly linked to the methane flow rate, which increased with supply pressure, at a constant operating pressure. The significance of this observation is that under real conditions, the supply pressure from the biogas digester will decrease as the biogas is used. Thus the rate at which food is cooked will decrease as the biogas is used. The supply pressure is thus an important variable and measures should be taken to reduce the pressure drop on the line between the digester and the hob to achieve the highest supply pressure.

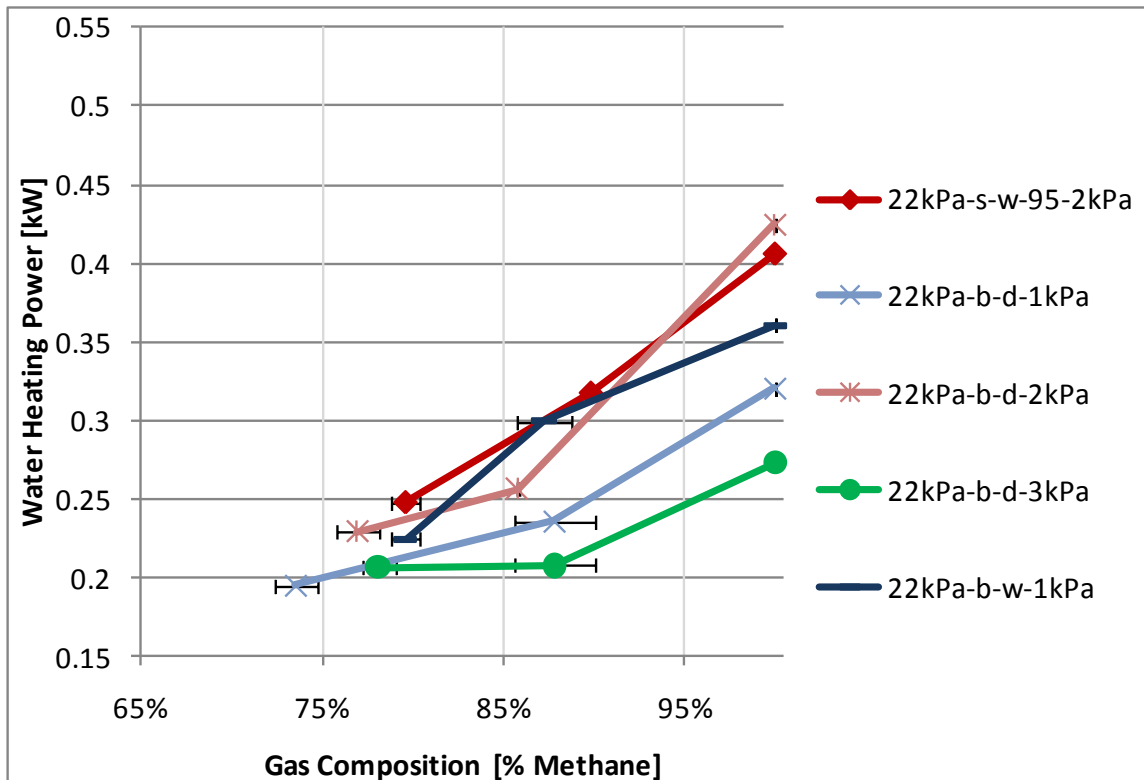


Figure 13 Water heating power versus gas composition (constant supply and operating pressure, low range)

Figure 14 provides the results for runs where the methane flow rate was kept constant, while the carbon dioxide flow rate was varied. The supply pressure was also constant for each run, but the operating pressure varied. In general, the higher heating rates were produced by the small burner, with the larger, 1.28 mm injector producing the highest heating rates. It is noted that the small burner generally produced higher heating rates than the big burner; this was primarily due to the pot size, which was too small for the big burner. The heating rates for the big burner were similar for the wet and dry runs, at the same supply pressure. For both the wet and dry runs with the small burner, the runs with the 1.28 mm injector produced higher heating rates than their 0.95 mm injector counterparts.

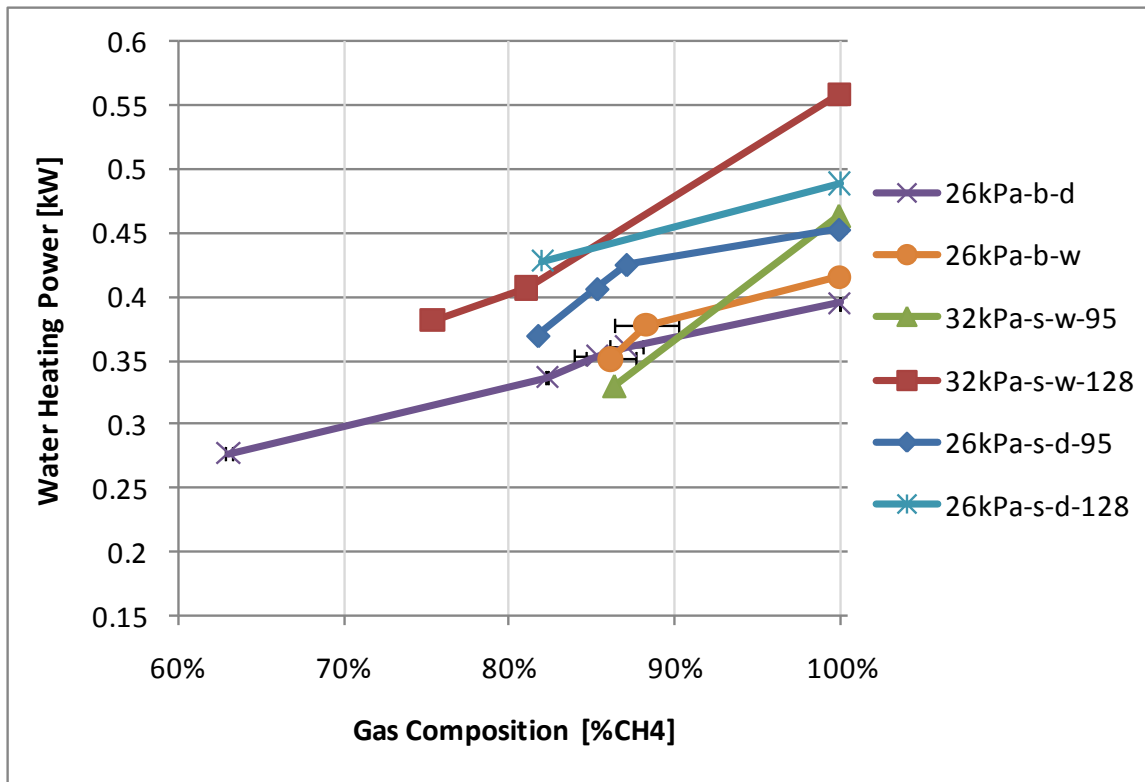


Figure 14 Water heating power versus gas composition (constant methane flow rate)

In summary, the water heating rate increased with an increase in the proportion of methane in the gas. Higher heating rates were achieved with the small burner at high supply pressures, while lower heating rates were observed with the big burner at low supply pressures, for runs where the supply and operating pressures were kept constant. The water heating rate increased with an increase in the supply pressure, for a constant operating pressure.

For a constant methane flow rate, the small burner fitted with the 1.28 mm injector produced the highest heating rate, followed by the small burner fitted with the 0.95 mm injector, with the big burner producing the lowest heating rates.

The addition of moisture to the gas mixture did not affect the results significantly, and any discrepancy between wet and dry runs may not only be due to the presence of water vapour, but perhaps also due to the sensitive nature of the system pressure dynamics.

4.2. Variation of Flame Power with Gas Composition

Figures 15 to 17 provide plots of flame power versus gas composition, with the supply and operating pressures constant for each run. The flame power refers to the potential heat available due to the combustion of methane; the magnitude of which depends on the methane flow rate. The results are also grouped and displayed on three graphs, according to magnitude of flame power.

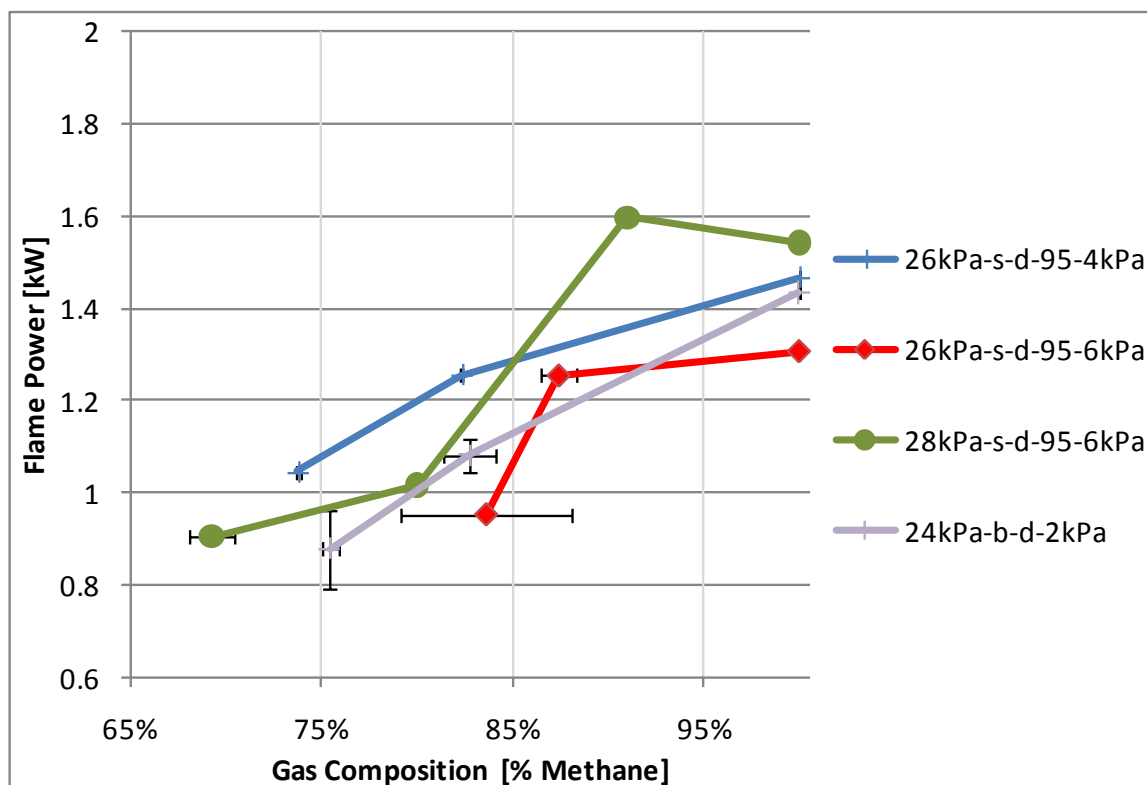


Figure 15 Flame power versus gas composition (constant supply and operating pressure, high range)

Figure 15 displays the results for the high flame power range. The results in Figure 15 were produced from runs with a mid to high supply pressure and mainly include runs with the small burner, like Figure 11. The flame power was higher for the small burner at a supply pressure of 28 kPa, compared to 26 kPa, for a constant operating pressure of 6 kPa. For a constant supply pressure of 26 kPa, the flame power was higher at a lower operating pressure of 4 kPa, compared to 6 kPa.

Figure 16 provides the results for the runs which produced the mid-range flame power. For a constant supply pressure of 24 kPa, a higher flame power was produced by the small

burner at a lower operating pressure of 2 kPa, compared to 3 kPa. The results for the big burner with a supply pressure of 22 kPa, and operating pressures of 1 and 2 kPa, were almost identical. However, the wet run for the big burner, displayed in Figure 17 (with a supply and operating pressure of 22 kPa and 1 kPa respectively), produced a lower flame power than its dry counterpart.

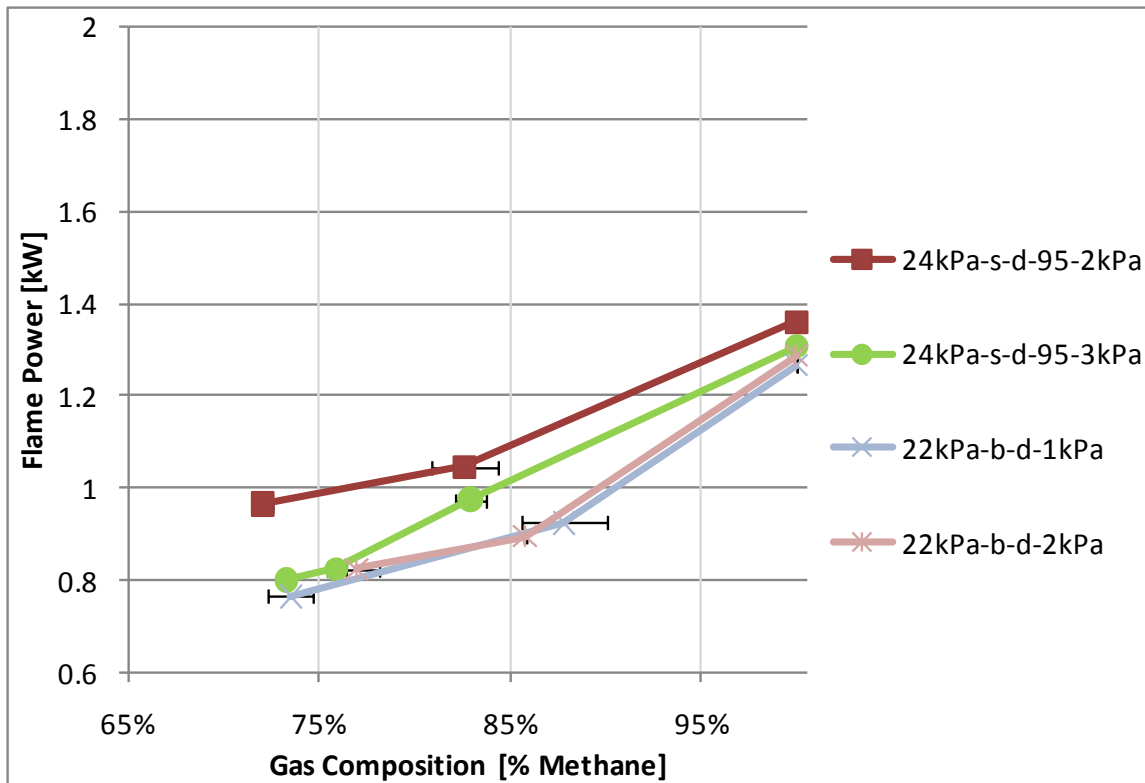


Figure 16 Flame power versus gas composition (constant supply and operating pressure, medium range)

Figure 17 provides the low flame power range, generally produced by runs at a low supply pressure. The results for the small burner, for wet and dry runs and for runs with different injector sizes, were very similar.

Two further observations may be made when all three graphs are compared. A higher flame power was produced by the big burner with a supply pressure of 24 kPa, compared to 22 kPa, for a constant operating pressure of 2 kPa. A similar result may be observed for the small burner with an operating pressure of 2 kPa and a supply pressure of 24 kPa, compared to 22 kPa.

A plot of flame power versus gas composition corresponding to Figure 14 was not included, as, since the methane flow rate was constant, the potential flame power remained constant for all gas compositions.

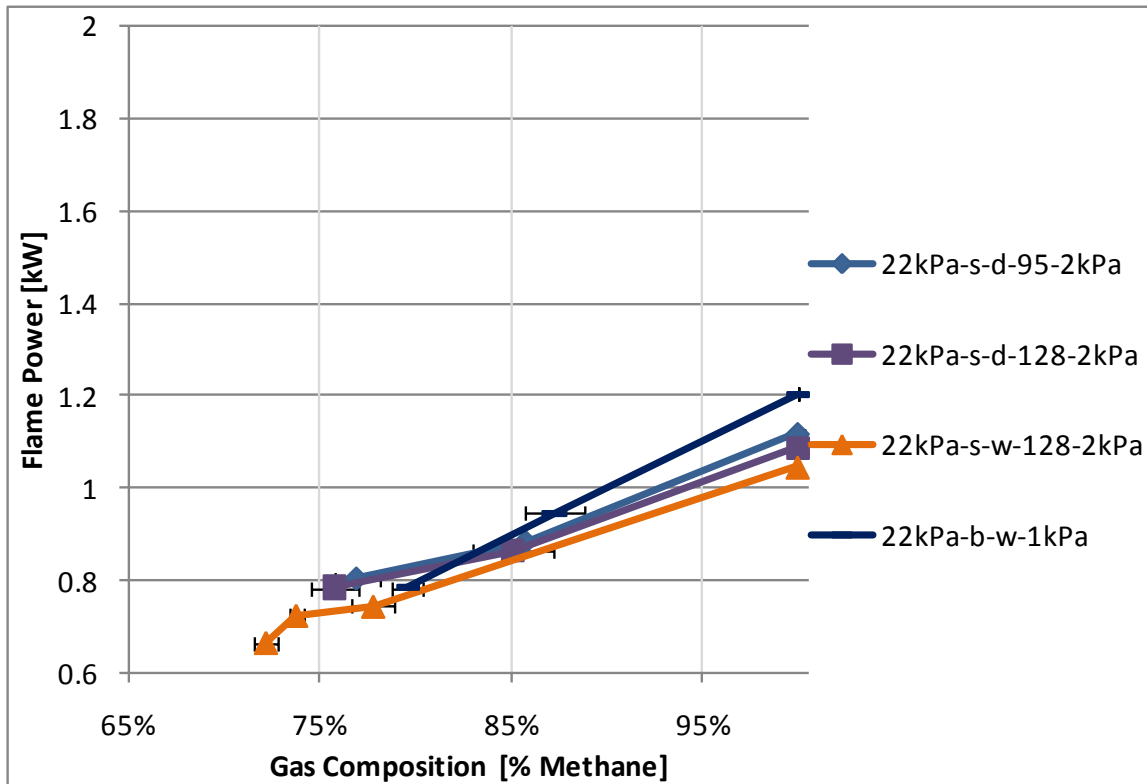


Figure 17 Flame power versus gas composition (constant supply and operating pressure, low range)

To summarize, the flame power increased with an increase in the content of methane in the gas mixture. The flame power was greatest at high supply pressures and lowest at low supply pressures. At the same supply pressure, the flame power was greater for the big burner than the small burner with the 0.95 mm injector, followed by the 1.28 mm injector. For a constant operating pressure, the flame power was greater for a higher supply pressure; and for a constant supply pressure, the flame power was greater at a lower operating pressure.

4.3. Hob Efficiency

Figure 18 displays the hob efficiency for two different runs where the gas composition and operating pressure remained constant, while the supply pressure was varied. The general trend is that as the supply pressure increased, the hob efficiency decreased. Additionally, the small burner was more efficient than the big burner.

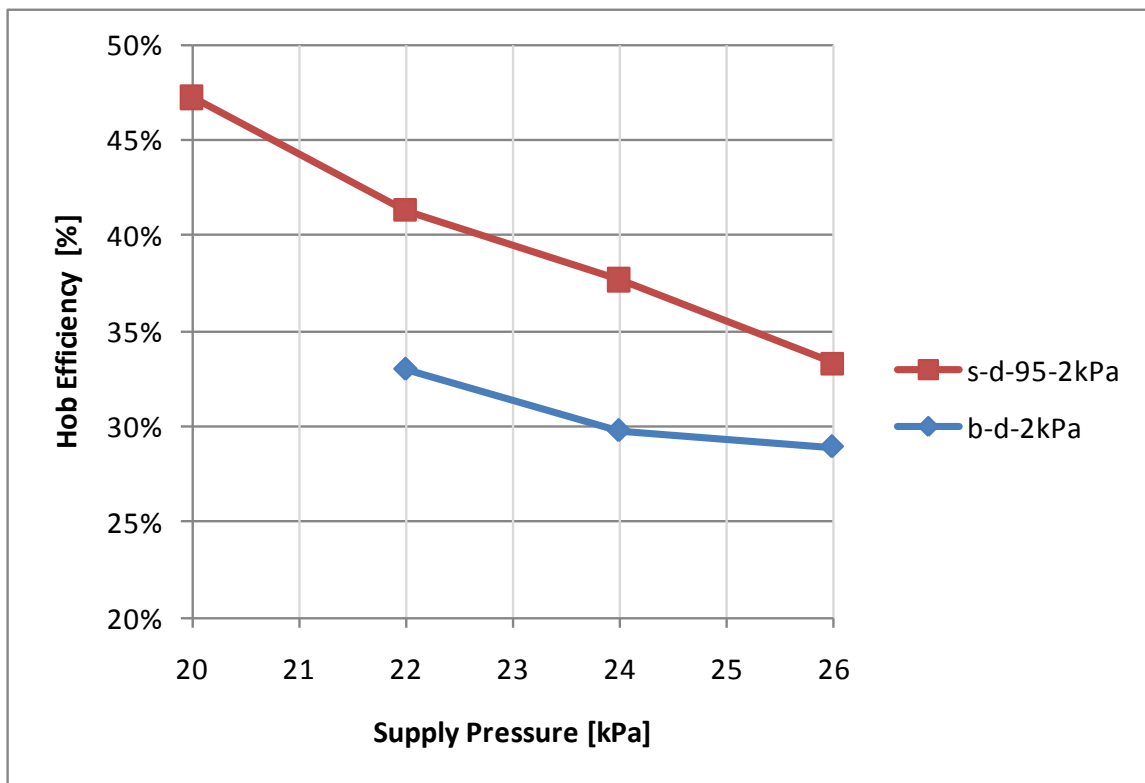


Figure 18 Supply pressure versus hob efficiency (constant gas composition of 99.95% methane and operating pressure of 2 kPa)

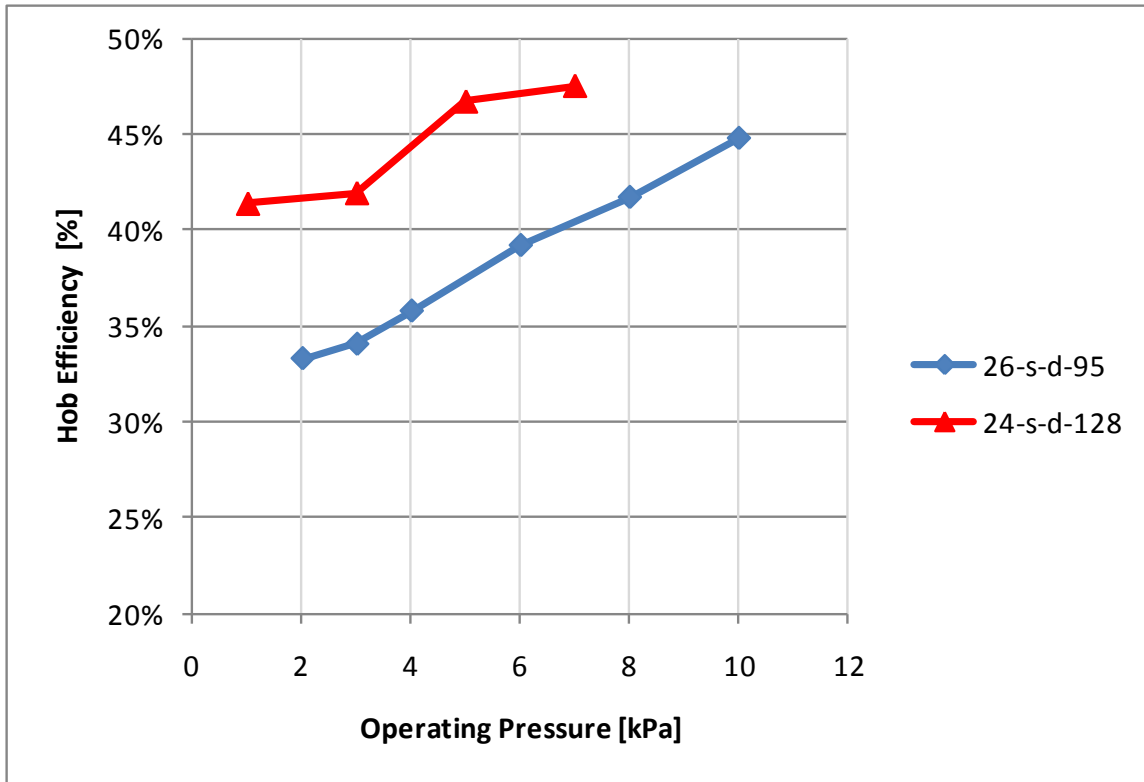


Figure 19 Operating pressure versus hob efficiency (constant gas composition of 99.95% methane and supply pressure)

Figure 19 displays the hob efficiency for runs where the gas composition and supply pressure remained constant, while the operating pressure varied. The trend shows that the hob efficiency increases with an increase in operating pressure. It may also be noted that the run with the lower supply pressure and large injector was more efficient than the run with the higher supply pressure and the small injector. This is important to note, since, under real conditions, the hob will need to operate with low supply pressures. The implications are that the injector size should be increased in order to increase the hob efficiency.

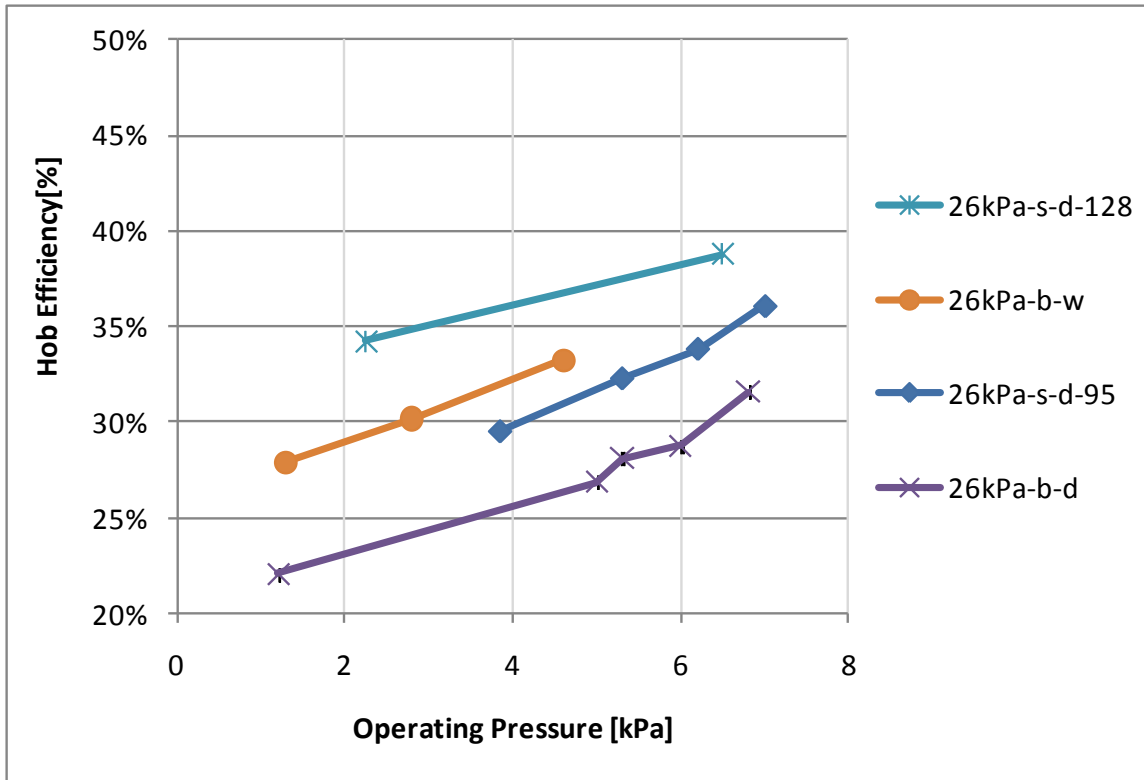


Figure 20 Operating pressure versus hob efficiency (constant methane flow rate of 1.25 kW and supply pressure)

Figure 20 also provides a plot of hob efficiency versus operating pressure for a constant supply pressure, but for a constant methane flow rate, rather than a constant gas composition. As it was seen in Figure 19, the efficiency increased with an increase in operating pressure. The small burner fitted with the 1.28 mm injector performed better than the small burner fitted with the 0.95 mm injector, followed by the big burner, for a constant supply pressure of 26 kPa. For the same supply pressure, the big burner performed better on the wet run compared to the dry run.

Figure 21 provides a plot of hob efficiency versus flow rate, at a constant gas composition and supply pressure. The general trend which may be observed is that the efficiency decreases with an increase in flow rate. As in Figure 19, the run with the lower supply pressure and the large injector proved to be more efficient than the run with the higher supply pressure and the small injector.

Figure 22 displays the same graph as Figure 21, but with results for runs with a constant operating pressure. The efficiency of the hob decreased with an increase in flow rate. The small burner was more efficient than the big burner.

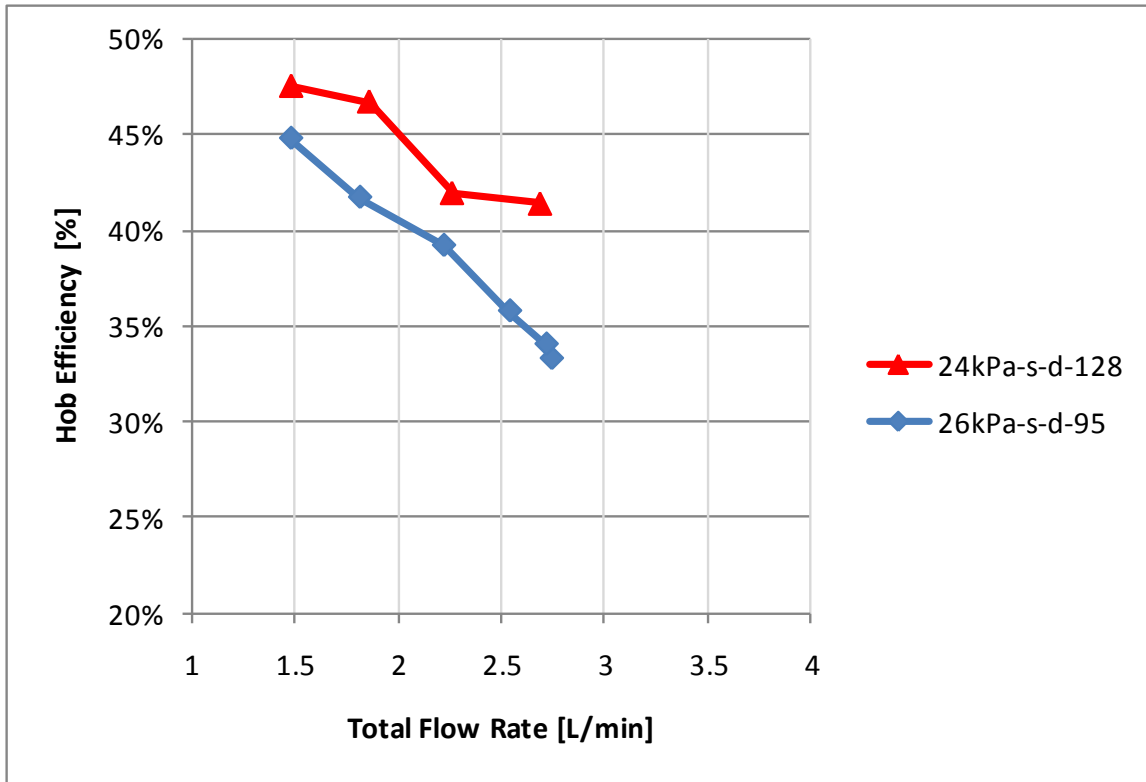


Figure 21 Flow rate versus hob efficiency (constant gas composition of 99.95% methane and supply pressure)

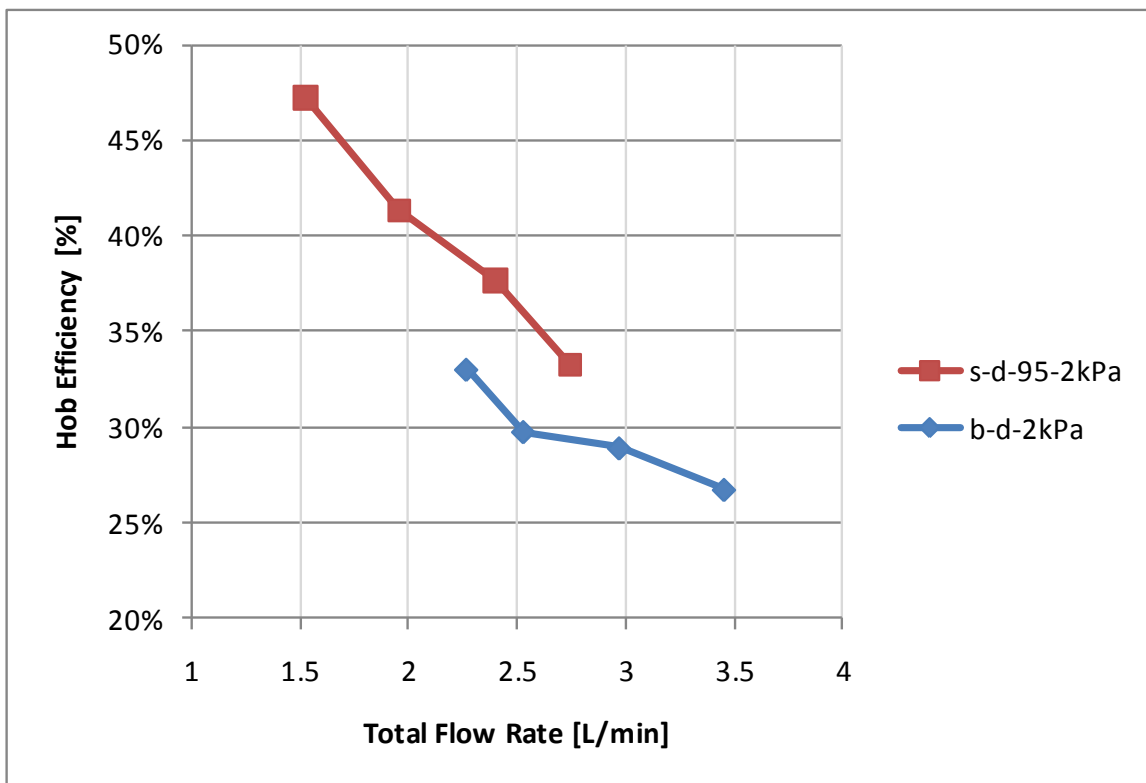


Figure 22 Flow rate versus hob efficiency (constant gas composition of 99.95% methane and operating pressure of 2 kPa)

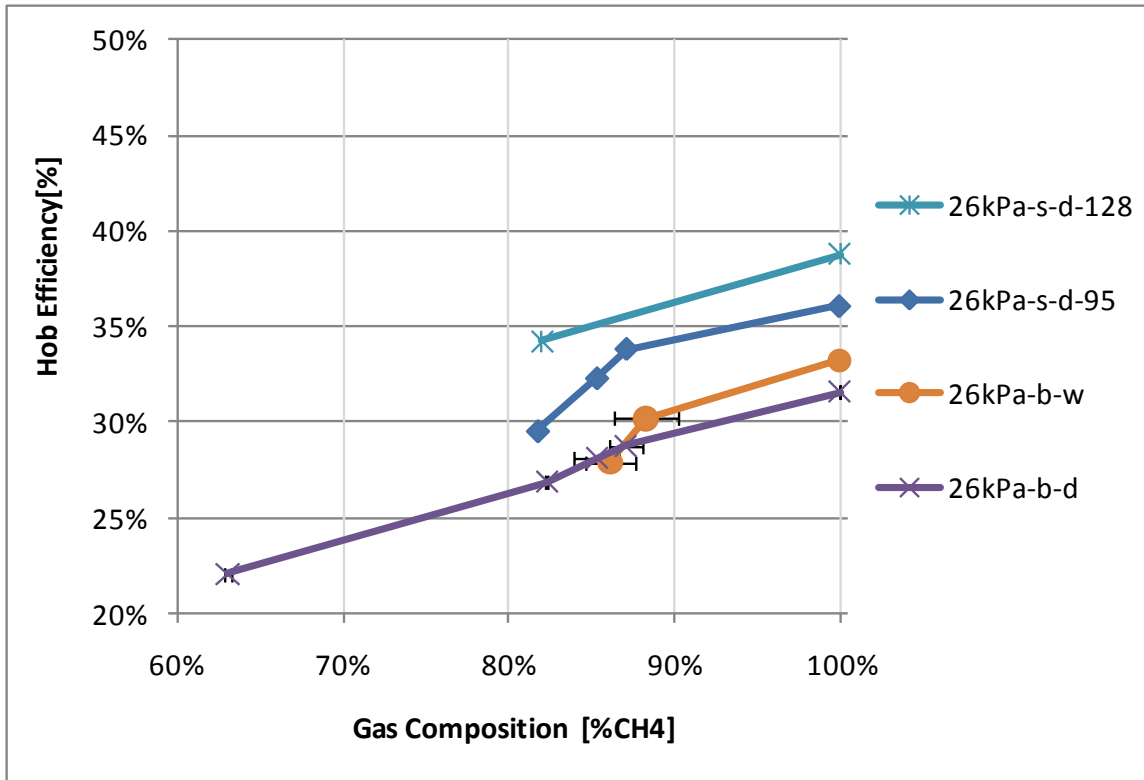


Figure 23 Gas composition versus hob efficiency (constant methane flow rate of 1.25 kW and supply pressure)

Figure 23 provides a plot of efficiency versus gas composition, for runs where the methane flow rate and supply pressure remained constant. This essentially shows that as the proportion of methane in the gas decreases, and thus as the flow rate increases, the efficiency of the hob decreases. The small burner fitted with the 1.28 mm injector performed better than the small burner fitted with the 0.95 mm injector, followed by the big burner, for a constant supply pressure.

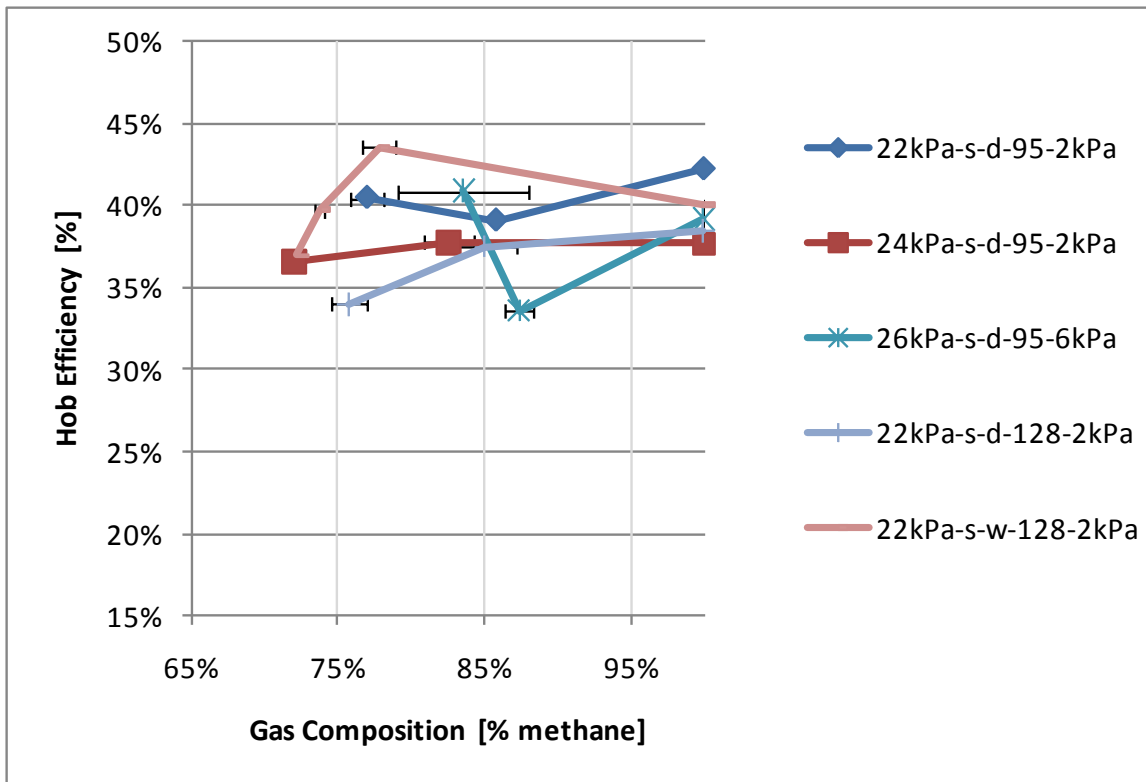


Figure 24 Gas composition versus hob efficiency (constant operating and supply pressure, high range)

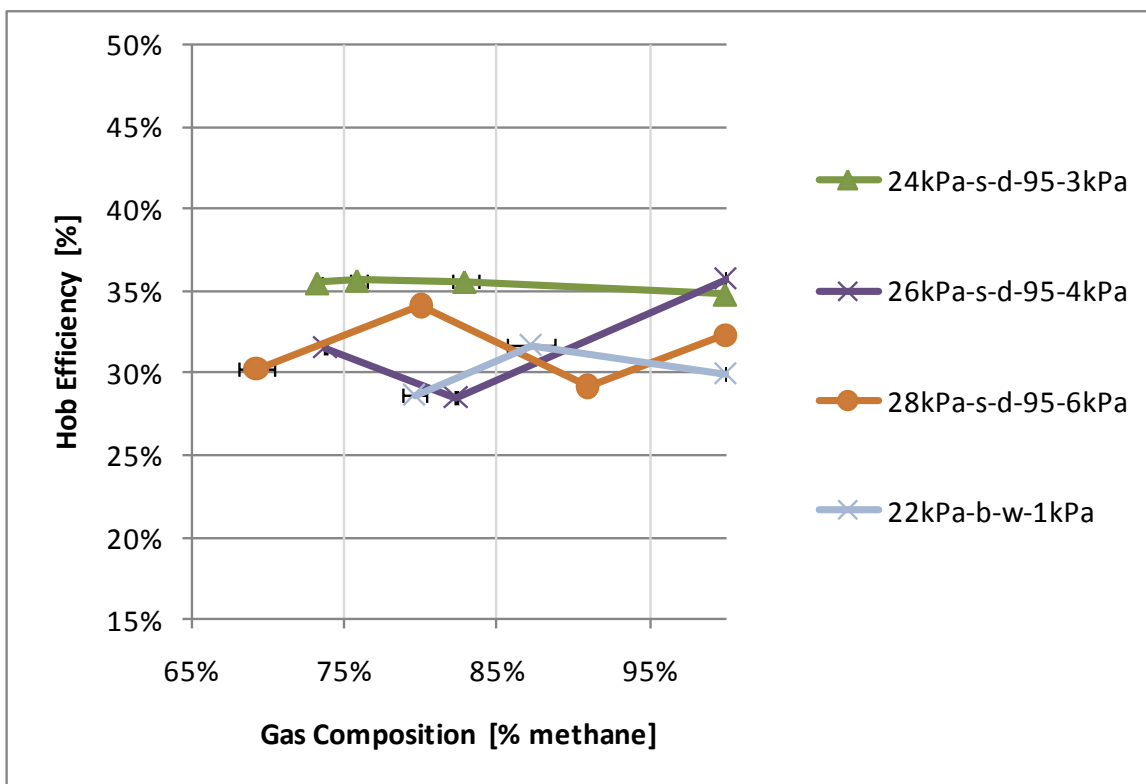


Figure 25 Gas composition versus hob efficiency (constant operating and supply pressure, mid range)

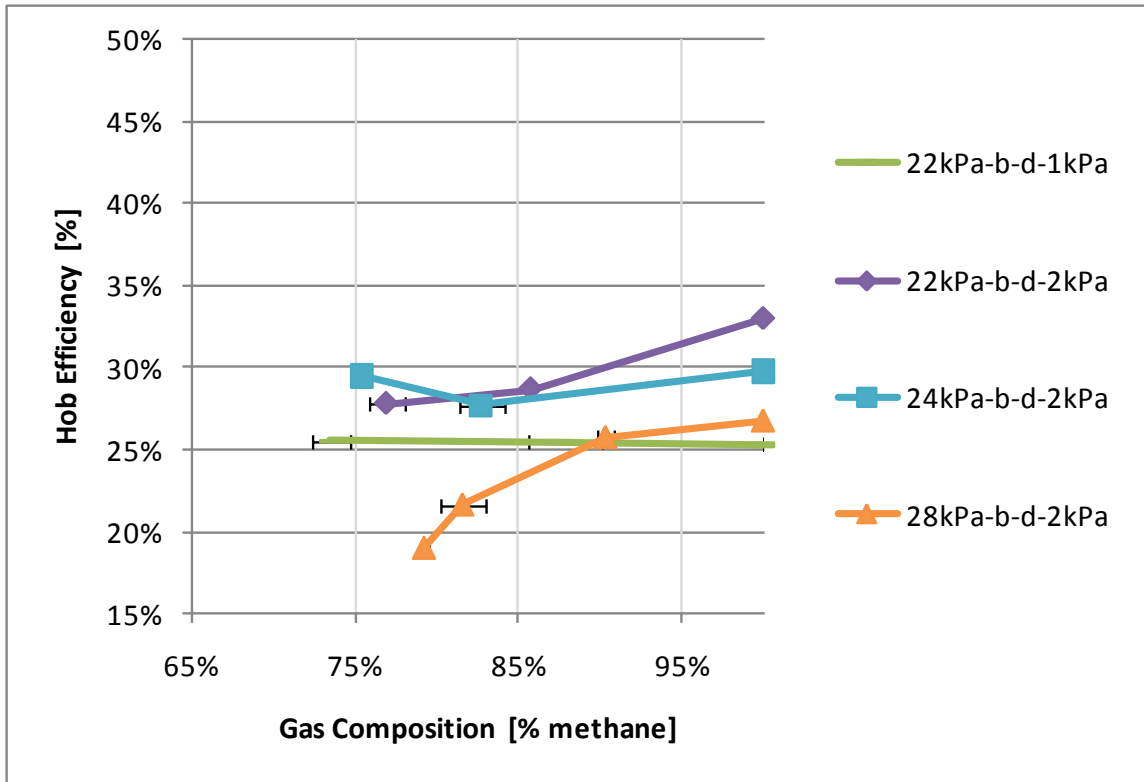


Figure 26 Gas composition versus hob efficiency (constant operating and supply pressure, low range)

Figures 24 to 26 are plots of hob efficiency versus gas composition, for a constant operating and supply pressure. The results have been grouped on the three graphs, from high to low efficiency. There is no clear trend for each individual run, and the hob efficiency seems to remain fairly constant for most runs. This is significant as it shows that under identical pressure conditions, the gas composition does not affect the efficiency of the hob.

An important comparison can be made between the different runs and how they relate to figures 11 to 13 and 15 to 17. Figures 11 to 13 provided the results for gas composition versus water heating rate and figures 15 to 17 provided the results for gas composition versus flame power, both for constant supply and operating pressures. The general trend of figures 11 to 13 showed that the water heating rate was higher at high supply pressures, with the small burner providing a higher heating rate than the large burner at the same supply pressure. This was consistent with the general trend of figures 15 to 17, which showed that the flame power was highest at high supply pressures, although the big burner provided a higher flame power than the small burner at the same supply pressure. In contrast to the results illustrated in figures 11 to 13 and 15 to 17, figures 24 to 26 show that the highest efficiencies were achieved by the small burner at low supply pressures, then by the small burner at mid-to-high supply pressures, and lastly by the big burner.

4.4. Cut-Off Compositions

Figure 27 presents the cut off compositions as a function of supply pressure. The cut off compositions are significant, as they provide an indication of the lowest quality of gas which can be used in the hob. In the context of this project, it is desirable that the hob can work with a low quality gas, that is to say the methane content of the gas is low. Thus, in this case, the performance of the hob is measured by how poor the gas quality was.

The cut off compositions were determined by gradually increasing the carbon dioxide flow rate and turning the hob on and off until it would no longer ignite. This was performed for both the small and the big burner, and under wet and dry conditions. The small burner was also tested with the two different injector sizes.

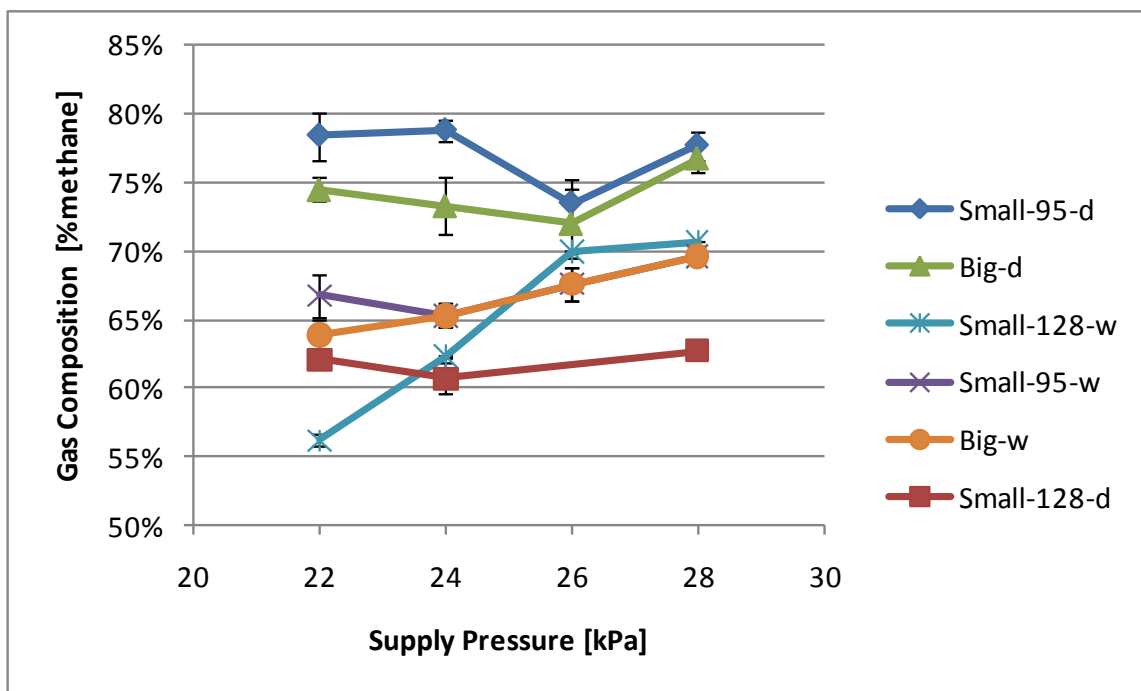


Figure 27 Cut-off compositions below which ignition was not possible

The cut off compositions for the dry results were fairly constant as the supply pressure increased. The small burner with the 0.95 mm injector and the big burner performed similarly, with cut off compositions in the range of 72-79 % methane. The small burner with the 1.28 mm performed significantly better, with cut off compositions in the range of 61-63 %.

The wet results were more erratic than the dry results. Like the dry results, the small burner with the 0.95 mm injector and the big burner performed similarly. However, the small

burner with the 1.28 mm injector seemed to perform better at low supply pressures and worse at high supply pressures, compared to the other two wet runs. A possible explanation for this behaviour is that the addition of water caused the system pressure dynamics to alter, which possibly skewed the results for the wet runs.

4.5. Error Analysis

As stated previously, the standard deviation of the gas composition could be calculated for every run, since gas samples were analysed in duplicate in the GC. The error in gas compositions have been displayed on figures as error bars.

Due to certain limitations, mainly including the amount of gas samples which could be analysed in the GC, many of the runs could not be carried out in duplicate. Nevertheless, the error in the various figures presented in the results should be accounted for. Since some runs were carried out in duplicate, the standard deviation of these runs could be calculated. The pooled standard deviation was determined to be an appropriate method of calculating the standard deviation of the other runs. This method may be used when one may assume that all the runs were carried out with the same precision, even though some variables were different for each run. The equation to calculate the pooled standard deviation is given by: (IUPAC, 2011)

$$S_p = \sqrt{\frac{(n_1 - 1)s_1^2 + (n_2 - 1)s_2^2 + \dots + (n_k - 1)s_k^2}{n_1 + n_2 + \dots + n_k - k}}$$

Where: S_p is the pooled standard deviation
 n is the sample size
subscripts 1, 2,..., k represent the various runs which were carried out in duplicate
 s is the standard deviation of a sample

The pooled standard deviations for the water heating power, flame power, hob efficiency and total flow rate were thus calculated and the results are presented in Table 9. The values provided may be applied to all the figures which display these variables. The data that was used to calculate the pooled standard deviation may be found in Table 20 in Appendix C.

Comparing the order of magnitude of the actual values to the pooled standard deviation, the percent of error range is fairly low, and deemed to be acceptable.

Table 9 Pooled standard deviation

Variable	Order of magnitude of actual values	Pooled standard deviation			Percent error - range
Water heating power	0.3 - 0.5	±	0.015	kW	3 - 5 %
Flame power	0.8 - 1.4	±	0.029	KW	2 - 4 %
Hob efficiency	25 - 45 %	±	0.94%	%	2 - 4 %
Total flow rate	1.5 - 3	±	0.093	L/min	3 - 6 %

4.6. Conclusions and Recommendations from the Experiments

4.6.1. Summary

The effect of a number of variables was investigated through the experimental work. The main findings are summarised here.

The water heating rate increased with an increase in the methane composition of the gas, for runs where the operating and supply pressures were constant. The highest heating rates were achieved with the small burner at high supply pressures, while the lowest heating rates were observed with the big burner at low supply pressures. Comparing runs with the same operating pressure, the water heating rate increased with an increase in the supply pressure.

The water heating rate was also found to increase with an increase in the methane composition of the gas, for runs where the methane flow rate and supply pressure were constant. The highest water heating rate was produced by the small burner fitted with the 1.28 mm injector, followed by the small burner fitted with the 0.95 mm injector, and then by the big burner.

The flame power increased with an increase in the composition of methane in the gas mixture, for runs where the operating and supply pressures were constant. The flame power was greatest at high supply pressures and lowest at low supply pressures. At the same supply pressure, the flame power was greater for the big burner than the small burner with the 0.95 mm injector, followed by the 1.28 mm injector. For a constant operating pressure, the flame power was greater for runs with a higher supply pressure; and for a constant supply pressure, the flame power was greater for runs at a lower operating pressure.

For a constant gas composition and operating pressure, the hob efficiency decreased as the supply pressure increased. Additionally, the small burner was more efficient than the big burner.

Hob efficiency increased with an increase in operating pressure, for a constant gas composition and supply pressure. It was also noted that the run with the lower supply pressure and large injector was more efficient than the run with the higher supply pressure and the small injector. This suggests that the injector size should be increased in order to increase the hob efficiency at low supply pressures.

Efficiency was found to decrease with an increase in flow rate, when the gas composition and supply pressure remained constant. The run with the lower supply pressure and the large injector proved to be more efficient than the run with the higher supply pressure and the small injector. Similarly, the efficiency of the hob decreased with an increase in flow

rate, for a constant operating pressure. The small burner was more efficient than the big burner.

For a constant supply pressure and methane flow rate, the efficiency increased with an increase in operating pressure. The small burner fitted with the 1.28 mm injector performed better than the small burner fitted with the 0.95 mm injector, followed by the big burner, for a constant supply pressure of 26 kPa. For the same supply pressure, the big burner performed better on the wet run compared to the dry run.

It was also found that as the proportion of methane in the gas increased, and thus as the flow rate decreased, the efficiency of the hob increased, for a constant methane flow rate and supply pressure. The small burner fitted with the 1.28 mm injector performed better than the small burner fitted with the 0.95 mm injector, followed by the big burner; this was an important finding as it demonstrated the effect that further modifications could have. Since the methane flow rate (and thus the flame power) was constant, the decrease in efficiency was likely caused by: the increase in the inert gas heating losses; as well as the increase in the flow rate which caused a larger, cooler flame and greater convective losses.

In contrast to the results where the supply and operating pressures remained constant, the highest efficiencies were achieved by the small burner at low supply pressures, then by the small burner at mid-to-high supply pressures, and lastly by the big burner.

One of the important objectives was to find the lowest possible composition of methane required to be able to use the hob. This objective was met out by determining the cut-off compositions, at which the gas could no longer be ignited in the hob. These were found to be approximately: 62% for the small burner fitted with the 1.28 mm injector; 77% for the small burner fitted with the 0.95 mm injector; and 74% for the big burner, which was fitted with the 1.28 mm injector throughout.

The addition of moisture to the gas mixture did not affect the results significantly, and any discrepancy between wet and dry runs may not only be due to the presence of water vapour, but perhaps also due to the sensitive nature of the experimental system pressure dynamics.

4.6.2. Conclusions

The purpose of this investigation was to determine the methane content of biogas required to be used in a standard gas hob. It has become clear that there is no simple solution to this problem.

The presence of inert gases was shown to decrease the water heating rate as well as the efficiency of the hob, for experiments where the methane flow rate and the supply pressure remained constant. This shows that upgrading the biogas would improve cooking rates and

efficiency, thus deeming it beneficial. Considering the cut-off compositions, it may be claimed that a gas consisting of 80% methane is acceptable to be used in a gas hob, thus leading to the conclusion that the biogas should be upgraded to this level. Disadvantages of this option may include the cost of upgrading the biogas as well as increasing the pressure drop along the line from the digester to the stove. Additionally, for a technology which is considered environmentally beneficial, the environmental impact of the absorber, especially the solvent, should be considered.

On the other hand, it was shown that the highest water heating rate and efficiency were produced by the small burner fitted with the 1.28 mm injector, followed by the small burner fitted with the 0.95 mm injector, and then by the big burner (although it must be noted that the efficiency of the latter was compromised by the small size of the pot). This was demonstrated for experiments where the methane flow rate and supply pressure were constant (varying gas composition). The higher efficiency was also produced for the small burner fitted with the 1.28 mm injector for experiments where the gas composition and supply pressure were constant (varying flow rate). For the experiments where the supply and operating pressures were kept constant, the hob efficiency was not affected by a change in the gas composition. In addition, the cut-off compositions were the lowest for the small burner fitted with the 1.28 mm injector. These findings point to the possibility that the biogas does not require upgrading, and rather that gas hobs could be retrofitted with larger injectors.

The possible benefits of a higher cooking rate and hob efficiency offered by the reduction of inert gases through upgrading thus need to be weighed up against the additional costs required to upgrade the gas, in order to determine if upgrading is preferable. There is also the possibility that a combination of both options may be optimal.

4.6.3. Recommendations

It is recommended that testing of a hob should be carried out under real conditions. The ambient temperature affects the moisture content of the gas, and thus the presence of moisture may have a more significant effect on the performance of the hob. The supply pressure from the digester plays an important role in the performance of the hob, and should thus be investigated further under real conditions.

It appears clear that larger injector sizes are an effective way of allowing ignition of a lower quality gas. Although larger injectors may need to be custom made, it is recommended that further investigations be carried out to determine the effect of larger injector sizes on the water heating rate and hob efficiency.

It was also observed that the efficiency of a gas hob appears to be a strong function of the match between pot size and hob size; this insight should form part of all technical advice given to gas hob users.

5. Absorber Design

Based on the experimental work, which was carried out with a gas hob, it was decided that the design of a carbon dioxide absorber should be undertaken as a basis for investigating the feasibility of upgrading the raw biogas, assumed to be 60% methane, to 80% methane. The feasibility of various upgrading technologies was assessed for use on a household scale in chapter 3. The criteria for assessment were: financial feasibility, safety, environmental impact, ease of operation, and technology maturity. It was decided that absorption was the most appropriate technology. The presentation and discussion of the design calculations, and of the feasibility of such an option, follow the approach that was described in chapter 3.

5.1. Mass Balance

When starting the design of an absorber, one typically has a number of restrictions in place already, allowing only a few degrees of freedom. For this design the inlet and outlet composition of the gas was fixed, as were the temperature, pressure and the inlet solvent concentration of CO₂ (at zero). It is important to note that under real digester conditions the composition of the inlet gas; the temperature and the pressure fluctuate daily and seasonally.

The absorber design needed to be based on a gas flow rate that would be typical of real life usage. Thus the flow rate was calculated based on the heat of combustion of methane and the production of a 3 kW flame, which is a typical rating of a rapid burner on a gas hob. Table 10 provides a summary of values which were used to determine the gas flow rates. Refer to Appendix D for sample calculations.

Table 10 Calculation of gas flow rate (¹ Sandler, 1999)

Heat of combustion CH ₄ ¹	802.32	kJ/mol
Rated Power	3	kW
CH ₄ in raw biogas	60%	%
Flow rate raw biogas	22.4	mol/h
	0.52	m ³ /h
Purity Scrubbed Biogas	80%	%
Flow rate scrubbed biogas	16.8	mol/h
	0.39	m ³ /h

Figure 28 presents the mass balance diagram for an absorber. X and Y are the mole ratios of CO₂ to the solvent and methane (non-transferring component) respectively, while x and y are the mole fractions of CO₂ in the liquid and gas phase respectively. Subscript number 1 represents the conditions at the bottom of the column, and 2 the top. The method used to calculate the solvent flow rate is explained in the next section.

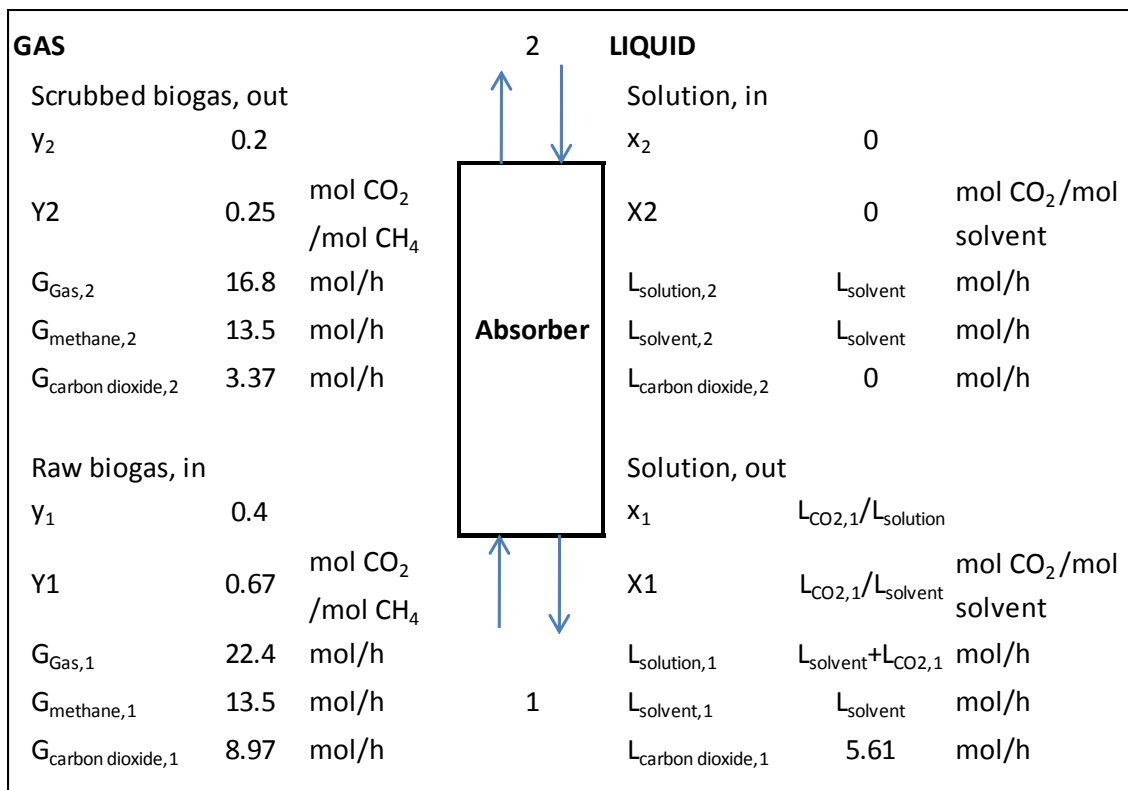


Figure 28 Mass balance diagram

5.2. Selection of Solvent

According to Perry and Green (2008), a high solubility of the solute and its selectivity over other components in the gas, are important qualities of a solvent. The higher the solubility of the solute in a solvent, the lower the solvent flow rate needs to be. In addition to these aspects, a solvent should not be volatile, expensive, corrosive, unstable, viscous, flammable, and should not foam. Usually, the more chemically similar the solvent is to the solute, the higher the solubility will be.

A solvent can either be classified as physical or chemical; the solute is merely absorbed into a physical solvent, while the solute will react with a chemical solvent. The main differences between the two types are given in Table 11. In general, for both types, solubility decreases with an increase in temperature. (Green & Perry, 2008)

Table 11 Comparison between physical and chemical solvents (Green & Perry, 2008)

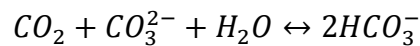
Characteristic	Physical solvent	Chemical solvent
Solubility variation with pressure	Relatively linear	Highly nonlinear
Low-pressure solubility	Low	High
High-pressure solubility	Increases with pressure	Levels off

Noting that solubility is low for a physical solvent at low pressures and that the system in question is at close to atmospheric conditions, it was anticipated that a chemical solvent would be required for the desired separation. Additionally, the most common solvents used for the removal of CO₂, or acidic gases in general, are aqueous solutions of monoethanolamine (MEA), diethanolamine (DEA), and potassium carbonate (K₂CO₃) (Green & Perry, 2008). These are all chemical solvents. By contrast though, physical absorption into water at high pressures seems to be the preferred, more efficient and least costly option for biogas upgrading (as discussed in section 2.3).

Due to the application of this absorber, it was aimed to keep the design as simple as possible, in order to limit capital costs as well as to keep the operation straightforward. Thus the inclusion of a stripper was not considered viable (refer to section 3.3), and the choice of solvent was restricted to a solvent that was not toxic and could be used further once it had been spent. MEA is a corrosive liquid, and MEA and DEA are both classified as being flammable, irritants and skin permeators (The Dow Chemical Company, 2003). The use of these toxic solvents was thus ruled out as a possible option. High gas pressures were also to

be avoided, as the inclusion of a compressor for a flammable gas was thought to add too much capital cost.

Solvents such as water or an alkaline salt solution could be used for crop irrigation if the biogas-digester is located on a farm, with the alkaline salt acting as a fertilizer. An aqueous solution of K_2CO_3 may itself be used as a fertilizer, but only for certain types of acid soil and within carefully specified application rates; potassium bicarbonate ($KHCO_3$) is the product of the reaction of K_2CO_3 with CO_2 and is also used as a fertilizer (Gowariker et al., 2009). The use of a K_2CO_3 solution was thus thought to be a good option for the solvent. The stoichiometry for CO_2 and K_2CO_3 is one-to-one. The overall reaction of absorbed CO_2 and an aqueous carbonate solution is (Knuutila et al., 2010):



The use of water as a solvent was still considered as an option, since the cost of a chemical solvent may prove to be prohibitively high; although it was anticipated that water would not be a viable solvent at close to atmospheric conditions. The next step was thus to search for the equilibrium solubility data in order to determine the required flow rates of the various solvents under consideration.

5.3. Equilibrium Solubility Data

The equilibrium solubility data is the basis for the design of an absorber as it is used to determine the flow rate of the solvent which is required for a desired separation. It is considered the most important and possibly the most time consuming part of the design process (Green & Perry, 2008).

Henry's Law is typically applicable for common solutes and solvents, when the system is dilute, non-reacting and at a low pressure (the solute partial pressure is less than 1 atm). Henry's Law is given by the following relationship, but may be modified according to the units of the constant (Green & Perry, 2008).

$$p_A = Hx_A$$

Where: p_A is the partial pressure of substance A in the gas in equilibrium with a liquid
 x_A is the mole fraction of A in the liquid at equilibrium
H is Henry's Law constant, which is dependent on the solute, solvent and temperature

The partial pressure is related to the gas phase mole fraction of the solute through Dalton's Law. This law is valid for non-reacting gases at low-to-moderate total pressures, and is given by:

$$p_A = P_{total} y_A$$

Where: y_A is the mole fraction of A in the gas phase

Henry's Law was applicable for the CO₂-water system, and the following equation was applicable at 25°C (Green & Perry, 2008):

$$p_{CO_2} = 1635 \text{ atm } x_{CO_2}$$

For less common equilibrium relationships and for chemical solvents, such as CO₂ dissolved in aqueous K₂CO₃, solubility data available in literature may be used. The data is typically found as liquid mole fractions or loadings (amount of solute/amount of active solvent) for a range of partial pressures of the solute, at a given temperature. It is important that the temperature, at which the solubility data is given, is the same as the operating temperature of the absorber. If no data is available, one may need to generate one's own experimental data. Fortunately, equilibrium solubility data was available for the CO₂-K₂CO₃ system, in the correct temperature and pressure range, and is provided in Table 21 in Appendix D.

5.4. Calculation of the Liquid-to-Gas Ratio

The solvent flow rate is determined through the use of a design diagram, shown in Figure 29. This consists of a plot of the equilibrium data and an operating line on the same set of axes; the x- and y-axis are occupied by the solute composition in the liquid and gas phase respectively. The operating line represents the gas and liquid compositions at the inlet and outlet of the absorber.

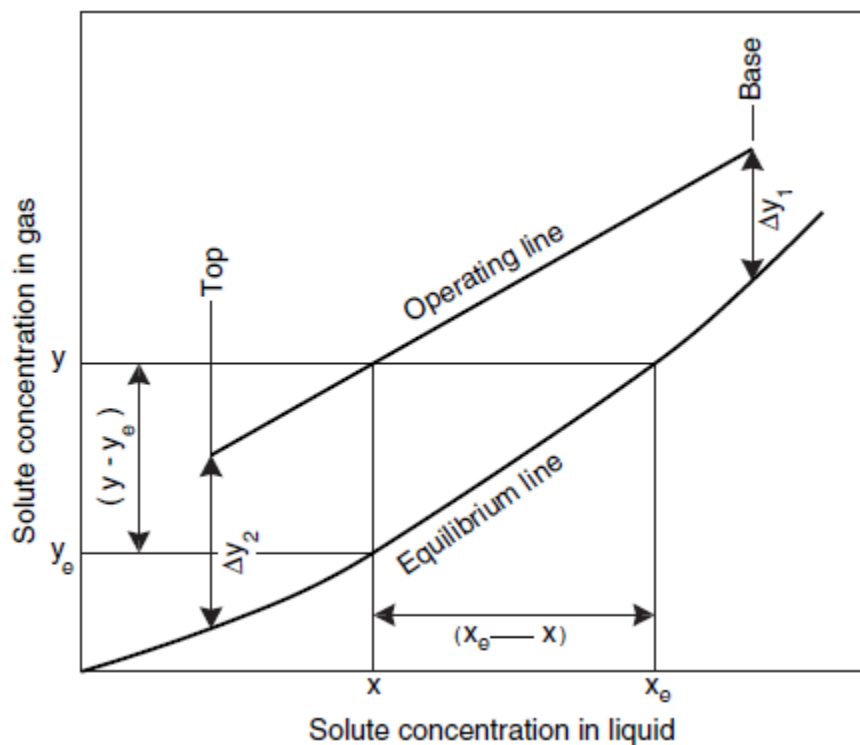


Figure 29 Design diagram, showing the gas absorption concentration relationships (Sinnott, 2005)

Three design diagrams representing CO₂ dissolved in water, and aqueous solutions of 5 and 10 mass % K₂CO₃ at 25°C are shown in Figures 30, Figure 31 and Figure 32 respectively. The Henry's Law constant for CO₂ dissolved in water was used to create the equilibrium curve in Figure 30, while equilibrium data provided by Park *et al.* (1997) was used to construct Figure 31 and Figure 32.

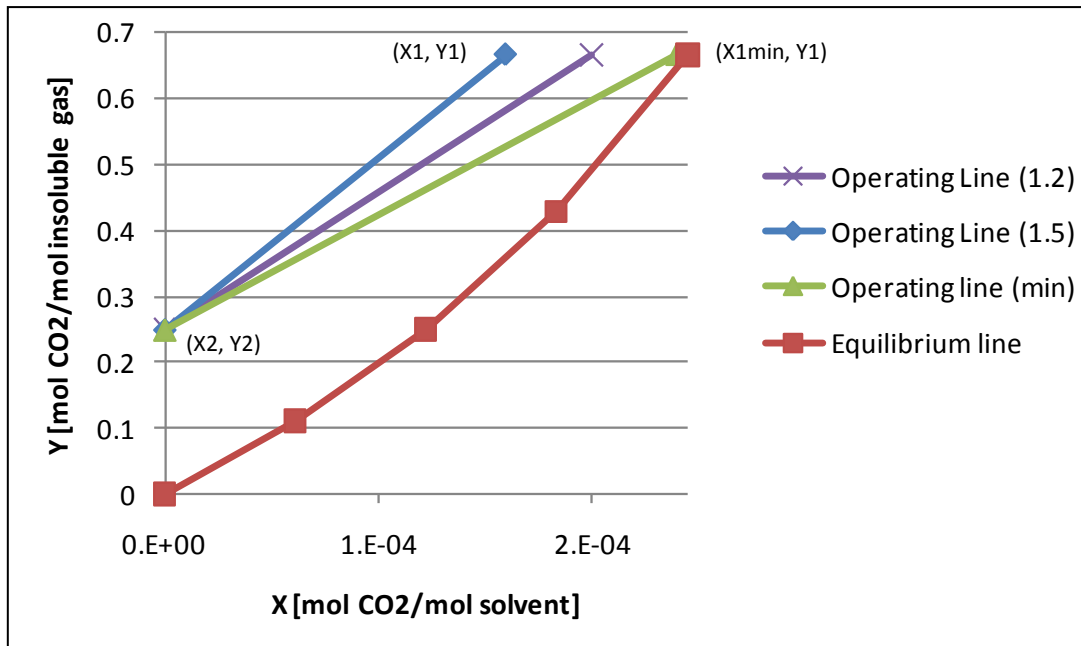


Figure 30 Design diagram for CO₂ dissolved water (Henry's constant from Green & Perry (2008))

The data are plotted as mole ratios of CO₂ to moles of non-transferring components in both the liquid and gas phase. It was necessary to use this method, rather than using mole fractions, since the gas was considered to be concentrated with CO₂, i.e. greater than 10% CO₂ (Sinnott, 2005). The minimum operating line is constructed by knowing the CO₂ content of the inlet (Y₁) and outlet gas (Y₂), and the inlet CO₂ solvent concentration (zero, X₂). The minimum outlet CO₂ solvent concentration (X_{1min}) is the point where the operating line intercepts the equilibrium line at Y₁. The gradient of this line is the ratio of the minimum CO₂-free solvent flow rate to the CO₂-free gas flow rate (L/G).

The actual operating line is then constructed by multiplying the gradient of the minimum operating line by a factor, which is usually 1.2 to 1.5. This factor is chosen through economic considerations as well as from experience (Green & Perry, 2008). The use of the minimum solvent flow rate would result in an infinitely tall column as equilibrium is never truly reached; the use of excess solvent will decrease the height of the column. A balance between capital and operating costs may be found in order to determine the optimum solvent flow rate. In this case a factor of 1.2 and 1.5 (or 20 and 50% excess solvent) was used. However, since a chemical solvent was necessary and a stripper will not be used to regenerate the solvent, a lower excess of 20% may be preferred. For expensive solvents, or in this case when the use of the solvent does not necessarily add monetary value to the product, the use of a smaller excess is preferable in order to keep the solvent purchase costs down. A smaller excess will result in a taller column, but since preliminary calculations indicated that the absorber in this design would not be very large, this appeared not to be an important factor.

Once the gradient of the operating line is known, the solvent flow rate may be calculated. The final CO₂ concentration in the outlet solvent (X₁) may also be determined, and is equal to the abscissa of Y₁ on the operating line.

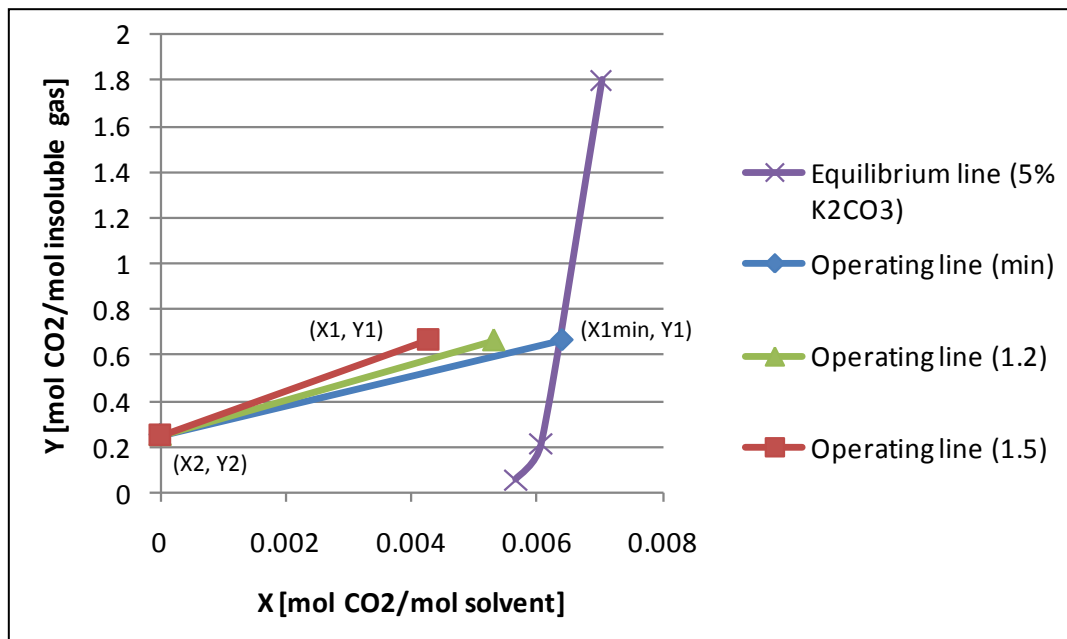


Figure 31 Design diagram for CO₂ dissolved in a 5 mass % K₂CO₃ solution (equilibrium data from Park et al. (1997))

The lowest solubility is offered by water, followed by the 5 % and then the 10 % K₂CO₃ solution; the lowest flow rate is associated with the solvent offering the highest solubility. It is clear from the results, presented in Table 12, that water is not a good choice as a solvent for CO₂ compared to the other two options. The main reason for this is that the column is operating under near atmospheric conditions, whereas, in practice, if water is used for CO₂ absorption, the operating pressure is much higher. This is because the solubility of CO₂ in water increases with pressure.

Table 12 Calculated solvent flow rate at 1.2 and 1.5 times the minimum rate

Solvent	Water		5% K ₂ CO ₃		10% K ₂ CO ₃		
	20%	50%	20%	50%	20%	50%	
Solvent excess							
Flow rate	28061	35077	1053	1317	532	665	mol/h
solvent (L _{solvent})	505	631	20	25	10	13	L/h

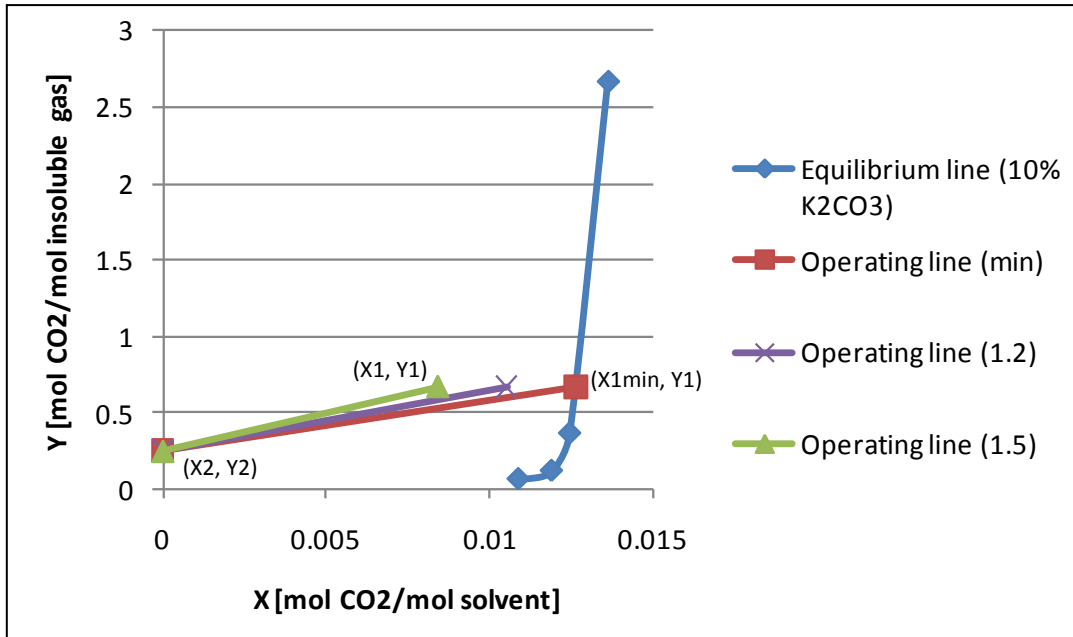


Figure 32 Design diagram for CO₂ dissolved in a 10 mass % K₂CO₃ solution (equilibrium data from Park et al. (1997))

5.5. Choice of Equipment

According to Green and Perry (2008), gas effluents containing CO₂ and H₂S are typically treated in packed or tray columns. These are also the two main types which are used for gas absorption, and are classified as liquid dispersed contacting devices. Based on the anticipated diameter size of the column (i.e. less than 0.6 m), a plate column was not suitable for the scrubbing of biogas, and thus a packed column was chosen. Packed columns also offer a lower pressure drop compared to tray columns.

Packed towers are cylindrical vessels, vertically orientated, which are filled with a packing. The two fluid streams are normally passed through the tower counter-currently. Counter-current contacting, as opposed to co-current contacting, provides the greatest driving force for mass transfer across the whole column. The purpose of the packing is to increase the interfacial surface area between the gas and liquid. The packing should distribute the liquid well across the whole column to prevent liquid channelling. There are two categories of packing: random and structured. Since the column diameter would be small, random packing would be more suitable than structured packing. (Green & Perry, 2008)

There are many different types of random packing, such as Pall rings, Intalox saddles and Berl saddles, which come in various sizes and materials. Various packing materials are available, including: metal, ceramic, glass and plastic. The choice of packing size is based on the column diameter, and the column diameter is based on the packing size, so selecting the packing size is typically an iterative process. It is recommended that columns with a diameter less than 0.3 m use a packing size of less than 25 mm (Sinnott, 2005). Green and Perry (2008) state that it is good practise to select a packing size which provides:

$$10 < \frac{D_c}{d_p} < 40$$

Where: D_c is the column diameter [m]

d_p is the packing size [m]

For very small applications, such as for laboratory use or for this absorber, Richardson et al. (2002) recommends the use of special packings which are typically too expensive for industry-size columns. These include: Dixon packings, which are Lessing rings, constructed from wire mesh or KnitMesh, which is a fine wire mesh packing.

Since the absorber was anticipated to have a small diameter, most commercially available packing would be too large. The calculations thus had to be carried out with the smallest size packing for which information was available, as well as with a special type of packing for small applications. The characteristics of the packings that were used in the calculations are presented in Table 13.

Table 13 Characteristics of Random Packings used in Calculations

Name	Material	Size mm	Packing factor (Fp) m^{-1}	Specific area (a) m^2/m^3	Reference
Intalox saddles	ceramic	6	2720	984	Green & Perry, 2008
Dixon rings	metal	3	none available [†]	2275	Pingxiang Naik Chemical Industry Equipment Packing Co., 2011
Raschig rings	ceramic	6	5250	794	Richardson et al., 2002

[†] packing factor for Intalox saddles used

5.6. Column Diameter

The diameter of a packed column depends on the flow rates of the gas and liquid, as well as the characteristics of the packing and the fluid properties. The diameter is typically designed according to a set pressure drop; the recommended pressure drop of an absorber is 15 to 50 mm of water (or 150-500 Pa) per metre of packed height (Sinnott, 2005). Another factor which needs to be considered is the flooding velocity, or the gas velocity at which the downward flow of liquid will be impeded so strongly that the column will fill with liquid, i.e. *flood*. This is an undesirable operating condition which is characterised by a low mass transfer rate and a high pressure drop. In order to prevent flooding, the gas velocity should be at 60 to 80 % of the flooding velocity (Green & Perry, 2008).

A generalized pressure drop correlation, which is available in various forms in most text books covering this subject, is used to calculate the column diameter. A copy of the correlation may be found in Figure 44 in Appendix D. The correlation is a plot of F_{LV} on the x-axis and K_4 on the y-axis, with a number of isobars (the uppermost line is the flooding line). The factors, F_{LV} and K_4 are given by the following equations (Sinnott, 2005):

$$F_{LV} = \frac{L_w}{V_w} \sqrt{\frac{\rho_V}{\rho_L}}$$
$$K_4 = \frac{13.1(V_w)^2 F_p \left(\frac{\mu_L}{\rho_L}\right)^{0.1}}{\rho_V(\rho_L - \rho_V)}$$

Where: L_w is the liquid mass flow rate per cross sectional area [$\text{kg}/\text{m}^2\text{s}$]

V_w is the gas mass flow rate per cross sectional area [$\text{kg}/\text{m}^2\text{s}$]

ρ_V and ρ_L are the gas and liquid densities [kg/m^3]

F_p is a packing factor, specific to the packing type, size and material of construction [m^{-1}]

μ_L is the liquid viscosity [$\text{Pa}\cdot\text{s}$ or Ns/m^2]

The method requires the calculation of the F_{LV} factor, which is used to find the K_4 factor at the desired pressure drop (between 15 and 50 mm water per metre of packed height) and the flooding line. The percentage of flooding is then calculated by taking the square root of

the ratio of K_4 at the desired pressure drop and at flooding; it should be between 60 and 80%. If the percentage flooding is in the correct range, the column will not flood; if not, the chosen pressure drop needs to be adjusted until the percentage flooding is in the correct range.

For the design in question, the biogas flow rate is fairly fixed, but the solvent flow rate may vary, depending on solvent strength. Considering the three solvents described already, the calculated flow rates vary significantly. Water was quickly ruled out as a viable solvent, since the flow rate was too high compared to the gas flow rate, which was calculated to result in a flooded column. This was established based on the F_{LV} factor, which was much greater than the acceptable range given in Figure 44.

The flow rates of the two K_2CO_3 solutions were significantly lower than the water flow rate, thus offering viable solutions. The column diameters were found to be in the range of 3 to 4 cm. The results are given along with the column heights in Table 14 and the sample calculations are provided in Appendix D.

5.7. Packed Tower Height

There are many text books available which provide correlations to calculate the height of a packed absorber column. Most of these books cover physical absorption for dilute conditions well, but some deductions and comparisons between books need to be made in order to understand absorption under concentrated conditions. In addition, the information provided for absorption with a chemical reaction under concentrated solutions is not covered well. It thus made the task of trying to estimate the height of this column fairly difficult.

To support this, the text books generally agree that such an absorber design cannot be done without experimental data or design software. While the column diameter and flow rates are determined by the same methods used for physical absorption, the column height depends on enhanced mass-transfer coefficients which are system specific. According to Green and Perry (2008), these calculations are complex and justify the use of a professional software package. Richardson et al. (2002) states that calculating the height of an absorber with a chemical reaction is difficult, and should always be supported by experimental data.

Nevertheless, some of the theory as well as various methods for predicting the height will be presented in this section, starting with some mass transfer theory.

5.7.1. Mass Transfer Theory

The determination of the height of a packed absorber is based on the principles of mass transfer. The film theory is used to understand physical absorption, while an extension of this theory is used to explain absorption with a chemical reaction (Richardson, Harker, & Backhurst, 2002). Figure 33 provides a graphical presentation of the process of absorption with a chemical reaction, which is applicable to the absorption of CO_2 into a solution of K_2CO_3 .

Starting on the left hand side, substance A (CO_2) in the bulk gas phase has a partial pressure (P_{AG}). A moves by diffusion through the non-transferring gas (in this case it is methane), through a stagnant gas film to the gas-liquid interface (U). The partial pressure of A decreases from P_{AG} in the bulk gas to P_{Ai} at the interface. The general theory is that A in the gas phase (P_{Ai}) is in equilibrium with A in the liquid phase (concentration C_{Ai}) at the interface, as long as the reaction is not instantaneous at the gas-liquid interface. This is the same for both physical and chemical absorption.

A crosses over the gas-liquid interface into the liquid film through diffusion. As this is happening, reactant B (K_2CO_3) diffuses through the bulk liquid, through the stagnant liquid

film, towards the interface. When A and B meet at the reaction zone (R), they react, causing the concentration of each to become zero as a new product is formed (AB).

This is a simplified case and there are many possible variations. The position of the reaction zone and the relative concentrations can change, depending on the speed of the reaction, the rate of diffusion of each species, and whether one of the reactants is in excess (Green & Perry, 2008). All of these variations may be applicable at different points in the column as the concentration of the solute in the gas phase changes, and the reactant (K_2CO_2) in the liquid is expended.

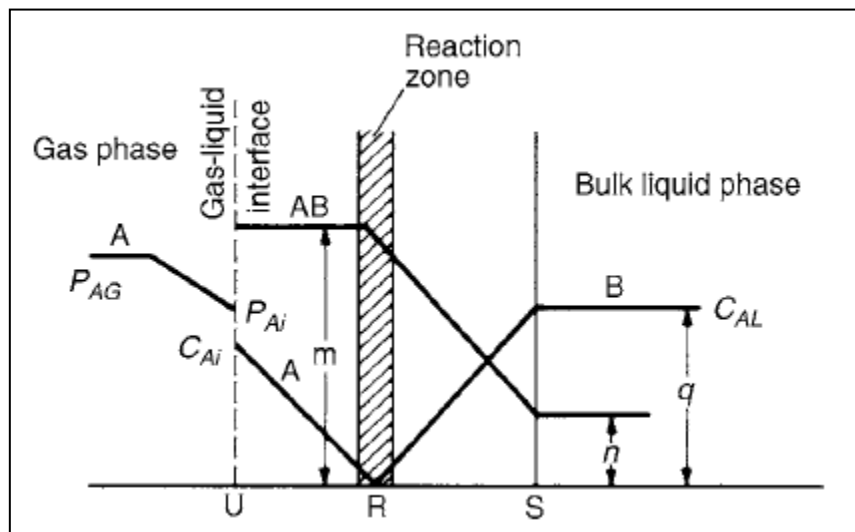


Figure 33 Concentration profile for absorption with chemical reaction (Richardson, Harker, & Backhurst, 2002)

In the case of physical absorption, A would continue to diffuse through the stagnant liquid film into the bulk liquid as a result of the concentration driving force from the interface to the bulk liquid ($C_{Ai} - C_{AL}$). By reducing the concentration of A to zero in the reaction zone, the driving force for absorption is increased. As long as the reaction rate is fast enough, the absorption will take place at a greater rate than that of physical absorption. If the reaction rate is slow, or B is not in excess, the reaction zone may be located in the bulk liquid. This would result in conditions similar to physical absorption. (Richardson, Harker, & Backhurst, 2002)

For physical absorption, the mass transfer flux of A in the gas phase is given by:

$$N_A = k_G(P_{AG} - P_{Ai})$$

The transfer of A in the liquid phase is given by:

$$N_A = k_L(C_{Ai} - C_{AL})$$

Where: k_G and k_L are the individual mass transfer coefficients based on the gas and liquid films respectively.

The absorption enhancement due to the chemical reaction in the liquid, may be represented by an enhancement factor, r . This factor has been shown to relate to the concentration of A at the interface (C_{Ai}), the diffusivity of A in the liquid (D_L), k_L , the concentration of B in the bulk (C_{BL}), and the second order rate constant (k_2), for CO_2 absorbed into alkaline solutions (Van Krevelen and Hoftzyer (1948), cited by Richardson et al., 2002). This work provided the following adjustment to the previous equation:

$$N_A = (C_{Ai} - C_{AL})(k_2 D_L C_{BL})^{0.5} \quad \text{Where} \quad r = \frac{(k_2 D_L C_{BL})^{0.5}}{k_L}$$

For slow reactions (i.e. k_2 is small), r is close to unity, and absorption may be considered physical. For large k_2 (fast reaction), $r \approx C_{BL} / i C_{Ai}$, where i refers to the number of moles of B that reacts with A. The absorption rate is proportional to reaction rate, for a moderate rate (Richardson et al., 2002). It is thus clear that this information needs to be supported by experimental values. The use of this relation is linked to the height of the absorber, which is explained in the next section.

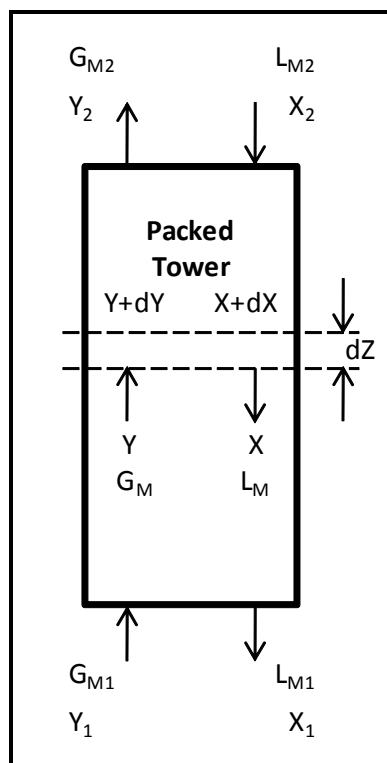


Figure 34 Nomenclature for material balances in a counter-current packed-tower absorber (Richardson et al., 2002)

5.7.2. Height Calculation

The height of a column depends on the rate of absorption, and thus the mass transfer coefficient is an essential value to have in order to design an absorber. The mass transfer coefficient is dependent on both the liquid and gas properties, but also on the characteristics of the packing and the dimensions of the column.

Richardson et al. (2002) provide derivations for various cases; the derivation for the concentrated case in terms of the gas film is presented here. The following equation describes a mass balance across a differential height, dZ , with the nomenclature illustrated in Figure 34.

$$AG_M dY = AL_M dX$$

If the flux of component A (CO_2) through a cross-sectional area (A) is given by:

$$N_A = K_G(P_{AG} - P_{A,e})$$

And the interfacial area for mass transfer is given by:

$$\text{interfacial area for mass transfer} = adV = aAdZ$$

If:

$$AG_M dY = N_A adV \quad \text{and} \quad P_{AG} = \frac{Y}{1+Y} P$$

Then:

$$G_M dY = K_G a P \left(\frac{Y_e - Y}{(1 + Y_e)(1 + Y)} \right) dZ$$

And the height (for concentrated systems) is thus given by:

$$Z = \frac{G_M}{K_G a P} \int_{Y_1}^{Y_2} \frac{(1 + Y_e)(1 + Y)}{Y_e - Y} dY$$

Where: G_M and L_M are the inert gas and liquid phase molar velocities per cross-sectional area respectively [mol/s.m^2]

X and Y are solute mole ratios in the liquid and gas phase respectively [$\text{mol CO}_2/\text{mol inert liquid or gas}$]

A is the cross-sectional area [m^2]

N_A is the mass transfer flux [mol/s.m^2]

K_G is the overall mass transfer coefficient based on the gas film [mol/Pa.s.m^2]

P_A is the partial pressure of A [Pa] (the subscript e denotes equilibrium)

P is the total system pressure [Pa]

a is the effective interfacial area [m^2/m^3]

V is volume [m^3]

Z is height [m]

This is one of a number of forms of the equation one could use to calculate the height. It is useful to have this equation in terms of the overall mass transfer coefficient as the integral is in terms of the equilibrium concentration (Y_e), which can be calculated. Also the overall coefficient may be determined experimentally, while the individual coefficient is only known under special circumstances (Richardson et al., 2002). When given in terms of the individual coefficient, Y_e is replaced with Y_i , the interface concentration, which is generally not known. An exception to this is if it is known that the absorption is gas or liquid film controlling. When absorption is liquid film controlling, as it is for this system (Green & Perry, 2008), then X_e is equal to X_i (Richardson et al., 2002).

The pre-integral term is sometimes considered as the height of a transfer unit, while the integral term is the number of transfer units. The simplified height equation may thus be written as:

$$Z = H_{OG}N_{OG} = H_{OL}N_{OL}$$

Where: H_{OG} and H_{OL} are the heights of the overall transfer units based on the gas and liquid phase respectively [m]

N_{OG} and N_{OL} are the number of transfer units based on the gas and liquid phase respectively

When the overall mass transfer coefficient is not known, the height of the overall transfer unit may be estimated based on the height of the individual gas and liquid phase transfer units. This method is applicable to cases where the equilibrium and operating lines are straight, or can be approximated as straight. The equation based on the gas phase is given as:

$$H_{OG} = H_G + \frac{m_{eL}}{m_{oL}} H_L$$

Where: H_G and H_L are the heights of the individual gas and liquid phase transfer units [m]

m_{eL} is the slope of the equilibrium line

m_{oL} is the slope of the operating line

As discussed previously, the rate of absorption is enhanced by a chemical reaction, which needs to be determined experimentally. Since experimental absorber testing was out of the scope of this thesis, height predictions based on physical absorption could be made with caution. The height of the transfer units was thus calculated in two different ways, in order to cross-check the various methods employed.

Cornell's method

This method, given by Sinnott (2005), is applicable to Berl saddles, and may be used to provide conservative estimates for Pall rings and Intalox saddles. It accounts for physical properties of the system, gas and liquid flow rates, and the column diameter. The column that was used in the experiments to determine this correlation was 0.305 m in diameter and 3.05 m in height. There are terms in the equations which correct for column dimensions; however, it is questionable as to whether these corrections can be extended to such a small column. Nevertheless, the correlation will be presented here. The results provided by this method are given in Table 14 and the sample calculations may be found in Appendix D. The equations are:

$$H_G = \frac{0.011\phi_h S_{C_v}^{0.5} \left(\frac{D_c}{0.305}\right)^{1.11}}{L_w f_1 f_2 f_3^{0.5}}$$

$$H_L = 0.305\phi_h S_{C_L}^{0.5} K_3$$

Where: H_G and H_L are the heights of the gas and liquid phase transfer units respectively [m]

S_{C_v} and S_{C_L} are the Schmidt numbers based on the gas and liquid phase respectively, given by: $Sc = \frac{\mu}{\rho D}$ [dimensionless]

D is the diffusivity, available for both the liquid and gas phase [m^2/s]

D_c is the column diameter [m]

K_3 , Ψ_h and ϕ_h are correction factors, which are read off Figure 45, Figure 46, and Figure 47, found in Appendix D)

L_w is the liquid flow rate per cross-sectional area [kg/m^2s]

f_1 , f_2 , and f_3 are viscosity, density and surface tension correction factors relative to water (taken as 1 in the calculations, as the solution is aqueous)

Onda's method

An alternative method, also provided by Sinnott (2005), provides equations to calculate the individual mass transfer coefficients, k_G and k_L , as well as the effective wetted area of the packing, a_w . These values may then be used to calculate height of the gas and liquid transfer units, H_G and H_L . The experimental work was based on Pall rings and Berl saddles. Once again, the results provided by this method are given in Table 14 and the sample calculations may be found in Appendix D. The equations are:

$$\frac{a_w}{a} = 1 - e^{-1.45 \left(\frac{\sigma_c}{\sigma_L}\right)^{0.75} \left(\frac{L_w}{a\mu_L}\right)^{0.1} \left(\frac{L_w^2 a}{\rho_L g}\right)^{-0.05} \left(\frac{L_w^2}{\rho_L \sigma_L a}\right)^{0.2}}$$

$$k_L \left(\frac{\rho_L}{\mu_L}\right)^{1/3} = 0.0051 \left(\frac{L_w}{a_w \mu_L}\right)^{2/3} \left(\frac{\mu_L}{\rho_L D_L}\right)^{-1/2} (ad_p)^{0.4}$$

$$\frac{k_G RT}{a D_v} = K_5 \left(\frac{V_w}{a\mu_v}\right)^{0.7} \left(\frac{\mu_v}{\rho_v D_v}\right)^{1/3} (ad_p)^{-2.0}$$

- Where:
- a_w is the effective wetted area of the packing [m^2/m^3]
 - a is the actual area of the packing [m^2/m^3]
 - σ_c is the critical surface tension of the packing material [N/m]
 - σ_L is the liquid surface tension [N/m]
 - ρ_L is the liquid density [kg/m^3]
 - g is the gravitational constant [$9.81 \text{ m}/\text{s}^2$]
 - k_L is the liquid film mass transfer coefficient [$\text{mol}/\text{m}^2\text{s.Pa}$]
 - d_p is the packing size [m]
 - k_G is the gas film mass transfer coefficient [m/s]
 - R is the ideal gas constant [$8.314 \text{ m}^3\text{Pa}/\text{K.mol}$]
 - $K_5 = 5.23$ for packing sizes larger than 15 mm, and 2.00 for sizes below this
 - V_w is the gas flow rate per cross-sectional area [$\text{kg}/\text{m}^2\text{s}$]

The following equations may then be used to calculate the height of the gas and liquid transfer units:

$$H_G = \frac{G_m}{k_G a_w P}$$

$$H_L = \frac{L_m}{k_L a_w C_t}$$

Where: P is the operating pressure [Pa]

C_t is the concentration ($C_t = \frac{\rho_L}{M_s}$) [mol/m³]

M_s is the molecular mass of the solvent [g/mol]

5.8. Results

Table 14 provides the column dimensions which were calculated by the methods presented in the previous sections. Results are given for both 20 and 50% excess solvent. As anticipated, the column diameters were found to be fairly small, in the range of 3.1 to 4.3 cm. The two methods used to predict the column height provided very different results. Cornell's method clearly underestimated the column height. As predicted, it is possible that the correlation does not extend to such small columns. These values should thus be ignored. Onda's method provided values which seemed more realistic than Cornell's method, with heights in the range of 5 to 15 cm. There is still large uncertainty associated with these values.

Table 14 Column dimensions

Solvent	5 mass % K ₂ CO ₃ solution		10 mass % K ₂ CO ₃ solution		
	Solvent excess	20%	50%	20%	50%
6mm Intalox saddles					
Column diameter [cm]		3.4	3.6	3.1	3.2
Column height [cm]					
<i>Cornell's method</i>		2.7	0.28	1.9	0.26
<i>Onda's method</i>		13	10	15	13
3mm Dixon rings					
Column diameter [cm]		3.4	3.6	3.1	3.2
Column height [cm]					
<i>Cornell's method</i>		2.7	0.28	1.9	0.26
<i>Onda's method</i>		6.9	5.3	7.7	6.4
6mm Raschig rings					
Column diameter [cm]		4.1	4.3	3.6	3.7
Column height [cm]					
<i>Cornell's method</i>		2.6	0.36	2	0.34
<i>Onda's method</i>		11	8.5	12	10

The height of the columns for the two different solutions were not very different, with the more concentrated solution associated with the taller column, owing to the smaller column diameter. The different packing types had a significant effect on the column height, with the packing with the highest surface area (the Dixon rings) requiring the shortest column. Comparing the excess solvent results, a taller column was calculated for the lower excess, as predicted. The differences in height were not substantial for Onda's method, but ranged by

as much as a factor 10 for Cornell's method when changing from 20% to 50% excess solvent – again indicating that this method might not apply for such a small column.

The column was designed for a pressure drop of 21 mm water, or approximately 200 Pa, per metre of packed height. Thus for a column height of 5 – 15 cm, the pressure drop across the absorber will be 10 – 30 Pa. This value is relatively low compared to supply pressures of 2000 – 7000 Pa (g) and should not have a great effect on the operation of the hob.

5.9. System Configuration and Integration

Figure 35 presents the proposed system integration for the absorber. The K_2CO_3 and water will need to be pre-mixed and stored in a tank, ready to be used when needed. A pump will transfer the solvent from the storage tank to the absorber where the biogas is scrubbed. In addition, it is recommended that the pressure of the raw biogas should be regulated. This is favourable for the correct operation of the gas hob, as well as allowing the pump speed to be fixed, thus simplifying the overall operation.

It is assumed that at start up, the line connecting the absorber to the hob will contain gas that was upgraded when the hob was previously used. It is also assumed that the absorber will not require a long start up period, based on the findings of Tippayawong & Thanompongchart (2010) that were discussed in the literature review. The implication of this is that only a small amount of gas, if any, will need to be purged before ignition is possible.

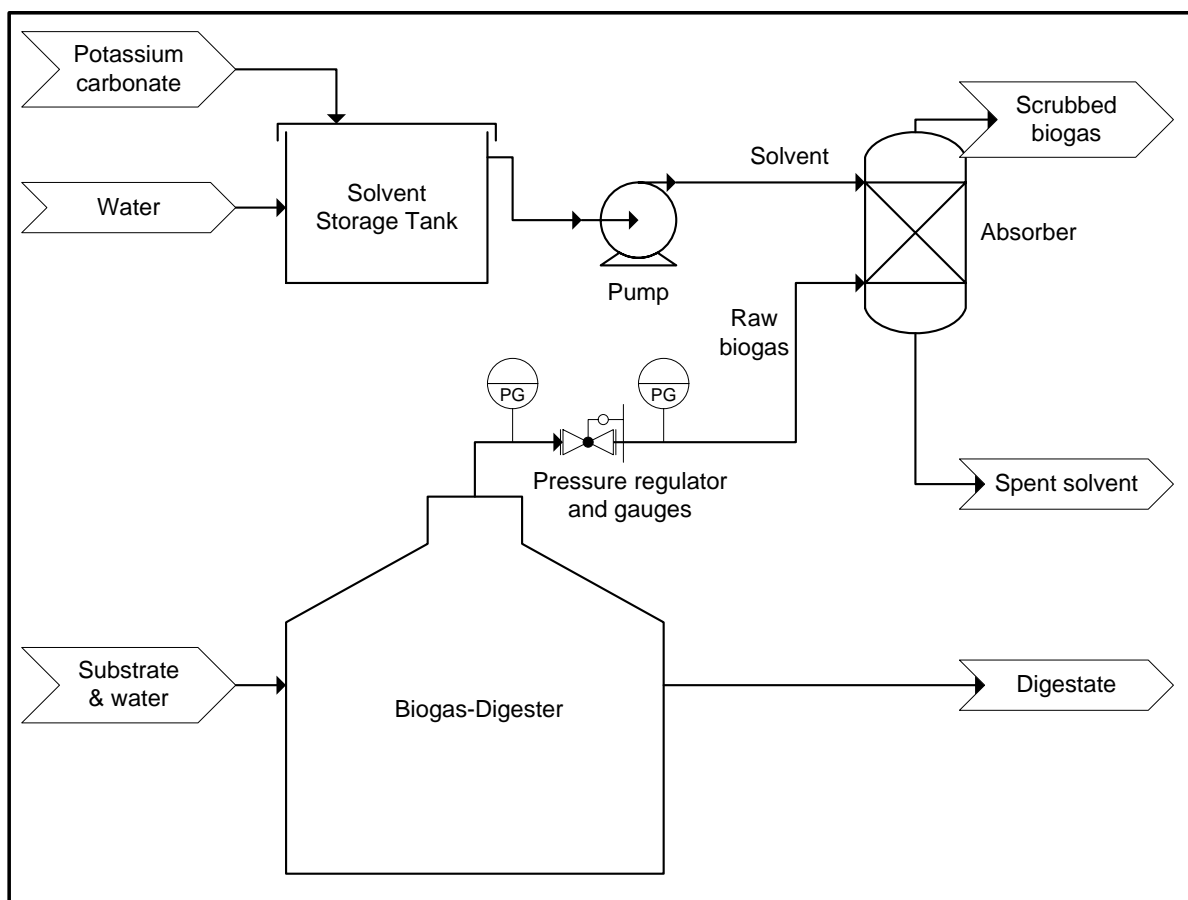


Figure 35 System Integration

The size of the storage tank required will depend on the biogas usage, the concentration of the solvent and the frequency with which the solvent is replenished. For example, for a solvent flow rate of 15 L/h and biogas required to produce a 3 kWh flame per day, used 7 days a week, a 250 L storage tank would be sufficient if the solvent is replenished fortnightly.

The pump size will depend on the solvent flow rate and the system configuration. The system configuration includes: the length, diameter, and material of construction of the pipe line connecting the storage tank to the pump, and the pump to the absorber; as well as the fittings that are installed along the line, such as bends, valves and flow metres.

Other options for the system configuration were to run the scrubber continuously as the biogas is being produced and store it for later use, with or without compressing it. This would have the benefit of reducing the size of the absorber required. Since the absorber was found not to be excessively large, and the compression and storage of the gas was seen as an unnecessary complication and additional cost, so it was decided that these options did not need to be considered.

5.10. Financial Viability

Possibly the most important aspect of this design is to determine if it is financially viable. As discussed in section Absorber Design 3.3, it was decided that the feasibility would be determined by a comparison of the operating costs (i.e. the solvent costs) to upgrade a certain amount of biogas and the cost of LPG that would be needed to produce an equivalent amount of energy.

On the basis of one hour of cooking time per day, for 30 days a month, the approximate consumption of K_2CO_3 could be calculated. This was considered to be the greatest operating cost. Other costs include electricity to run the pump and water. For a general usage comparison, the cost of K_2CO_3 may be compared to the cost of LPG, based on a 3 kW flame used for one hour of cooking per day. LPG was chosen over natural gas since it is the typical fuel used in South Africa that the biogas would replace. If the costs are on par, or the K_2CO_3 costs less than the LPG, then the absorber could possibly be considered viable.

Table 15 Price comparison

Solvent	5 % solution		10% solution		
	20%	50%	20%	50%	
Solvent excess					
K_2CO_3 required	30	37	31	39	kg/month
K_2CO_3 price	11.60	11.60	11.60	11.60	R/kg
K_2CO_3 cost	345	431	365	457	R/month
LPG price	19.44	19.44	19.44	19.44	R/kg
LPG calorific value	46.1	46.1	46.1	46.1	MJ/kg
LPG cost (3 kW flame)	137	137	137	137	R/month

Table 15 provides a comparison of the costs for both the 5 and 10 wt % solutions at 20 and 50% excess solvent. The K_2CO_3 price was based on a verbal quote from Crest Chemicals for food grade K_2CO_3 sold in 25 kg bags (Crest Chemicals, 2011). Four companies based in Cape Town were contacted for a quote; the cheapest quote was provided by Crest Chemicals. None of the four companies stocked industrial grade K_2CO_3 , which would be sufficient for the absorber, they only stocked food grade. The price was quoted excluding value added tax (Vat) and is subject to exchange rate fluctuations. The LPG price is the maximum retail price specified under the Petroleum Products Act, valid for 05 October 2011 to 01 November 2011 in the Cape Town zone (Department of Energy, 2011).

Based on the quote from Crest Chemicals, the cost of K_2CO_3 is significant compared to the cost of LPG. The cost is high enough to render an absorber infeasible, and possibly can only be justified if the spent solution was to be used as fertilizer. This may be a possibility if the digester is on a farm which requires this type of fertilizer in this quantity or more. The absorber could possibly become feasible with a lower grade K_2CO_3 at a price of about R4.50 per kg or less; this is the price at which the K_2CO_3 would be on par with the LPG cost.

Other options which could be considered include:

- Cheaper solvents
- A recycle stream could be included in the absorber design to reduce the amount of K_2CO_3 needed, although the reduction will be limited to the stoichiometry of the reaction between CO_2 and K_2CO_3 and the new equilibrium conditions. Based on the stoichiometry alone, the price would be decreased by a maximum of 40%. In practise this will be less as there are equilibrium constraints. This reduction is still not enough to make the design feasible.
- A stripper could be an option, although this would significantly complicate the system. The absorber would become significantly taller and an additional piece of equipment would be required, increasing the capital cost; as well as increasing the operating costs for the additional energy required to heat the solvent in the stripping process.

A further financial consideration is the effectiveness of the absorber not only to remove the CO_2 , but also to remove hydrogen sulphide (H_2S) present in the biogas. Presently a method for H_2S removal is necessary, as this gas is corrosive and has to be removed in order to protect the gas appliances (Petersson & Wellinger, 2009). The K_2CO_3 solvent is appropriate for the removal of acid gases in general, and could thus also be used for the removal of H_2S (Green & Perry, 2008). If the absorber can replace the H_2S removal device, its capital and operating cost could be saved.

5.11. Conclusions and Recommendations from the Absorber Design

5.11.1. Conclusions

Based on the experimental work, which was carried out with a gas hob, it was decided that the design of a CO₂ absorber should be undertaken. An aqueous K₂CO₃ solution was chosen as a suitable solvent, as the spent solvent had the potential to be used as fertilizer. The use of water as a solvent was excluded as it would require an impractically high flow rate, due to the low solubility of CO₂ in water at the low pressures created in fixed dome biogas digesters. The design was based on an upgraded biogas flow rate which would be required to produce a 3 kW flame, calculated to be approximately 0.4 m³/h.

It was decided that a packed column was the most suitable absorber type. The packed column was designed as well as possible, without experimental data or a professional software package. The column diameter was calculated to be 3 to 4 cm, and depended on the column packing and the flow rate of the solvent. The height could not be predicted with much confidence but appeared to be of the order of only 5-15 cm: experiments would be necessary to determine the required column height.

The feasibility of the absorber is ultimately dependent on the cost, thus the financial viability was studied. The cost of the K₂CO₃ which would be required to run the absorber was compared to the cost of LPG, which would provide approximately the same cooking time and flame power as the biogas. Only the K₂CO₃ cost was considered as this was anticipated to be fairly significant. Other costs included: the capital cost of the absorber, solvent tank and pump; and the operating costs, including: the electricity for the operation of the pump and water. It was found that if only the cost of the K₂CO₃ was considered, the absorber was already financially infeasible, unless there was a need for KHCO₃ fertiliser on the premises.

5.11.2. Recommendations

There are a number of options which could be considered in order to reduce the operating cost of the absorber, such as the use of a different solvent, and the inclusion of a stripper to regenerate the solvent. It is, however, not anticipated that the extra cost of an absorber will be justified for the benefits gained from using scrubbed biogas. It is thus recommended that more effort should rather be spent on the alteration of domestic gas appliances for their use with biogas.

Three different commercial packing types were used to calculate possible column dimensions, but in reality, due to the need to keep the cost down, the packing that will actually be used in the column may not be a packing that is commercially available. The

shape and material of construction greatly influences the way that the liquid is distributed and thus the rate of mass transfer. The rate of mass transfer is an important factor that affects the efficiency of a column and thus the height. Additionally, the packing size has an influence on the required column diameter. It is thus strongly recommended that various types of packing be tested in order to finalize the absorber design.

In addition to experimenting with different types of packing, sensitivity tests should be carried out at various temperatures. Solubility is strongly dependant on temperature, and should thus be a key consideration in the final design.

6. Conclusions and Recommendations

6.1. Purpose and Motivation

Household scale biogas production and use was the focus of this dissertation. Biogas is used for cooking, heating and lighting. Raw biogas is of a lower quality compared to typical household gaseous fuels: natural gas and LPG. It is similar to natural gas, as it is a methane-based fuel; but is not as concentrated as natural gas, with only 55 to 70% methane.

In general it is necessary to purchase special biogas appliances in order to utilize biogas. It is also possible to modify standard appliances or upgrade the biogas to a quality that is compatible with standard gas equipment.

Biogas upgrading is performed on an industrial scale, but has not been reported on a household scale, possibly as it is a relatively expensive and complicated process. It could have an application in cases where certain biogas appliances are not readily available, or if a household has existing standard gas appliances.

A need to test a standard gas appliance with a range of synthesized gas mixtures, similar to that of biogas and natural gas, was identified. The aim was to determine if biogas upgrading was required and, if it was, to what methane concentration it needed to be upgraded. Following on from this, the need to design a household scale biogas upgrading system was also established.

6.2. Hypotheses

A standard gas hob was chosen as the appliance that should be tested. The design and operation of a hob were reviewed. Two features were identified that could be fairly easily adjusted on a standard gas hob in order to make it compatible with biogas. These features were the injector size and the air intake.

In line with the purpose of the dissertation, various biogas upgrading technologies were reviewed and assessed in terms of their feasibility for use on a household scale. The technologies were assessed according to the following criteria: financial feasibility, safety,

environmental impact, ease of operation, and technology maturity. Absorption was found to be the most appropriate technology.

Informed by the literature, it was hypothesised that a standard gas appliance, namely a gas hob, would not operate when run on a gas that has the same composition as biogas if the hob had not been modified. Additionally, it was hypothesised that a household scale absorber for the upgrading of biogas, whilst technically feasible, would not be financially attractive.

6.3. Experimental Work

6.3.1. Approach

In order to either prove or disprove the first hypothesis, a standard gas hob was tested. Conditions expected in a real household biogas production and usage situation needed to be represented in the laboratory. Since biogas is typically composed of 55-70% methane and 30-45% carbon dioxide, 55% methane was chosen as the lowest limit. The gas compositions that were tested thus ranged from 55 to 100% methane, representing biogas as well as various levels of upgraded biogas.

Another important variable was identified as the gas supply pressure. This is dependent on the amount of biogas present in the digester. It is required to overcome the pressure drop in the line from the digester to the hob and to provide a driving force for the gas to flow. The available pressure decreases as the biogas is used. The effect of supply pressure on the operation of the hob was thus investigated.

In addition to the supply pressure, the operating pressure of the hob also needed to be considered. Most tests were carried out at the mid-range recommended operating pressure for natural gas (2 kPa), however, a range of pressures were also investigated in order to account for possible variations in the supply pressure.

Besides the various gas mixtures that were tested, the hob could be modified to be more compatible with biogas. The modification of the hob was limited to changing the injector size, while the air intake was kept constant.

6.3.2. Summary of Findings

The effect of a number of variables was investigated through the experimental work. The main findings are summarised here.

The results for gas composition versus water heating rate, for constant supply and operating pressures, showed that the water heating rate was higher at high supply pressures, with the small burner providing a higher heating rate than the large burner at the same supply pressure. The results for gas composition versus flame power showed that the flame power was highest at high supply pressures, although the big burner provided a higher flame power than the small burner at the same supply pressure. In contrast to these results and under the same conditions, the highest efficiencies were achieved by the small burner at low supply pressures, then by the small burner at mid-to-high supply pressures, and lastly by the big burner.

Table 16 Hob Efficiency Summary

Variable	Constant 1	Constant 2	Comment
Supply pressure	Gas composition	Operating pressure	Efficiency decreased as supply pressure increased The small burner was more efficient than the big burner
Operating pressure	Gas composition	Supply pressure	Efficiency increased with an increase in operating pressure The small burner performed better fitted with the 1.28 mm injector and at a lower supply pressure compared to the small burner fitted with the 0.95 mm injector
Operating pressure	Methane flow rate	Supply pressure	Efficiency increased with an increase in operating pressure The small burner fitted with the 1.28 mm injector performed better than the small burner fitted with the 0.95 mm injector, followed by the big burner
Flow rate	Gas composition	Supply pressure	Efficiency decreased with an increase in the flow rate The small burner performed better fitted with the 1.28 mm injector and at a lower supply pressure compared to the small burner fitted with the 0.95 mm injector
Flow rate	Gas composition	Operating pressure	Efficiency decreased with an increase in the flow rate The small burner was more efficient than the big burner
Gas composition	Methane flow rate	Supply pressure	Efficiency decreased with a decrease in the methane content of the gas (and thus an increase in the flow rate) The small burner fitted with the 1.28 mm injector performed better than the small burner fitted with the 0.95 mm injector, followed by the big burner
Gas composition	Supply pressure	Operating pressure	The small burner, at low supply pressures was most efficient, followed by the small burner at high supply pressures, and lastly the big burner The gas composition did not effect the hob efficiency

For experiments where the operating pressure varied, but the methane flow rate and the supply pressure were constant, the highest water heating rate was produced by the small

burner fitted with the larger (1.28 mm) injector, followed by the small burner fitted with the 0.95 mm injector, and then by the big burner. The flame power was greater at a higher supply pressure, with a constant operating pressure; and at a lower operating pressure, with a constant supply pressure.

The hob efficiency was investigated for a number of system variables under different conditions; Table 16 provides a summary of the findings. The title *variable* refers to the graphs that were plotted against hob efficiency. The system only allowed for two variables to be kept constant at a time. In general the small burner performed better than the big burner since a small pot was used during the experiments; it was the correct size for use with the small burner but inadequate for use with the big burner thus decreasing the efficiency.

One of the important objectives was to find the lowest possible composition of methane required to be able to use the hob. The cut-off composition was approximately 10-15% lower (at ~62%) for the small burner fitted with the 1.28 mm injector, compared to ~ 77% for the small burner fitted with the 0.95 mm injector and ~74% for the big burner, which throughout was fitted with the 1.28 mm injector. A methane content of 80% was thus considered sufficient to be compatible with a standard hob.

6.4. Absorber Design

6.4.1. Approach

Based on the findings of the experimental work, a household scale absorber was designed. The first step was to decide on the system configuration. The simplest option was to have an inline absorber, which could upgrade the biogas as it was being used. The flow rate of the upgraded biogas was specified by the flow rate required to produce a 3 kW flame in a hob, while the required composition was specified by the experimental findings (80% methane). The absorber design was carried out based on theory.

Most of the typical steps that are taken when designing an industrial absorber were applied to this design. These included: solvent and equipment choice, solvent flow rate determination, and column dimension calculations. In the interest of specifying a robust and simple to operate unit, a stripper was not included in the design and the column was restricted to operating at ambient conditions.

6.4.2. Summary of Findings

Due to the restrictions on the operating temperature and pressure, a chemical solvent was required. A suitable solvent was found to be an aqueous K_2CO_3 solution, due to its potential to be used as a fertilizer once reacted to $KHCO_3$ by absorbing CO_2 from the biogas. A packed column type absorber was chosen due its suitability to the small scale. Since three different types of packing and two different solvent strengths, at two different flow rates each, were used to calculate the column dimensions, a range for column diameter and height resulted. The column diameter and a height were calculated to be 3 to 4 cm and 5 to 15 cm respectively; although experiments are recommended to confirm these values.

It was determined that the absorber would cost more to run, in terms of the cost of the required K_2CO_3 , than it would cost to buy the amount of LPG required to produce a 3 kW flame (based on local South African prices). The lowest K_2CO_3 price was found to be ZAR 11.60 /kg; while the calculations showed that a maximum price of ZAR 4.59 /kg would be required for the upgraded biogas to be competitive with LPG.

6.5. Conclusions

This dissertation had two main objectives:

1. To investigate the performance of a standard home appliance run on synthesized biogas, with varying methane content.
2. To design a CO_2 scrubber that may be used in a household biogas digester system.

It is safe to state that these objectives have been met; however, linked to the first objective were a number of sub-objectives that needed to be considered. The first sub-objective of the experimental work was to determine the minimum methane content of biogas required to be used in a standard gas hob. It became clear that there was no simple solution to this objective. It may be claimed that it is acceptable that the biogas should be upgraded to 80% methane, when the cut off compositions are considered.

However, there is an alternative option, which accords with the second sub-objective. The small burner fitted with the 1.28 mm injector produced the highest efficiency, followed by the small burner fitted with the 0.95 mm injector, and then by the big burner, for experiments where the methane flow rate and supply pressure were constant (varying gas composition). A higher efficiency was also produced for the small burner fitted with the 1.28 mm for experiments where the gas composition and supply pressure were constant (varying flow rate). The small burner fitted with the 1.28 mm injector also demonstrated the ability

to ignite the lowest quality gas. It may thus be argued that the biogas does not require upgrading; and rather that hob modification may be sufficient.

Conversely, the water heating rate and hob efficiency were both shown to decrease with an increase of inert gas, i.e. carbon dioxide, for experiments where the methane flow rate and the supply pressure remained constant. An advantage of upgrading the biogas could thus include faster cooking rates and higher appliance efficiency. The main disadvantage is the cost of upgrading the biogas, as well as the additional pressure drop due to the absorber. A further concern is the environmental impact of the absorber, especially in the context of being used with a technology which is considered to be environmentally beneficial. These concerns were addressed during the absorber design.

Both of these options thus demonstrated their own advantages and disadvantages, corresponding to the third sub-objective. An absorber was thus designed in order to determine more certainly if the option of upgrading biogas is feasible.

The feasibility of the absorber was dependent on certain criteria outlined with the objectives. While the other criteria were used as guidelines for the design of the absorber, the cost of the absorber was rather an outcome of the design. It was thus the ultimate deciding factor for the absorber feasibility.

The method of determining the financial feasibility was to compare the cost of the K_2CO_3 , which would be required to run the absorber, to the cost of LPG, which would provide a 3 kW flame. The K_2CO_3 cost was anticipated to be significant, and was thus estimated before other costs, including: the capital cost of the absorber, solvent tank and pump; and the operating costs, including: the electricity for the operation of the pump and water. The result was as anticipated: the cost of the K_2CO_3 was significant, enough so that the absorber was determined to be infeasible before other costs were taken into account.

Based on these findings, it can be concluded that the modification of a standard gas hob is preferable over upgrading the biogas. Furthermore, the first hypothesis could be supported: with a large injector the hob could indeed operate, and with reasonable efficiency, at typical biogas compositions. The second hypothesis could also be supported, since the solvent costs were found to be prohibitively high compared to the possible economic advantages of using this device, and thus a financially feasible absorber design was not found.

6.6. Recommendations

A number of recommendations have already been mentioned, based on both the experimental work and the absorber design. These are re-stated and elaborated on in this final section of the dissertation.

Further testing with a hob should be carried out with real biogas, in order to account for some factors which may not have been included during this experimental work. One of these factors is the ambient temperature, which varies daily and seasonally. The temperature affects the moisture content of the gas, which may affect the performance of the hob. The biogas supply pressure should be investigated under real conditions, since this variable plays an important role in the performance of the hob.

Since the experimental work showed that larger injector sizes allow for the ignition of a lower quality gas than what was specified, a range of injector sizes should be tested. Thus the optimum size may be found, in terms of the water heating rate and hob efficiency. Additionally, the effect of the air intake was not explored in this dissertation, and further experiments could be carried out to determine its effect.

In addition to further tests carried out with a gas hob, other gas appliances should be investigated to determine if they could be modified to be compatible with biogas.

Although the absorber design was found to be infeasible, there are some options which could still be considered in order to reduce the operating cost of the absorber; with the main ones being the use of a different solvent and the inclusion of a stripper. The benefits of this exercise may not, however, be justified, and it is the author's opinion that the time would be better spent modifying and testing standard gas appliances.

There are a number of recommendations that can be made, if it is desired that the absorber design should be taken further. First and foremost, a prototype should be built and tested with various types of packing, packing heights, solvents, solvent strengths, and solvent flow rates. Variations in temperature should also be included in order to finalize the design.

References

Afrox. (2001). *Material Safety Data Sheet: Methane*. Afrox.

Agama Energy (a). (2011, June 22). *Product Datasheet*. Retrieved 12 16, 2011, from BiogasPro: <http://www.biogaspro.com/download/product-information-download-supporting-documentation.html>

Agama Energy (b). (2011, June 22). *BiogasPro Information Overview*. Retrieved 11 22, 2011, from BiogasPro: http://www.biogaspro.com/download/product-information-download-supporting-documentation/item/information-overview-2.html?category_id=3

Austin, G. (2011, June 19). *About Biogas*. Retrieved July 11, 2011, from BiogasPro: <http://www.biogaspro.com/about-biogas.html>

Crest Chemicals. (2011, 10 20). Potassium carbonate quote.

de Hullu, J., Maassen, J. I., van Meel, P. A., Shazad, S., & Vaessen, J. M. (2008). *Comparing different biogas upgrading techniques*. Eindhoven: Dirkse Milieutechniek and Eindhoven University of Technology.

Department of Energy. (2011, 10 4). *Maximum Retail Price for Liquefied Petroleum Gas*. Retrieved 10 20, 2011, from Liquefied Petroleum Gas Safety Association of South Africa: <http://www.lpgas.co.za/page34/page34.html>

Deublein, D., & Steinhauser, A. (2008). *Biogas from Waste and Renewable Resources: An Introduction*. Weinheim: Wiley-VCH.

Eze, J. I. (2010). Preliminary Studies on Biogas Scrubbing System for Family Sized Biogas Digester. *Global Journal of Science Frontier Research*, vol. 10, Issue 3 , 12-17.

Fraenkel, P. L. (1986). *Water Lifting Devices*. Retrieved July 11, 2011, from Food and Agriculture Organization of the United Nations (FAO): <http://www.fao.org/docrep/010/ah810e/ah810e00.htm>

Gowariker, V., Krishnamurthy, V. N., Gowariker, S., Dhanorkar, M., & Paranjape, K. (2009). *The Fertilizer Encyclopedia*. New Jersey: John Wiley & Sons Inc.

Green, D. W., & Perry, R. H. (2008). *Perry's Chemical Engineers' Handbook, 8th edition*. McGraw-Hill.

International Union of Pure and Applied Chemistry (IUPAC). (2011, 10 11). *Compendium of Chemical Terminology Gold Book, version 2.3*. Retrieved 10 26, 2011, from IUPAC Gold Book: <http://goldbook.iupac.org/PDF/goldbook.pdf>

IPCC. (2007). *IPCC Fourth Assessment Report: Climate Change 2007*. Retrieved 2012, from http://www.ipcc.ch/publications_and_data/ar4/wg1/en/ch2s2-10-2.html

Kapdi, S. S., Vijay, V. K., Rajesh, S. K., & Prasad, R. (2004). Biogas scrubbing, compression and storage: perspective and prospectus in Indian context. *Renewable Energy* , 1-8.

Kapdi, S., Vijay, V., Rajesh, S., & Prasad, R. (2006). Upgrading biogas for utilization as a vehicle fuel. *Asian Journal on Energy and Environment* , 387-393.

Khandelwal, K. C., & Gupta, V. K. (2009). *Popular Summary of the Test Reports on Biogas Stoves and Lamps prepared by testing institutes in China, India and the Netherlands*. The Hague: SNV Netherlands Development Organisation.

Knuutila, H., Juliussen, O., & Svendsen, H. F. (2010). Kinetics of the reaction of carbon dioxide with aqueous sodium and potassium carbonate solutions. *Chemical Engineering Science* 65 , 6077-6088.

Melamu, R. (2011, 01). African Biogas Experts meeting in Addis Abbaba. (C. Trautmann, Interviewer)

Park, S.-B., Shim, C.-S., Lee, H., & Lee, K.-H. (1997). Solubilities of carbon dioxide in the aqueous potassium carbonate and potassium carbonate-poly(ethylene glycol) solutions. *Fluid Phase Equilibria* 134 , 141-149.

Perry, R. H., Green, D. W., & Maloney, J. O. (1997). *Perry's Chemical Engineers' Handbook, Seventh Edition*. McGraw-Hill.

Persson, M. (2003). *Evaluation of Upgrading Techniques for Biogas*. Lund: School of Environmental Engineering, Lund University.

Petersson, A., & Wellinger, A. (2009, 10). *Biogas upgrading technologies- developments and innovations*. Retrieved 10 27, 2011, from IEA - Biogas: http://www.iea-biogas.net/_download/publi-task37/upgrading_rz_low_final.pdf

Pingxiang Naik Chemical Industry Equipment Packing Co. (2011). *Dixon Ring*. Retrieved 10 20, 2011, from <http://www.laiko.net/pdlistone/products/7123503.html>

Poling, B., Thomson, G., Friend, D., Rowley, R., & Wilding, W. (2008). *Perry's Chemical Engineers' Handbook, 8th Edition, Section 2: Physical and Chemical Data*. The McGraw-Hill Companies, Inc.

REN21. (2011). *Renewables 2011 Global Status Report*. Paris: REN21 Secretariat.

Richardson, J. F., Harker, J. H., & Backhurst, J. R. (2002). *Particle Technology and Separation Processes, 5th Edition*. Butterworth-Heinemann.

SGE Analytical Science. (2011). *GC Columns > SolGel-WAX*. Retrieved 10 27, 2011, from SGE Analytical Science: http://www.sge.com/products/columns/gc-columns/forte-solgel-wax/product-table2-1?func=viewDetails;webgui_id=YP-A_ZxfeARnOnDZQa8WXQ

Sinnott, R. K. (2005). *Chemical Engineering Design, Volume 6*. Oxford: Elsevier.

Sustainable Development Department, Food and Agriculture Organization of the United Nations (FAO). (1997). *A System Approach to Biogas Technology*. Retrieved 7 11, 2011, from SD Dimensions: <http://www.fao.org/sd/EGdirect/EGre0022.htm>

The Dow Chemical Company. (2003, 12 03). *Material Safety Data Sheet for DEA*. Retrieved 12 2011, from The Dow Chemical Company: http://msdssearch.dow.com/PublishedLiteratureDOWCOM/dh_0044/0901b803800447ea.pdf?filepath=amines/pdfs/noreg/111-01401.pdf&fromPage=GetDoc

The Dow Chemical Company. (2003, 06 17). *Material Safety Data Sheet for MEA*. Retrieved 12 2011, from The Dow Chemical Company: http://msdssearch.dow.com/PublishedLiteratureDOWCOM/dh_0044/0901b80380044789.pdf?filepath=amines/pdfs/noreg/111-01388.pdf&fromPage=GetDoc

Tippayawong, N., & Thanompongchart, P. (2010). Biogas quality upgrade by simultaneous removal of CO₂ and H₂S in a packed column reactor. *Energy* 35 , 4531-4535.

Wheeler, P., Jaatinen, T., Lindberg, A., Hom-Nielsen, J., Wellinger, A., & Pettigrew, A. (2000). *Biogas Upgrading and Utilisation*. Retrieved 08 2011, from IEA Biogas: http://www.iea-biogas.net/_download/publi-task37/Biogas%20upgrading.pdf

Whirlpool Corporation. (n.d.). *Product Description Sheet*. Retrieved 7 12, 2011, from Whirlpool: <http://www.whirlpool.co.za/ifudocs/501931962030GB.pdf>

Whirlpool, C. (2011, May). Whirlpool Hob Information. (C. Trautmann, Interviewer)

Zanussi. (n.d.). *Mixed fuel cooker ZCM 631: Instruction Booklet*. Retrieved 07 13, 2011, from http://www.manualshark.org/manualshark/files/6/pdf_13074.pdf

Appendix A

Methane Material Safety Data Sheet



MATERIAL SAFETY DATA SHEET

METHANE

DATE: April 2001

1 PRODUCT AND COMPANY IDENTIFICATION

PRODUCT IDENTIFICATION

Product Name METHANE
Chemical Formula CH₄
Trade Names Methane (N2.5)
Methane (N3.5)
Colour Coding Signal Red (A.11) body with a Black band round the centre of the cylinder
Valve Neri - Brass 5/8 inch left hand female
Company Identification African Oxygen Limited
23 Webber Street
Johannesburg, 2001
Tel. No: (011) 490-0400
Fax No: (011) 490-0506

2 COMPOSITION/INFORMATION ON INGREDIENTS

Chemical Name Methane
Chemical Family Paraffins
CAS No. 74-82-8
UN No. 1971
ERG No. 115
Hazard Warning 2A flammable gas

3 HAZARDS IDENTIFICATION

Main Hazards All cylinders are portable gas containers, and must be regarded as pressure vessels at all times. Methane poses hazards to personnel through its flammability. All the precautions necessary for the safe handling of any flammable compressed gas must be observed in working with Methane.

Adverse Health Effects Methane is classified as a simple asphyxiant. It is practically physiologically inert, except when it lowers the partial pressure of oxygen in the air enough to cause systemic effects due to oxygen-deficiency.

Chemical hazards No known hazards
Biological Hazards No known effect
Vapour Inhalation No known effect
Eye contact No known effect
Skin contact No known effect
Ingestion No known effect

4 FIRST AID MEASURES

The conscious person who becomes aware of nausea and pressure on the forehead and eyes should go promptly to an uncontaminated area and inhale fresh air or oxygen. However, in the event of a massive exposure the victim may become unconscious or symptoms of asphyxiation may persist. In that case the person should be removed to an uncontaminated area, and given artificial respiration and then oxygen, after breathing has been restored. Treat symptomatically thereafter.

5 FIRE FIGHTING MEASURES

Extinguishing media Dry powder. Carbon dioxide. Fog-water spray. (In the absence of fog equipment a fine spray of water may be used).

Specific hazards Highly flammable. May form explosive gas mixtures with air. Is a simple asphyxiant.

Emergency actions If possible, shut off gas flow at source. Evacuate area. Post warning to prevent persons from approaching with lit cigarettes or open flames. Using water, keep all cylinders in the vicinity of the fire cool. Remove cylinders from the vicinity of the fire if possible. Allow small fires on cylinders to remain burning if they are not posing a hazard. CONTACT THE NEAREST AFROX BRANCH.

Protective clothing Exposed fire fighters should wear approved self-contained breathing apparatus with full mask.

Environmental precautions. As the gas is lighter than air, ensure that it is not trapped in confined spaces. This could lead to the formation of a highly explosive gas-air mixture. Ventilate all confined spaces using forced-draught if necessary. Ensure that all electrically powered equipment is flameproof.

6 ACCIDENTAL RELEASE MEASURES

Personal precautions. As Methane is a simple asphyxiant care should be taken when entering confined spaces where leaks have occurred. Do not enter any potentially hazardous area with any source of ignition such as a lit cigarette or match.

Environmental precautions. Methane does not pose a hazard to the environment. An explosive gas-air mixture could be formed when leaks occur, so eliminate all forms of ignition.

Small spills Small leaks should be extinguished by shutting off the source of supply, e.g. closing the valve on the cylinder, or tightening the gland nut. If unable to stop small leaks the cylinder should be moved into the open, well away from any source of ignition. Should a small leak have ignited, use a multi-purpose dry powder or carbon dioxide extinguisher. Should there be no extinguisher available, a welders glove or heavy cloth, soaked in water may be used to extinguish the flame.

Large spills Stop the source if it can be done without risk. Eliminate all sources of ignition and static discharges. Restrict access to the area until completion of the clean-up procedure. Post relevant warning signs. Wear adequate protective clothing when working near the source of the leak. Ventilate the area using forced-draught if necessary. Ensure that all equipment is flameproof.

7 HANDLING AND STORAGE

Do not allow cylinders to slide or come into contact with sharp edges. Methane cylinders may be stacked horizontally provided that they are firmly secured in order to prevent rolling. Ensure that equipment is adequately earthed. Conspicuous signs should be posted in the storage area forbidding smoking or the use of naked lights. Use a "first-in - first-out" inventory system to prevent full cylinders from being stored for excessive periods of time. Compliance with all relevant legislation is essential. Keep out of reach of children.

8 EXPOSURE CONTROLS/PERSONAL PROTECTION

Occupational exposure hazards No known effect.

Engineering control measures. Engineering control measures are preferred to reduce exposures. General methods include mechanical ventilation, process or personal enclosure, and control of process conditions. Administrative controls and personal protective equipment may also be required. Use a suitable flameproof ventilation system separate from other exhaust ventilation systems. Exhaust direct to outside. Supply sufficient replacement air to make up for air removed by exhaust system.

Personal protection Use self-contained breathing apparatus when fighting large fires.

Eyes. Use safety glasses when working with cylinders.

Hands. Use suitable protective gloves when working with cylinders.

Feet. Wear protective footwear when working with cylinders.

Skin. No known effect.

9 PHYSICAL AND CHEMICAL PROPERTIES

PHYSICAL DATA

Chemical Symbol	CH ₄
Molecular Weight	16,04
Specific volume @ 20°C & 101,325 kPa	1474,0 ml/g
Relative density of gas @ 101,325 kPa (Air=1)	0,555
Flammability limits in air	5,0 - 15,4% (by vol)
Autoignition temperature	537°C
Colour	None
Taste	None
Odour	Sweet, oil-type

10 STABILITY AND REACTIVITY

Conditions to avoid Overheating of cylinders. Keep sparks and flames away from cylinder, and under no circumstances allow a torch flame to come into contact with any part of the cylinder. Never test for leaks with a flame. Use soapy water when testing for leaks. Never use cylinders as rollers or supports, or for any other purposes other than the storing of Methane.

Incompatible materials. Methane is non-corrosive and may be contained at ambient temperatures by most common metals used in installations designed to have sufficient strength for the working pressures involved.

Hazardous Decomposition Products. No hazardous compounds are formed when Methane / air mixtures burn.

11 TOXICOLOGICAL INFORMATION

Acute Toxicity	No known effect
Skin & eye contact	No known effect
Chronic Toxicity	No known effect
Carcinogenicity	No known effect
Mutagenicity	No known effect
Reproductive Hazards	No known effect

For further information see Section 3. Adverse Health Effects

12 ECOLOGICAL INFORMATION

As Methane is lighter than air it will disperse rapidly in open areas. It does not pose a hazard to the ecology.

13 DISPOSAL CONSIDERATIONS

Disposal Methods Small amounts may be blown to the atmosphere under controlled conditions. No sources of ignition should be in the vicinity. Large amounts should only be handled by the gas supplier.

Disposal of packaging. The disposal of containers must only be handled by the gas supplier.

14 TRANSPORT INFORMATION

ROAD TRANSPORTATION

UN No.	1971
Class	2.1
Subsidiary risk	Asphyxiant
ERG No	115
Hazchem warning	2 A Flammable gas

SEA TRANSPORTATION

IMDG	1971
Class	2.1
Label	Flammable gas

AIR TRANSPORTATION

ICAO/IATA Code	1971
Class	2.1
Subsidiary risk	Flammable gas
Packaging instructions	
- Cargo	200

- Passenger	Forbidden
Maximum quantity allowed	
- Cargo	150 kg
- Passenger	Forbidden

15 REGULATORY INFORMATION

EEC Hazard class	Flammable gas
Risk phrases	R11 Highly flammable R18 In use may form flammable explosive vapour-air mixture R44 Risk of explosion if heated under confinement
Safety phrases	S2 Keep out of reach of children S3 Keep in a cool place S9 Keep container in a well ventilated place S16 Keep away from sources of ignition S33 Take precautionary measures against static discharges S37 Wear suitable gloves S39 Wear eye/face protection S51 Use only in well ventilated areas

National legislation

Refer to SABS 0265 for explanation of the above

16 OTHER INFORMATION

Bibliography
Compressed Gas Association, Arlington, Virginia
Handbook of Compressed Gases - 3rd Edition
Matheson. Matheson Gas Data Book - 6th Edition
SABS 0265 - Labelling of Dangerous Substances

17 EXCLUSION OF LIABILITY

Information contained in this publication is accurate at the date of publication. The company does not accept liability arising from the use of this information, or the use, application, adaptation or process of any product described herein.



A member of The AFROX Group

The Stripe Symbol and the word AFROX are AFROX Group Trademarks.

For product and safety enquiries please phone

EMERGENCY N°:
0860020202 (24 hr)

Photographs of the Experimental Apparatus



Pressure gauge - measures supply pressure

Pressure gauge - measures operating pressure

Gas sampling point

Cylinder - used to add moisture to the gas

Rotameter - carbon dioxide

Shield - used to reduce the draught caused by the fume hood

Rotameter - methane

Figure 36 Experimental apparatus



Figure 37 Whirlpool gas hob



Figure 38 Gas hob, showing burner heads and caps



Figure 39 Burner head, with injection candle and injector nozzle



Figure 40 Small burner in operation with a weak flame that was not well-dispersed by the burner crown



Figure 41 Small burner in operation with large, strong flames

Gas Chromatograph Details

Table 17 Gas Chromatograph details (SGE Analytical Science, 2011)

Brand	SGE
Part number	54788
Type	Sol Gel- WAX
Length [mm]	30
Inner diameter [mm]	0.32
Film thickness [um]	0.25
Max temperature [°C]	30 to 260/280

Appendix B

Raw Data

Table 18 Raw data

Water start temp	Water end temp	Supply Pressure	Operating Pressure	Rotameter CH ₄	Rotameter CO ₂	Time	Burner	Gas composition	Injector	Wet/dry
°C	°C	kPa	kPa	cm	L/min air	s	big/small	% CH ₄	mm	
19.5	58	26	3	1.2		1067.2	small	72%	0.95	dry
20	50	26	3	1.55		873.3	small	70%	0.95	dry
20.5	58	26	2	2.8		754.2	big	70%	1.28	dry
19	52	28	2	3.7		621.2	big	75%	1.28	dry
19.5	55	28	2	3.85		580.4	big	75%	1.28	dry
19.6	53	28	3.2	2.6		616.5	small	75%	0.95	dry
18.5	56	28	2	3.4	0.4	679	big	78%	1.28	dry
19.7	57	28	2	3.25	0.4	718.3	big	78%	1.28	dry
19.5	56	28	3.4	5		489.5	small	100%	0.95	dry
20	58	28	3.4	4.9		461.6	small	100%	0.95	dry
18.5	50	28	2	3.8	0.35	481.5	big	84%	1.28	dry
19	48	26	3	2.4	0.4	541.3	small	80%	0.95	dry
19	51	26	0.8	2.9	0.4	425.1	big	80%	1.28	dry
19	58	26	2.6	2.35	0.1	412.4	small	87%	0.95	dry
19	52	24	2	2		349.2	small	83%	0.95	dry
19	53	24	2	1.6	0.15	402.8	small	72%	0.95	dry
17	45	22	2	0.8		359.8	small	77%	0.95	dry
16.4	45	20	2	1.1	0	293.2	small	100%	0.95	dry
17.5	47	22	2	2.4	0	253.5	small	100%	0.95	dry
18.2	46	24	2	3.5	0	226.8	small	100%	0.95	dry
17.8	50	26	2	4.4	0	260.2	small	100%	0.95	dry
18	51	28	3	5.1	0	260.8	small	100%	0.95	dry
17.4	47	22	1	3	0	289	small	100%	0.95	dry
18	59	22	2	2.3	0	374	small	100%	0.95	dry
19.5	56	26	3	4.4	0	288.3	small	100%	0.95	dry
19.5	50	26	4	4	0	242.9	small	100%	0.95	dry
19.5	50	26	6	3.25	0	248.9	small	100%	0.95	dry
19.5	45	26	8	2.2	0	235	small	100%	0.95	dry
19.3	51	26	10	1.3	0	327.3	small	100%	0.95	dry
18.8	45	26	4	2.6		259.4	small	84%	0.95	dry
18.5	46	26	6	1.55		294.4	small	84%	0.95	dry
19.3	55	24	3	3.2	0	274.3	small	100%	1.28	dry
19.3	54	24	5	2.2	0	285.5	small	100%	1.28	dry
19.3	45	24	7	1.2	0	255.8	small	100%	1.28	dry
17.4	55	26	2	5	0	322.4	big	100%	1.28	dry
17.7	50	28	3.2	5.2	0	230.8	small	100%	0.95	dry
18.5	50	28	2	6.15	0	244.3	big	100%	1.28	dry
19.3	50	22	2	1.2		371.2	small	86%	0.95	dry
19.8	50	22	2	1.25		492.1	big	86%	1.28	dry
20.7	50	22	2	0	0.1	494.2	small	80%	0.95	wet
20.5	50	22	1	0.7	0.15	548.5	big	80%	1.28	wet

Raw data continued

Water start temp °C	Water end temp °C	Supply Pressure kPa	Operating Pressure kPa	Rotameter CH ₄ cm	Rotameter CO ₂ L/min air	Time s	Burner big/small	Gas composition % CH ₄	Injector mm	Wet/ dry
16.8	50	24	3	0.55	0.2	504.3	small	79%	0.95	dry
17	50	24	2	0.75	0.25	579.4	big	79%	1.28	dry
18.2	50	24	3	0.9	0.35	452.5	small	76%	0.95	dry
19	53	24	3	0.78	0.2	500.5	small	73%	0.95	dry
19.6	50	24	3	1.65		366.2	small	83%	0.95	dry
20.1	50	24	2	2.35		403.2	big	83%	1.28	dry
20.1	51	26	4	1.4	0.15	347.6	small	82%	0.95	dry
20.5	50	26	2	2.68	0.2	376.6	big	82%	1.28	dry
20.5	50	26	4	2	0.3	373.3	small	74%	0.95	dry
20.8	50	26	4	4.2		264.1	small	77%	0.95	dry
20.8	50	26	2	4.8		295	big	77%	1.28	dry
17.5	50	28	6	4.6		291.5	small	91%	0.95	dry
18.5	50	28	2	4.3	0.1	353.9	big	90%	1.28	dry
19.1	53	28	6	1.85	0.3	408.7	small	80%	0.95	dry
18.8	50	28	2	4.75	0.25	369.4	big	82%	1.28	dry
20	50	28	6	1.3	0.45	458.5	small	69%	0.95	dry
19.5	50	28	2	4.35	0.1	303.5	big	91%	1.28	dry
19.8	50	28	2	4	0.65	452.2	big	79%	1.28	dry
19.8	51	26	6.4	3		304.2	small	87%	0.95	dry
16.5	50	26	6	3		370.1	big	87%	1.28	dry
16.2	50	26	6	3		335.2	small	87%	0.95	dry
16.3	50	26	6	3		410.4	big	87%	1.28	dry
17.5	50	26	5.3	3	0.05	334.5	small	85%	0.95	dry
18.6	51	26	5.3	3	0.05	383.2	big	85%	1.28	dry
19	50	26	4	3	0.1	362.4	small	82%	0.95	dry
19.6	50	26	5	3	0.1	377.3	big	82%	1.28	dry
19.8	50	26	3.7	3	0.2	330.9	small	81%	0.95	dry
20.3	51	26	1.2	3	0.7	462.9	big	63%	1.28	dry
20	50	22	2	3.15	0	295.3	big	100%	1.28	dry
20.7	50	24	2	3.85	0	286.6	big	100%	1.28	dry
20.8	50	28	6	4.35	0	244.6	small	100%	0.95	dry
20.5	50	28	2	6.3	0	242	big	100%	1.28	dry
20.9	50	26	7	3	0	268.7	small	100%	0.95	dry
20.9	50	26	6.8	3	0	307.7	big	100%	1.28	dry
20.4	53	26	4.3	3	0	311.9	small	100%	0.95	wet
19.5	50	26	4.6	3	0	306.9	big	100%	1.28	wet
20.3	50	22	2	1.95	0	306.1	small	100%	0.95	wet
20.3	50	22	1	2.75	0	344.6	big	100%	1.28	wet
20.8	50	22	2	2.95	0	285.4	small	100%	0.95	dry
20.8	51	24	3	3.25	0	277.5	small	100%	0.95	dry
20.3	51	22	1	2.5	0	302	small	100%	1.28	wet
20.7	52	22	2	2	0	312.3	small	100%	1.28	wet
20.5	51	26	4.7	3	0	266.7	small	100%	1.28	wet
20.9	50	26	5.1	3	0	257	small	100%	1.28	wet
20.7	50	22	1	2.6	0	267	small	100%	1.28	dry
20.5	50	22	2	2.2	0	294.7	small	100%	1.28	dry
20.6	50	26	6.5	3	0	251.4	small	100%	1.28	dry
17.2	52	22	1	1	0.25	411.2	small	72%	1.28	wet
17	50	22	2	0.5	0.35	425.8	small	78%	1.28	wet

Raw data continued

Water start temp °C	Water end temp °C	Supply Pressure kPa	Operating Pressure kPa	Rotameter CH ₄ cm	Rotameter CO ₂ L/min air	Time s	Burner big/small	Gas composition % CH ₄	Injector mm	Wet/ dry
17.1	53	22	1	0.2	0.55	727.5	small	72%	1.28	wet
17.2	50	22	2	0.1	0.4	557.5	small	72%	1.28	wet
17.5	50	32	12	3	0	243	small	100%	1.28	wet
16.6	50	32	4.5	3	0.85	366.31	small	75%	1.28	wet
16.5	50	32	6.2	3	0.55	344.2	small	81%	1.28	wet
20.8	53	32	8	3	0.2	409.9	small	86%	0.95	wet
20.5	50	32	8	3	0.15	370.2	small	86%	0.95	wet
20.8	50	26	3.7	3	0.1	272.7	small	82%	1.28	dry
21.1	50	26	0.8	3	0.25	295.5	small	82%	1.28	dry
20.5	50	22	2	0.7	0.1	462.7	small	76%	1.28	dry
21	50	22	2	1.1		374.4	small	85%	1.28	dry
18.5	50	22	1	0.6	0.4	675.5	big	74%	1.28	dry
20.7	41	22	3	0	0.2	410.9	big	78%	1.28	dry
21	50	26	2.8	3		320.8	big	88%	1.28	wet
21.3	50	26	1.3	3	0.15	341.7	big	86%	1.28	wet
20.9	51	22	2	0.9		396.5	small	90%	0.95	wet
21	50	22	2	0.4	0.1	421.2	small	74%	1.28	wet
20.8	50	22	1	1.5		407.5	big	87%	1.28	wet
21.1	50	32	11.6	3	0	260.3	small	100%	0.95	wet

Table 19 Cut-off compositions: Raw data

Supply pressure kPa	Rotameter CH ₄ cm	Rotameter CO ₂ L/min air	Burner big/small	Gas composition % CH ₄	Injector mm	Wet/ dry
22	-	0.2	small	78%	0.95	dry
24	0.4	0.3	small	79%	0.95	dry
26	1	0.35	small	75%	0.95	dry
28	1.25	0.5	small	80%	0.95	dry
22	-	0.65	small	62%	1.28	dry
24	0.5	0.75	small	61%	1.28	dry
28	1.8	1	small	63%	1.28	dry
22	-	0.3	small	67%	0.95	wet
24	0.5	0.4	small	65%	0.95	wet
26	1.2	0.45	small	68%	0.95	wet
28	1.8	0.5	small	70%	0.95	wet
20	-	-	small	58%	1.28	wet
22	-	0.6	small	56%	1.28	wet
24	0.5	0.85	small	62%	1.28	wet
26	1.3	0.8	small	70%	1.28	wet
28	2.3	0.85	small	71%	1.28	wet
22	0.5	0.4	big	74%	1.28	dry
24	1.2	0.6	big	71%	1.28	dry
26	1.5	0.75	big	70%	1.28	dry
28	2.5	0.6	big	79%	1.28	dry
22	0.7	0.4	big	64%	1.28	wet
24	1.4	0.45	big	65%	1.28	wet
26	2.2	0.55	big	68%	1.28	wet
28	3.1	0.55	big	70%	1.28	wet
28	3.5	0.5	big	74%	1.28	dry
28	3.5	0.5	big	79%	1.28	dry
26	2.8	0.4	big	82%	1.28	dry
24	1.6	0.3	big	79%	1.28	dry
22	0.3	0.15	big	84%	1.28	dry
20	0	0	big	95%	1.28	dry
24	1.3	0.35	big	76%	1.28	dry
26	2.4	0.4	big	74%	1.28	dry
28	3.1	0.6	big	77%	1.28	dry
32	3	1.05	small	72%	1.28	wet
28	1.85	0.45	small	74%	0.95	dry
28	2.2	0.4	small	79%	0.95	dry
26	1.5	0.4	small	82%	0.95	dry
24	0.7	0.4	small	79%	0.95	dry
20	0	0	small	95%	0.95	dry
26	0	-	small	77%	0.95	dry
26	0.8	0.5	small	69%	0.95	dry

Appendix C

Gas Composition

Methane content calculation using reference gas and GC output:

$$\begin{aligned}\text{Methane content [\%]} &= \frac{\text{Methane content reference gas} \times \text{Area}}{\text{Area reference gas}} \\ &= \frac{99.95\% \times 8626631}{10797378} \\ &= 79.9\%\end{aligned}$$

Flow Rate

Calibration chart:

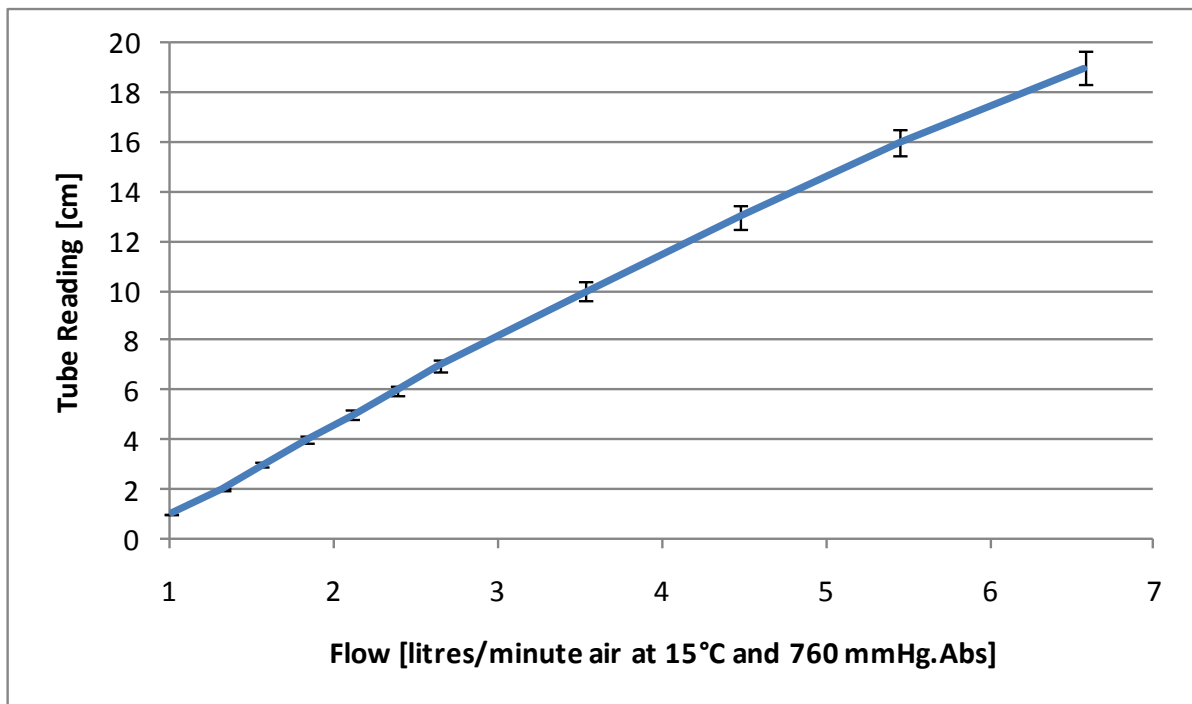


Figure 42 Air calibration chart for metric series rotameter tube size 7 with float type A, showing ±3.5% error bars

Methane flow rate calculation using capacity factors to correct for the different gas:

$$\begin{aligned} \text{Flow rate methane at 0kPa} &= \text{Flow rate air} \times \frac{\text{Capacity factor for methane}}{\text{Capacity factor for air}} \\ &= 1.3 \times \frac{14.5}{10} \\ &= 1.9 \text{ L/min} \end{aligned}$$

Methane flow rate calculation, correcting for pressure:

$$\begin{aligned} \text{Flow rate methane at 1 kPa} &= \text{Flow rate methane at 0kPa} \times \frac{P_{\text{atm}}}{P} \\ &= 1.9 \times \frac{101.3}{101.3 + 1} \\ &= 1.9 \text{ L/min} \end{aligned}$$

Sample chart used to aid the calculation of methane flow rates:

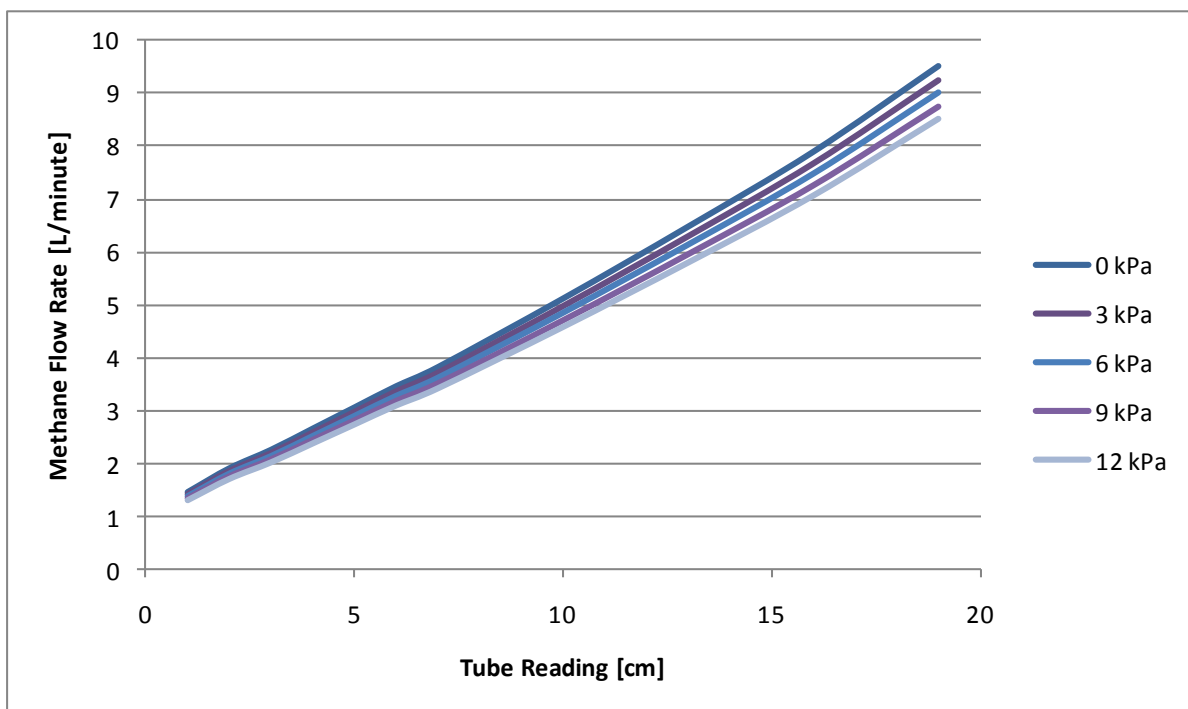


Figure 43 Sample chart, showing graphs plotted for flow rates at different pressures

Carbon dioxide flow rate calculation:

$$\begin{aligned} \text{Flow rate } CO_2 &= \text{Flow rate methane} \times \left(\frac{1}{\% \text{methane in gas}} - 1 \right) \\ &= 1.9 \times \left(\frac{1}{80\%} - 1 \right) \\ &= 0.47 \text{ L/min} \end{aligned}$$

Energy Transferred to the Water

Energy calculation:

$$\begin{aligned} H &= \int_{T_1}^{T_2} 2.7637 \times 10^5 - 2.0901 \times 10^3 T + 8.1250 T^2 - 1.4116 \times 10^{-2} T^3 + 9.3701 \times 10^{-6} T^4 \\ &= \left[2.7637 \times 10^5 T_2 - 2.0901 \times 10^3 \frac{T_2^2}{2} + 8.1250 \frac{T_2^3}{3} - 1.4116 \times 10^{-2} \frac{T_2^4}{4} + 9.3701 \right. \\ &\quad \left. \times 10^{-6} \frac{T_2^5}{5} \right] \\ &\quad - \left[2.7637 \times 10^5 T_1 - 2.0901 \times 10^3 \frac{T_1^2}{2} + 8.1250 \frac{T_1^3}{3} - 1.4116 \times 10^{-2} \frac{T_1^4}{4} \right. \\ &\quad \left. + 9.3701 \times 10^{-6} \frac{T_1^5}{5} \right] \end{aligned}$$

$H = 2400 \text{ J/mol}$, for $T_1 = 18.2^\circ\text{C}$ and $T_2 = 50^\circ\text{C}$:

Power calculation:

$$\begin{aligned} P &= \frac{H \times \text{mass of water}}{t \times \text{molar mass of water}} \\ &= \frac{2400 \times 1}{452.5 \times 18.015} \end{aligned}$$

$P = 0.29 \text{ kW}$, for $t = 452.5 \text{ s}$

Flame Power

Calorific value calculation:

The calorific value refers to the lower heating value. It is usually given as per mass or mole, and thus needs to be converted to a per volume basis. LHV_v stands for the lower heating value on a per volume basis, while LHV_m refers to the lower heating value on a per mole basis. The LHV_m was taken from Perry (1997). The ambient temperature was assumed to be 293.15 K.

$$\begin{aligned}LHV_v &= LHV_m \times \frac{P_{operating,abs}}{R \times T} \\&= 802.6 \times \frac{101.3 + 3}{8.314 \times 293.15} \\&= 34.35 \text{ kJ/L}\end{aligned}$$

Flame power calculation:

$$\begin{aligned}\text{Flame power} &= \text{Methane flow rate} \times \text{Calorific value methane} \\&= 1.4 \text{ L/min} \times 34.35 \text{ kJ/L} \\&= 0.82 \text{ kW}\end{aligned}$$

Efficiency

Efficiency calculation:

$$\begin{aligned}\text{Efficiency} &= \frac{\text{Power due to heat added to water}}{\text{Flame power}} \\&= \frac{0.29}{0.82} \\&= 36\%\end{aligned}$$

Error Analysis

Table 20 Data used to calculate the pooled standard deviation

n	Water heating power kW		Flame power kW		Efficiency %		Total flow rate L/min	
	std dev	std dev ²	std dev	std dev ²	std dev	std dev ²	std dev	std dev ²
2	0.014	2.0E-04	0.010	1.1E-04	0.009	7.7E-05	0.018	3.3E-04
2	0.010	1.0E-04	0.036	1.3E-03	0.000	4.6E-08	0.072	5.2E-03
2	0.021	4.3E-04	0.085	7.3E-03	0.005	2.5E-05	0.293	8.6E-02
2	0.003	7.6E-06	0.000	0.0E+00	0.002	5.2E-06	0.000	0.0E+00
2	0.015	2.2E-04	0.017	2.9E-04	0.010	9.7E-05	0.030	9.0E-04
2	0.024	5.8E-04	0.005	2.9E-05	0.015	2.2E-04	0.011	1.2E-04
2	0.019	3.8E-04	0.001	5.5E-07	0.016	2.5E-04	0.045	2.0E-03
2	0.002	5.6E-06	0.000	0.0E+00	0.002	3.6E-06	0.001	8.2E-07
2	0.004	1.3E-05	0.002	5.5E-06	0.002	4.8E-06	0.009	7.4E-05
2	0.012	1.4E-04	0.002	3.2E-06	0.010	9.9E-05	0.019	3.6E-04
2	0.018	3.1E-04	0.000	0.0E+00	0.014	2.0E-04	0.009	7.4E-05

Appendix D

Raw Biogas Flow Rate

$$\text{Flow rate raw biogas} = \frac{3kW \times 3600}{802. \frac{32kJ}{mol} \times 60\%} = 22.4 \text{ mol/h}$$

$$\text{Volumetric flow rate raw biogas} = \frac{22.4 \text{ mol/h} \times 8.314 \text{ m}^3 \text{ Pa/molK} \times 298 \text{ K}}{107 \times 10^3 \text{ Pa}}$$

Equilibrium Solubility Data

Table 21 Equilibrium solubility data (Park, Shim, Lee, & Lee, 1997)

5 mass % K ₂ CO ₃		10 mass % K ₂ CO ₃	
Partial pressure CO ₂ kPa	Loading mol CO ₂ / mol K ₂ CO ₃	Partial pressure CO ₂ kPa	Loading mol CO ₂ / mol K ₂ CO ₃
5.7	0.83	6.15	0.762
18.61	0.889	11.05	0.833
68.79	1.03	28.35	0.872
129.3	1.127	77.8	0.955
		294.8	1.058

Correlations and Correction Factors

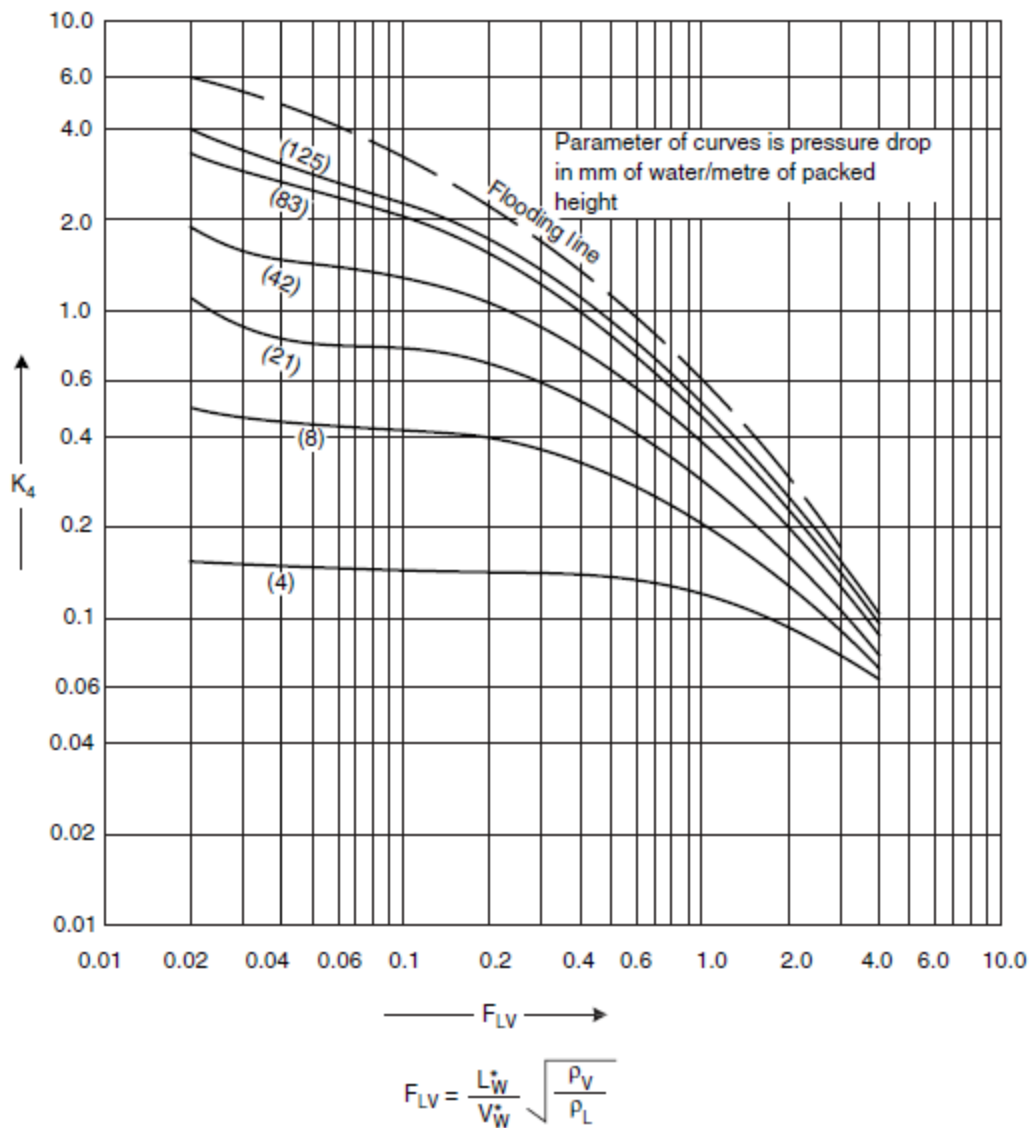


Figure 44 Generalised pressure drop correlation (Sinnott, 2005)

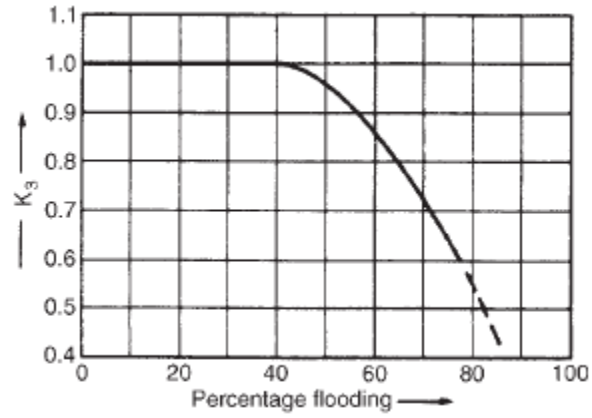


Figure 45 Percentage flooding correction factor (Sinnott, 2005)

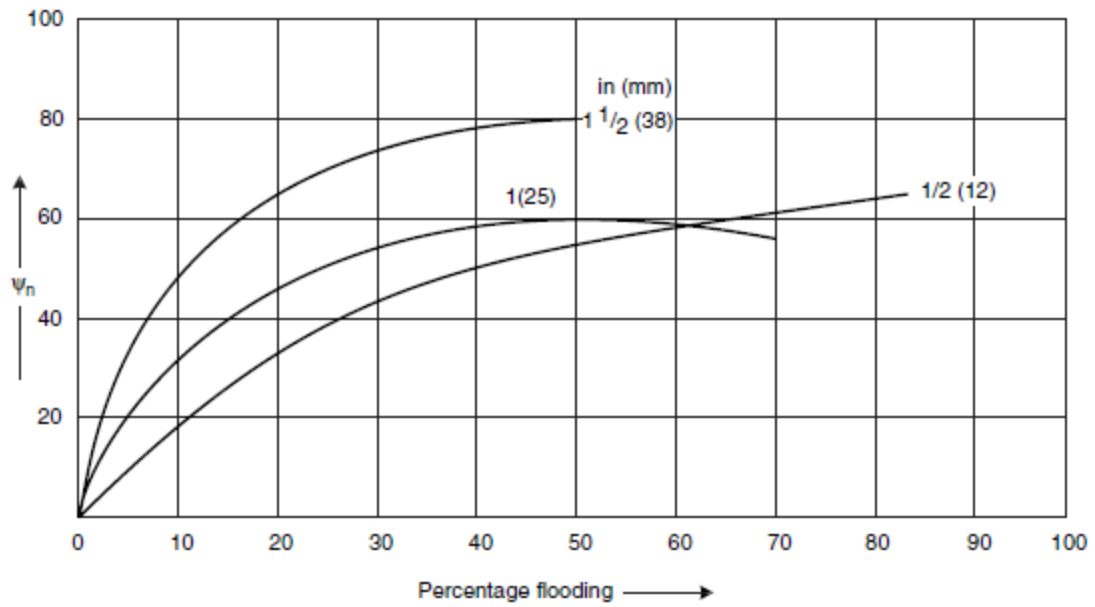


Figure 46 Factor for H₆ for Berl saddles (Sinnott, 2005)

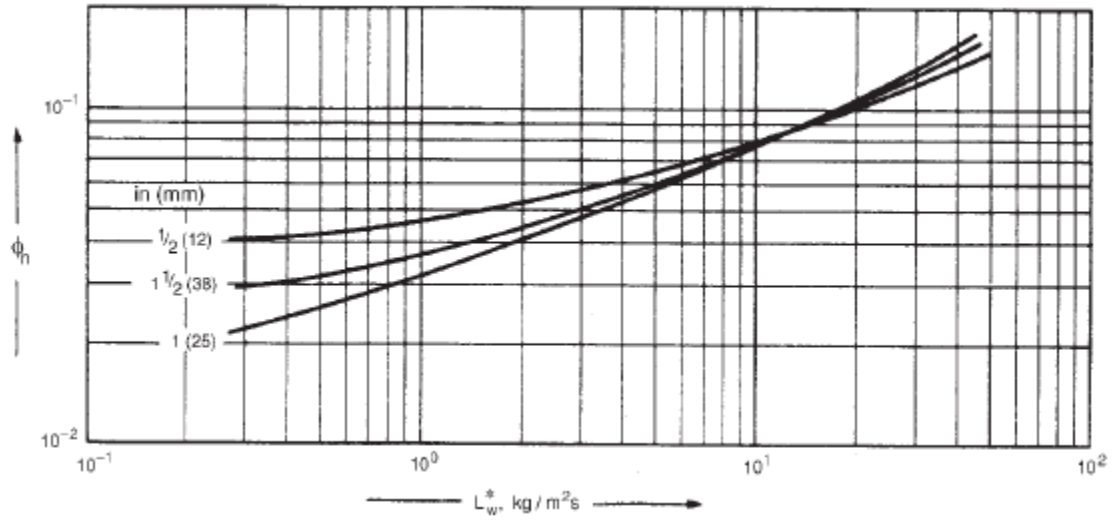


Figure 47 Factor for H_L for Berl saddles (Sinnott, 2005)

Absorber Design: Sample Calculations

Carbon Dioxide Absorber Design - 10% K₂CO₃ solvent

Key: M - molar mass ρ - density μ - viscosity
 G - gas molar flow rate P - pressure T - temperature
 m - mass flow rate L - liquid molar flow rate Q - volumetric flow rate
 y - gas mole fraction x - liquid mole fraction rate
 sub a - solute (carbon dioxide) sub b - solvent (water) sub c - methane
 sub G - gas sub L - liquid sub 1 - bottom of tower
 sub 2 - top of tower

$$M_a := 44.011 \frac{\text{gm}}{\text{mol}} \quad M_b := 18.015 \frac{\text{gm}}{\text{mol}} \quad M_c := 16.043 \frac{\text{gm}}{\text{mol}} \quad M_d := 138.21 \frac{\text{gm}}{\text{mol}}$$

$$g := 9.807 \frac{\text{m}}{\text{s}^2} \quad P := 107 \text{kPa} \quad R := 8.314 \frac{\text{J}}{\text{mol}\cdot\text{K}} \quad T := 298 \text{K}$$

GAS :

$$y_{c1} := 0.60 \quad y_{a1} := 0.4 \quad y_{c2} := 0.8 \quad y_{a2} := 0.2 \quad \mu_G := 12.97 \cdot 10^{-6} \text{Pa}\cdot\text{s}$$

$$M_G := y_{a1} \cdot M_a + y_{c1} \cdot M_c \quad M_G = 0.027 \frac{\text{kg}}{\text{mol}} \quad G_1 := 22.43 \frac{\text{mol}}{\text{hr}} \quad m_G := G_1 \cdot M_G$$

$$\rho_G := \frac{P \cdot M_G}{R \cdot T} \quad Q_g := \frac{m_G}{\rho_G} \quad G_2 := 16.83 \frac{\text{mol}}{\text{hr}} \quad m_G = 1.697 \times 10^{-4} \frac{\text{kg}}{\text{s}}$$

$$\rho_G = 1.176 \frac{\text{kg}}{\text{m}^3} \quad Q_g = 1.443 \times 10^{-4} \frac{\text{m}^3}{\text{s}}$$

LIQUID :

$$x_{k2co3} := 0.1 \quad \text{weight percent K}_2\text{CO}_3 \text{ in solution} \quad L_2 := 532 \frac{\text{mol}}{\text{hr}}$$

$$\rho_L := 1000 \frac{\text{kg}}{\text{m}^3} \quad \mu_w := 8.90 \cdot 10^{-4} \text{Pa}\cdot\text{s} \quad \mu_L := \mu_w$$

$$M_s := \frac{1}{\frac{x_{k2co3}}{M_d} + \frac{1 - x_{k2co3}}{M_b}} \quad M_s = 0.02 \frac{\text{kg}}{\text{mol}}$$

$$m_{L2} := L_2 \cdot M_s \quad L_{a1} := G_1 - G_2 \quad m_{La} := L_{a1} \cdot M_a$$

$$m_{L2} = 2.916 \times 10^{-3} \frac{\text{kg}}{\text{s}} \quad L_{a1} = 1.556 \times 10^{-3} \frac{\text{mol}}{\text{s}} \quad m_{La} = 6.846 \times 10^{-5} \frac{\text{kg}}{\text{s}}$$

$$m_{L1} := m_{L2} + m_{La} \quad Q_L := \frac{m_{L2}}{\rho_L}$$

$$m_{L1} = 2.984 \times 10^{-3} \frac{\text{kg}}{\text{s}} \quad Q_L = 2.916 \times 10^{-6} \frac{\text{m}^3}{\text{s}}$$

For 6 mm ceramic Raschig rings: $F_p := 5250 \text{ m}^{-1}$ $a := 794 \frac{\text{m}^2}{\text{m}^3}$ $\rho_P := 960 \frac{\text{kg}}{\text{m}^3}$

$X := \frac{mL1}{mG} \left(\frac{\rho_G}{\rho_L} \right)^{0.5}$ $X = 0.603$ From fig. 36, with a pressure drop of 21 mm water

$K_4 = 0.4$ $K_{4f} := 0.9$ Percentage flooding: $Pf := \left(\frac{K_4}{K_{4f}} \right)^{0.5}$ $Pf = 0.667$

$V_w := \left[\frac{K_4 \cdot \rho_G \cdot (\rho_L - \rho_G)}{13.1 \text{ m}^{-1} \cdot 1.2 \cdot \text{s}^{2.1} \cdot F_p \cdot \left(\frac{\mu_L}{\rho_L} \right)^{0.1}} \right]^{0.5}$ $V_w = 0.166 \frac{\text{kg}}{\text{m}^2 \cdot \text{s}}$

$\dot{A}_w := \frac{mG}{V_w}$ $A = 1.023 \times 10^{-3} \text{ m}^2$ $D := \left(\frac{4 \cdot A}{\pi} \right)^{0.5}$ $D = 0.036 \text{ m}$

Check this for packing size $D = 0.036 \text{ m}$ $D_p := 6 \text{ mm}$ $\frac{D}{D_p} = 6.014$ **A bit low**
(10 < D/Dp < 40 (up to 100)):

$\text{Flood_check} := Pf \cdot \frac{A}{\frac{\pi}{4} \cdot D^2}$ $\text{Flood_check} = 0.667$ **Applicable when D is rounded off to a standard size**

$\dot{A}_w := \pi \cdot \left(\frac{D}{2} \right)^2$ $A = 1.023 \times 10^{-3} \text{ m}^2$

Type of packing material	$v_{L, \text{min}}$ [mm/s]		
Ceramic	0.15	$v_L := \frac{QL}{A}$	$v_L = 2.851 \times 10^{-3} \frac{\text{m}}{\text{s}}$ ok
Oxidized or etched metal	0.30		
Bright metal	0.90		
Plastic	1.20		

Number of transfer units

$\frac{Y1}{\dot{m}_w} = \frac{ya1}{1 - ya1}$ $Y1 = 0.667$ $Y2 := \frac{ya2}{1 - ya2}$ $Y2 = 0.25$

$Ye(Y) := 10^{32} \cdot \left(\frac{Y - 0.25}{39.526} \right)^{17.077}$ From the equilibrium and operating line equations

$\text{Nog} := \int_{Y1}^{Y2} \left[\frac{(1 + Y) \cdot (1 + Ye(Y))}{Ye(Y) - Y} \right] dY$ $\text{Nog} = 1.4$

Height of transfer units - method from C&R vol. 6

Cornell's method May be used for Berl saddles, but also gives a conservative estimate for Pall rings and Intalox saddles

Vapour diffusivity

va := 26.9 vc := 16.5 + 4·1.98 vc = 24.42 atomic diffusion volumes

T_w := 298 K M_a := 44.011 M_c := 16.043 $\frac{g}{mol}$ P_b := 1.07 bar

$$DG := \frac{1.013 \cdot 10^{-7} \cdot T^{1.75} \left(\frac{1}{M_a} + \frac{1}{M_c} \right)^{0.5}}{P_b \left(\frac{1}{v_a^3} + \frac{1}{v_c^3} \right)^2}$$

DG = 1.697 × 10⁻⁵ m² / s

Check: (Benetiz)

$$Mac := 2 \cdot \left(\frac{1}{M_a} + \frac{1}{M_c} \right)^{-1}$$

Mac = 23.514

σ_a := 3.941 σ_c := 3.758 A e_{ka} := 195.2 e_{kc} := 148.6 K

$$\sigma_{ac} := \frac{\sigma_a + \sigma_c}{2}$$

e_{kac} := $\sqrt{e_{ka} \cdot e_{kc}}$ T_s := $\frac{T}{e_{kac}}$

$$\Omega := \frac{1.06036}{T_s^{0.15610}} + \frac{0.19300}{e^{0.47635 \cdot T_s}} + \frac{1.03587}{e^{1.52996 \cdot T_s}} + \frac{1.76474}{e^{3.89411 \cdot T_s}}$$

$$DG_{check} := \frac{0.00266 \cdot T^{\frac{3}{2}}}{P_b \cdot Mac^{0.5} \cdot \sigma_{ac}^2 \cdot \Omega}$$

DG_{check} = 0.158 cm² / s
 DG_{check} · 0.0001 = 1.577 × 10⁻⁵ m² / s close

Height of gas phase transfer unit

$$Sc_G := \frac{\mu_G}{\rho_G \cdot DG} \cdot \frac{m^2}{s}$$

Sc_G = 0.65

Ψ_h := 60 Estimated from fig 38, based on Berl saddles, lowest size is 12 mm (Ψ_h increases with an increase in packing size)

$$L_w := \frac{mL_1}{A} \quad L_w = 2.918 \frac{\text{kg}}{\text{m}^2 \cdot \text{s}}$$

$$f_1 := \left(\frac{\mu_L}{\mu_w} \right)^{0.16} \quad \rho_w := 1000 \frac{\text{kg}}{\text{m}^3} \quad f_2 := \left(\frac{\rho_w}{\rho_L} \right)^{1.25} \quad \sigma_w := 70 \quad \sigma_L := 70 \quad f_3 := \left(\frac{\sigma_w}{\sigma_L} \right)^{0.8}$$

$$HG := \frac{0.011 \cdot \Psi_h \cdot \text{ScG}^{0.5} \cdot \left(\frac{D}{3.05 \text{m}} \right)^{1.11}}{\left(L_w \frac{\text{m}^2 \cdot \text{s}}{\text{kg}} \cdot f_1 \cdot f_2 \cdot f_3 \right)^{0.5}} \quad HG = 2.262 \times 10^{-3} \quad \text{m}$$

Height of liquid phase transfer unit

$$\Phi_h := 0.059 \quad \text{From fig 39, for Berl saddles, smallest size is 12 mm}$$

$$DL := 1.92 \cdot 10^{-5} \frac{\text{cm}^2}{\text{s}} \quad \text{CO}_2 \text{ in water, at 298 K}$$

$$\text{ScL} := \frac{\mu_L}{\rho_L \cdot DL} \quad \text{ScL} = 463.542$$

$$K_3 := 0.74$$

$$HL := 0.305 \cdot \Phi_h \cdot \text{ScL}^{0.5} \cdot K_3 \quad HL = 0.287 \quad \text{m}$$

Overall height of transfer unit

$$m_e := 1.638 \quad \text{mopl} := 39.5$$

$$\text{HOG} := \frac{m_e}{\text{mopl}} \cdot HL + HG \quad \text{HOG} = 0.014 \quad \text{m}$$

Column height

$$Z := \text{HOG} \cdot \text{Nog} \quad Z = 0.02 \quad \text{m} \quad \text{Very small}$$

Onda's method

$K5 \approx 2$	$Lw = 2,918 \frac{\text{kg}}{\text{m}^2 \cdot \text{s}}$	$Vw = 0.166 \frac{\text{kg}}{\text{m}^2 \cdot \text{s}}$
$a = 794 \frac{1}{\text{m}}$	$dp := 6 \text{ mm}$	$dp = 6 \times 10^{-3} \text{ m}$
$\rho_{\text{w}} := 61 \cdot 10^{-3} \frac{\text{N}}{\text{m}}$	$\rho_{\text{L}} := 70 \cdot 10^{-3} \frac{\text{N}}{\text{m}}$ (water)	$R = 8.314 \frac{\text{m}^2 \cdot \text{kg}}{\text{mol} \cdot \text{K} \cdot \text{s}^2}$
$aw := a \cdot \left[1 - e^{-1.45 \left(\frac{\rho_{\text{c}}}{\rho_{\text{L}}} \right)^{0.75} \cdot \left(\frac{Lw}{a \cdot \mu_{\text{L}}} \right)^{0.1} \cdot \left(\frac{Lw^2 \cdot a}{\rho_{\text{L}}^2 \cdot g} \right)^{-0.005} \cdot \left(\frac{Lw^2}{\rho_{\text{L}} \cdot \sigma_{\text{L}} \cdot a} \right)^{0.2}} \right]$		$aw = 247.921 \frac{1}{\text{m}}$
$kL := 0.0051 \cdot \left(\frac{Lw}{aw \cdot \mu_{\text{L}}} \right)^{\frac{2}{3}} \cdot \left(\frac{\mu_{\text{L}}}{\rho_{\text{L}} \cdot DL} \right)^{-0.5} \cdot (a \cdot dp)^{0.4} \cdot \left(\frac{\rho_{\text{L}}}{\mu_{\text{L}} \cdot g} \right)^{-\frac{1}{3}}$		$kL = 5.092 \times 10^{-5} \frac{\text{m}}{\text{s}}$
$kG \approx K5 \cdot \left(\frac{Vw}{a \cdot \mu_{\text{G}}} \right)^{0.7} \cdot \left(\frac{\mu_{\text{G}}}{\rho_{\text{G}} \cdot DG \cdot \frac{\text{m}^2}{\text{s}}} \right)^{\frac{1}{3}} \cdot (a \cdot dp)^{-2} \cdot \frac{a \cdot DG \cdot \frac{\text{m}^2}{\text{s}}}{R \cdot T \cdot K}$		$kG = 2.904 \times 10^{-6} \frac{\text{mol} \cdot \text{s}}{\text{m} \cdot \text{kg}}$
$Gm := \frac{G1}{A}$	$Gm = 6.092 \frac{\text{mol}}{\text{m}^2 \cdot \text{s}}$	$\text{mol} \cdot \text{s} / \cdot \text{m}^2 \cdot \text{kg}$
$Lm := \frac{L2}{A}$	$Lm = 144.486 \frac{\text{mol}}{\text{m}^2 \cdot \text{s}}$	$\text{mol} \cdot \text{s} / \cdot \text{m}^2 \cdot \text{kg}$
$Ct \approx \frac{\rho_{\text{L}}}{Ms}$	$Ct = 5.068 \times 10^4 \frac{\text{mol}}{\text{m}^3}$	
$HGo := \frac{Gm}{kG \cdot aw \cdot P}$	$HLo \approx \frac{Lm}{kL \cdot aw \cdot Ct}$	$HOGO := \frac{me}{mopl} \cdot HLo + HGo$
$HGo = 0.079 \text{ m}$	$HLo = 0.226 \text{ m}$	$HOGO = 0.088 \text{ m}$
$Zo := \text{Nog} \cdot HOGO$	$Zo = 0.124 \text{ m}$	